KAUNAS UNIVERSITY OF TECHNOLOGY

JONAS MATULEVIČIUS

FORMATION AND INVESTIGATION OF FILTRATION PROPERTIES OF THE ELECTROSPUN NANOFIBER MATERIALS

Doctoral dissertation
Technological science, Chemical Engineering (05T)

2016, Kaunas

UDK: 66.074.2 + 677.022.3/.5] (043.3)

The dissertation was prepared at Kaunas University of Technology, Faculty of Chemical Technology, Department of Environmental Technology during the period 2011-2015. Research was supported by Research Council of Lithuania

Scientific Supervisor:
Prof., Dr. Linas Kliučininkas (Kaunas University of Technology, Technological Sciences, Chemical Engineering, 05T).

The Lithuanian Language Editor:
Aurelija Gražina Rukšaitė
Publishing house "Technologija"

The English Language Editor:
Brigita Brasienė
Publishing house "Technologija"

ISBN

KAUNO TECHNOLOGIJOS UNIVERSITETAS

JONAS MATULEVIČIUS

NANOPLUOŠTINIŲ MEDŽIAGŲ FORMAVIMAS ELEKTRINIO VERPIMO BŪDU IR FILTRAVIMO SAVYBIŲ TYRIMAS

Daktaro disertacija
Technologijos mokslai, chemijos inžinerija (05T)

2016, Kaunas

UDK: 66.074.2 + 677.022.3/.5] (043.3)

Disertacija rengta 2011-2015 m. Kauno technologijos universitete, Cheminės technologijos fakultete, Aplinkosaugos technologijos katedroje. Mokslinius tyrimus rėmė Lietuvos mokslo taryba.

Mokslinis vadovas:
Prof. dr. Linas Kliučininkas (Kauno technologijos universitetas, technologijos mokslai, chemijos inžinerija, 05T)

Lietuvių kalbos redaktorė
Aurelija Gražina Rukšaitė
Leidykla „Technologija“

Anglų kalbos redaktorė
Brigita Brasienė
Leidykla „Technologija“

ISBN

ACKNOWLEDGEMENTS

First and foremost, the author of this dissertation would like to thank his supervisor Prof., Dr. Linas Kliučininkas for his guidance, constant support and valuable advice throughout the research work.

The author as well wishes to express sincere thanks to Assoc. Prof., Dr. Dainius Martuzevičius for his discussions and useful suggestions in terms of aerosols and filtration.

The author is grateful to all the co-authors: Assoc. Prof., Jonas Baltrušaitis (for performing SEM images and improving the manuscript), Dr. Edvinas Krugly (for ideas when constructing the device of electrospinning), Dr. Tadas Prasauskas (for improving the drawings and suggestions) and Martynas Tichonovas (for sharing the DC power supply and other electric equipment).

Special thanks to all the colleagues from the Department of Environmental Technology of Kaunas University of Technology: Prof., Dr. Ginatas Denafas; Assoc. Prof., Dr. Viktoras Račys; Assoc. Prof., Dr. Violeta Kaunelienė; Assoc. Prof., Dr. Dalia Jankūnaitė; Dr. Inga Radžiūnienė; Dr. Inga Stasiulaitienė; Darius Čiužas and Rūta Sidaravičiūtė for direct and indirect help during the PhD.

The author of this dissertation wants to thank other colleagues at Wastewater Treatment Plant in Kaunas and JSC "Kauno Vandenys" for providing favourable conditions for work, which contributed to the PhD.

Finally, the author expresses heartfelt thanks to his wife Miglė for her endless love and care. The author as well thanks his daughter (for good sleeping at nights and amazing energy at days), parents (for encouraging and understanding) and grandparents (especially for taking care of his little daughter during the preparation of PhD).

LIST OF TABLES

LIST OF FIGURES

TABLE OF CONTENTS

LIST OF ABBREVIATIONS

α – packing density;
AA – acetic acid;
AFM – atomic force microscopy;
CA – cellulose acetate;
DCM – dichloromethane;
DMAc - *N*,*N*-dimethylacetamide;
DMF - *N*,*N*-dimethylformamide;
FA – formic acid;
FD - fiber diameter;
FSN – fragmented spider-net structure;
ID – filter name;
Kn - Knudsen number;
MPPS - most penetrating particle size;
MW - molecular weight;
PA – polyamide;
PA6 – polyamide 6;
PA6/6 - polyamide 6/6;
PAN – polyacrylonitrile;
PEO - polyethylene oxide;
PLS - partial least squares;
PS – polystyrene;
PSL - polystyrene latex;
PU – polyurethane;
PVA - polyvinyl alcohol;
PVAc - polyvinyl acetate;
PVC - polyvinyl chloride;
SD - standard deviation;
SEM – scanning electron microscopy;
SN – spider-net structure;
ST - stick-together fibers;
QF – quality factor;
TTCD – tip to collector distance;
UF – uniform fibers;
W – basis weight;
Z – thickness.

Symbols	**Explanation**
v/v/v	concentration in volume/volume/volume;
wt%	mass fraction (percentage by weight);
w/v	weight/volume concentration;
w/w	concentration in weight/weight.

INTRODUCTION

Air pollution is a major environment related health threat to human and a risk factor for both acute and chronic respiratory diseases (World health organization, 2005). The main sources of air pollution still remain automotive exhausts, power generation, industrial air emissions and other human activities like home heating and cooking (Colvile et al., 2001; Chen et al., 2015; Kibble and Harrison, 2005). Aerosols affect more people than any other pollutants (World health organization, 2005). Aerosols consist of complex mixtures of solid particles and droplets of liquids of inorganic and organic substances suspended in the air. Due to the better ability to penetrate and lodge deep inside the lungs, fine particles with aerodynamic diameter less than 2.5 μm are considered to be the most health damaging particles. Air filters and other particle air cleaners are used extensively in various industrial processes to remove particles from the incoming or recirculated air (Fisk et al., 2002). The conventional filters consist of quite high performance filtration medium, including glass fibers, meltblown fibers and spunbonded fibers, and are based on the micro sized fiber diameter. However, the fact that the decreasing fiber diameter leads to a better filtration efficiency makes the submicron filter media (including nano scale) attractive for the filtration applications (Hinds, 1999). The usage of nanofiber media filters becomes a viable area, since the development of electrospinning has been accelerated during the recent years. Electrospinning is a simple and widely used technique to fabricate fibers in a submicron scale (Askari et al., 2014; Barhate et al., 2011; Maze et al., 2007; Oh et al., 2008). Electrospun fibers have unique characteristics such as large surface area to the volume ratio, low basis weight, small pore size and relatively uniform fiber size (Leung et al., 2010). Because the fiber diameter is very small, the increase of pressure drop due to the gas phase "slips" around the fibers is not as large as in the case of an equivalent surface area of micron size fibers (Brown, 1993; Sambaer et al., 2011). The gas slip effect increases the single fiber capture efficiency of impaction, interception and diffusion due to the increased contact of air and small particles with the fiber surface (Hosseini and Tafreshi, 2010; Sambaer et al., 2011).

Numerous experimental studies were carried out to examine the filtration performance of electrospun fibers. The effects of some electrospinning parameters (Zhang et al., 2009) as well as nanofiber filter characteristics (Hung and Leung, 2011; Leung et al., 2010; Sambaer et al., 2011; Wang et al., 2008a) on filtration performance were extensively studied theoretically and experimentally. The influence of fiber media properties to achieve the enhanced filtration quality factor were gained by using multi-ply layer fiber mats (Leung et al., 2010; Wang et al., 2014; Zhang et al., 2010). This shows that the effects of various parameters and media properties on air filtration performance are quite well examined; however, there are no studies that are specifically focused on the comparative assessment of filtration characteristics of the nanofibers produced from various polymeric materials. Thus, the detailed characterization of polymer solution parameters, electrospinning conditions as well as nanofiber filtration characteristics in the airflow is a relevant task for the experimental research.

Aim of the thesis

To produce nanofibers by using electrospinning and investigate the characteristics as well as to perform the comparative evaluation of filtration properties of nanofiber media in an air stream.

Objectives of the thesis

1. To prepare and optimize the formation of nanofibers in electrospinning.
2. To assess the effects of the polymer concentration as well as electrospinning parameters on the characteristics of nanofiber media.
3. To perform a comparative evaluation of filtration properties of nanofiber media produced from various polymeric materials.
4. To assess and compare filters quality factors of one-ply and multi-ply nanofiber media.
5. To assess and compare filtration efficiency of polystyrene latex and sodium chloride aerosol particles through the nanofiber media.

Scientific novelty

1. The formation of nanofiber media for filtration applications was performed from various polymeric materials (including polyamide 6, polyamide 6/6 and polyacrylonitrile), while, for the first time, the electrospun cellulose acetate and polyvinyl acetate nanofiber media were used for filtration applications.
2. The novel ternary solvent system consisting of acetone/ dichloromethane/*N*,*N*-dimethylformamide at the ratio of 2/1/1 (v/v/v) was developed for the electrospinning of cellulose acetate nanofiber media. The suggested composition of the solvents ensured the continuous formation of cellulose acetate nanofiber media.
3. The unique data covering the comparison of filtration performance of various nanofiber media, the comparison of single-ply to multi-ply nanofiber mats as well as the comparison of the penetration ability of polystyrene latex and sodium chloride aerosol particles through the nanofiber media were obtained.

Practical value of the work

1. The findings of the thesis provide new knowledge and data associated with the electrospun nanofiber media characterization and testing of filtration properties in the airflow. For better understanding of the interplay between the nanofiber formation in the electrospinning process and nanofiber filter media characteristics, the operational parameters were defined.

2. The main challenges of nanofiber media filters were identified, and the subsequent recommendations were provided in order to adapt nanofiber filters as closely as possible in practical air filtration processes.
3. The experimental setups for electrospun nanofiber media formation and filtration testing were developed by supporting the improved methodologies of further knowledge-based experimental work.

Structure and outline of the dissertation

The dissertation is divided into the following parts: list of abbreviations, introduction, literature review, experimental part, results and discussion, conclusions, list of 168 references, list of publications on the dissertation topic. The literature survey and results of the research are presented in 83 pages, including 10 tables and 21 figures.

Publication of the research results

The results of this thesis are presented in three (3) publications corresponding to the list of the Web of Science database by Thomson Reuters; one (1) publication referred in international databases, reported at five (5) international conferences and two (2) local conferences as well as presented in one (1) local scientists contest.

1. LITERATURE REVIEW

1.1 Particles separation by filtration media

The basis of the filter is filter media. The filter media is defined as any permeable material used in filtration and upon which, or within which, the solids are deposited (Wakeman, 1985). The definition "nanofiber filter media" used in this work is a porous media composed of random electrospun nanofibers whose function is to capture aerosol of air gas stream transported through the medium. The scale "nano" in nanofiber is not the same, according to different sources. According to the definition provided by the International Standardization Organization (ISO), the word "nano" is nano-object material with one, two or three external dimensions in the nanoscale. The nanoscale size range is approximately from 1 nm to 100 nm. However, the non-woven industry uses the definition nanofiber for diameter less than 0.5 μm (Ford, 2011; Wang et al., 2008a). Moreover, Barhate and Ramakrishna (2007) consider nanofibers as having a diameter ranging from 100 to 1000 nm (0.1-1 μm). Leung and Hung (2012) proposed additional definition of nanofibers: ultrafine nanofibers are nanofibers with a diameter below 100 nm, while nanofiber is defined as fibers with a diameter up to 500 nm. According to these sources, the author of this thesis uses the definition of nanofiber for all the fiber filter media produced and tested in this work ranging from 60-535 nm of diameter.

According to filtration theories, the filtration is a mechanism or device for separating one substance from another (Butler, 1999). The filtration according to the phase of separating substances can be classified to these separations categories: gas-gas, gas-liquid, liquids-liquids, solids-solids, solids-liquids and solid-gases. The last is the most related to the thesis, and it will be analysed in more details.

In the filter media, some fundamental filtration mechanisms can exist theoretically (Hutten, 2007):

- Surface straining. This type of mechanism traps particles larger than the pore size on the top surface of the media. Particles that are smaller than the pore size may pass through the filter. Surface straining is common in the filtration of gases with high particle concentrations. This type of filtration is generally more associated with media that has uniform pore openings. Examples are membranes, screens and mesh fabrics.
- Depth straining. In this case, filter media is relatively thick compared to their pore size. The particles travel along the pore, until they are captured by the narrowest pore point, where the particle is too large to go ahead.
- Depth filtration. This mechanism allows particles to penetrate into the filter media and be captured throughout the depth of the filter media as well as on the surface of the media. In depth filtration compared to the depth straining has mechanisms, which are able to remove a particle from a gas stream, even though the particle may be smaller than the diameter at any point in the pore structure. The mechanisms (aka particle deposition mechanisms), which are responsible for doing this, are discussed later. Depth filtration is most commonly applied to rather lower concentrations of

particles in the upstream region to reduce particle concentrations to very low levels. Depth filters are more associated with the mats of random metallic, polymeric or inorganic materials. These filters are characterized by a broad pore size distribution. Examples are fibrous filters (high-efficiency air filters).

- Cake filtration. In this case, particles are mostly collected on the surface or near the surface of the filter media by building the layer of captured particles. Then, this layer (aka filter cake) acts as the additional filter medium for subsequent filtration. Cake filtration can occur for larger or smaller particles, even when the particles are smaller than the pores, especially when the particle concentration is relatively high. This happens with the bridging of the particles across the entrance to a pore to form a layer (base), upon which the cake begins to grow.

Generally, any real filtration process will probably involve a combination of two or more of the above-mentioned mechanisms (Sutherland and Purchas, 2002). As mentioned above, the depth filtration is more associated with the nonwoven filter media, including nanofiber filter media. Depth filtration is more concerned with other mechanisms for particle deposition. Particles can be captured through straining (sieving), inertial impaction, interception, diffusion and electrostatic attraction mechanisms (Hinds, 1999). Each mechanism has a certain size range, where it is the dominant factor for the filtration of particles. A typical particle capturing efficiency as a function of the aerosol particle diameter that is accounting for the different mechanisms is shown in Fig. 1.1.

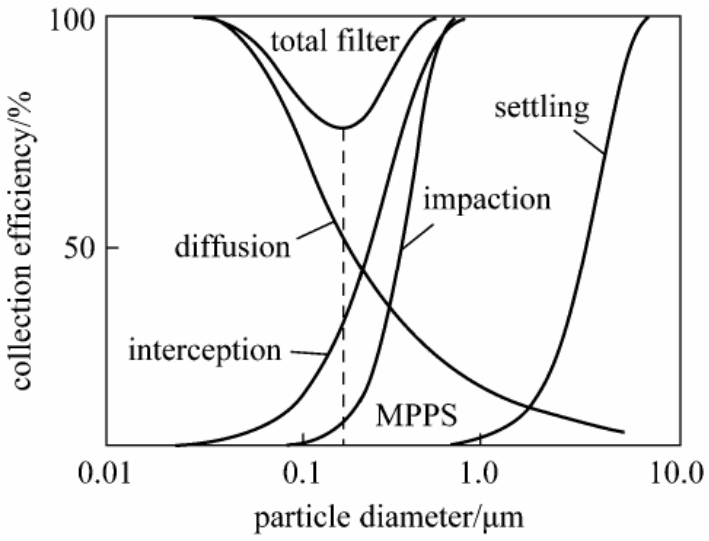

Fig. 1.1. Collection efficiency for individual single-fiber mechanisms and total efficiency (Hinds, 1999)

Sieving (Fig. 1.2.), the most common and the simplest mechanism in filtration, occurs when the particle is too large to fit between the fiber spaces. This principle

spans across the most filter designs, and it is entirely related to the diameter of the particle, media spacing and media density. Sieving is efficient for very large particles; the mechanisms start from ~1μm.

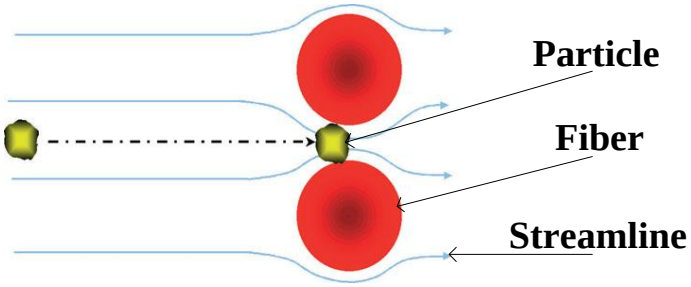

Fig. 1.2. The principle illustration of the sieving filtration mechanism (adapted from Camfil, 2015)

Inertial impaction (Fig. 1.3.) uses a rapid change in the air direction and the principles of inertia to separate heavier particles from the air stream. Particles at a certain velocity tend to remain at that velocity and travel in a continuous direction. This principle is normally applied when there is a high concentration of the course particulate and in many cases as a prefiltration mode to higher efficiency final filters. This mechanism starts working for particles greater than ~0.1 μm and is sufficient for particles greater than ~0.6 μm.

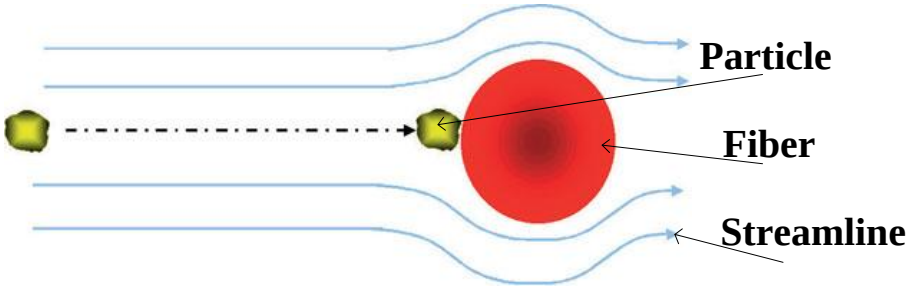

Fig. 1.3. The principle illustration of inertial impaction filtration mechanism (adapted from Camfil, 2015)

In the interception mechanism (Fig. 1.4.), a particle must come within a distance from a fiber of one radius of itself. Thus, the particle makes a contact with the fiber and becomes attached. The interception can be contrasted with the impaction mechanism in that a particle, which is intercepted, is smaller, and its inertia is not strong enough to cause the particle to continue in a straight line. Therefore, it follows the air stream until it comes into contact with a fiber. This mechanism starts to capture particles from ~0.05 μm by diameter and is effective for particles greater than ~0.5 μm.

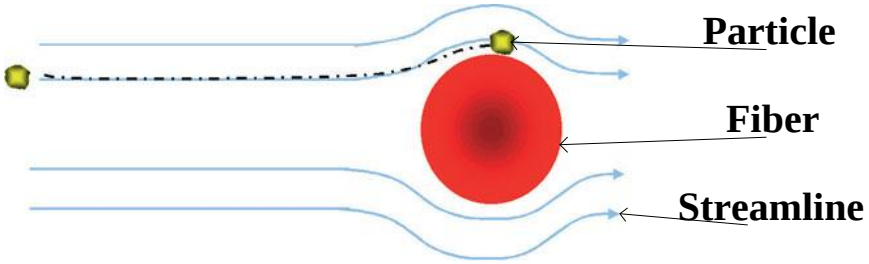

Fig. 1.4. The principle illustration of the interception filtration mechanism (adapted from Camfil, 2015)

Diffusion (Fig. 1.5.) occurs when the random Brownian motion of a particle causes that particle to contact the fiber (Boss and Day, 2009). As a particle vacates an area within the media, by attraction and capture, it creates an area of lower concentration within the media to which another particle diffuses only to be captured. In order to enhance the possibility of this attraction, filters that are employed in this principle must operate at low face velocities, and the filter media must be characterized by the larger volume fraction. The bigger is the retention time of a particle in the "capture zone", the greater is the volume fraction of the fiber media, and the greater are the chances of capture. Diffusion works on the smallest particles (<0.1 μm).

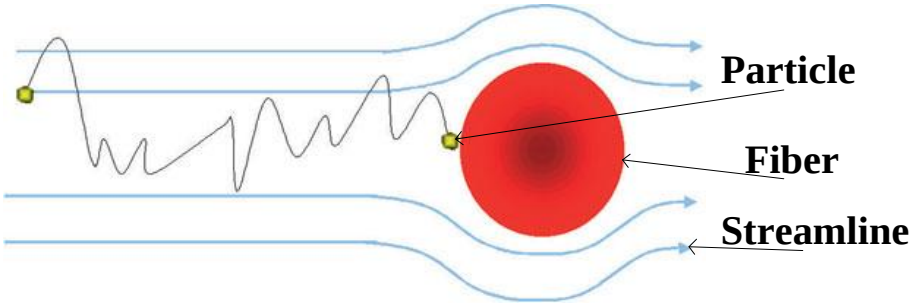

Fig. 1.5. The principle illustration of the diffusion filtration mechanism (adapted from Camfil, 2015)

Electrostatic attraction (Fig. 1.6.) usually stands for filters with a larger fiber diameter, and the electrostatic charges are responsible for increasing filters efficiency of fine particle removal. Filter media with a larger fiber diameter is normally chosen due to the low cost and airflow resistance. However, these filters often lose their electrostatic charge over time, because the particles that are captured on their surface occupy the charged sites thereby neutralizing their electrostatic charge. Electrostatic attraction is obtained by charging the media as a part of the manufacturing process.

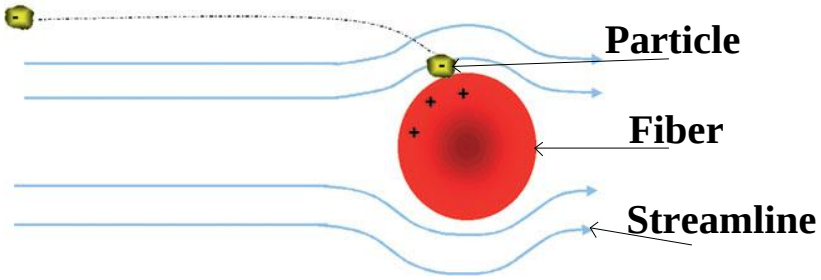

Fig. 1.6. The principle illustration of the electrostatic attraction filtration mechanism (adapted from Camfil, 2015)

As shown in Fig. 1.1., there is a vertical line indicated as the most penetrating particle size (MPPS). MPPS is defined as the one corresponding to the lowest overall filtration efficiency (Chuanfang, 2012). This is a characteristic size of a filter media, typically around ~0.3 μm. Exactly 0.3 μm particles are characterized as MPPS in high efficiency particulate air (HEPA) filters (European Standard EN1822-1). Efficiency ratings in EN1822-1 for HEPA and ultra-low penetration air (ULPA) media are based on MPPS. Particles in the mentioned size range are too large to be effectively pushed around by diffusion and too small to be effectively captured by interception or impaction. For nanofiber filter media, MPPS is in the smaller range of sizes (<<0.3 μm). According to the filtration theories (Hinds, 1999; Lee and Liu, 1980; Leung et al., 2010; Wang et al., 2008a), the decreasing fiber diameter (nanofiber) and increasing packing density of filters transfer the MPPS to the smaller range of sizes.

Practically, the most important particle filtration mechanisms for the nanofiber filter media are diffusion, impaction and inertial interception. This is because sieving and electrostatic attraction mechanisms are not of specific importance for the nanofiber filter media. Sieving mechanism effects very large particles (1-10 μm); therefore, these large particles are collected at a very high efficiency (equal or near 100 %) in most of the filters (including microfibers and nanofibers). While electrostatic attraction must be obtained by additionally charging the media. Charged filter media can be only explored as an additional subject, because according to the European filtration standards, (EN1822) all the new filters must be neutralized before testing in order to remove the electrostatic charge of the filter media. Studies associated with the investigation of nanofiber filters (Hung and Leung, 2011; Yun et al., 2010; Leung et al., 2010; Leung and Hung, 2012; Sambaer et al., 2011; Zhang et al., 2009; Zhang et al., 2010; Wang et al., 2008a; Wang et al., 2013; Wang et al., 2014) that are revealed in the literature review perform the filtration tests with particles smaller than 1 μm, most of them below 0.5 μm to several tens of nm. This as well shows that the mechanisms of interception and diffusion are more significant for the nanofiber filter media than the inertial impaction (Hung and Leung, 2011) (see Fig. 1.1.).

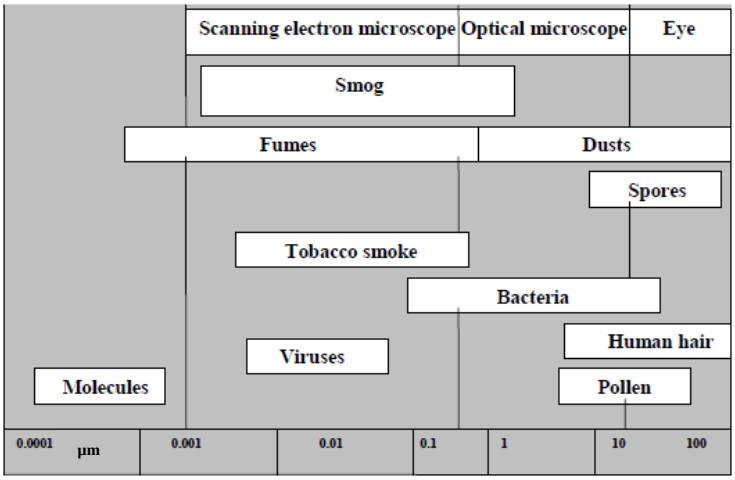

Fig. 1.7. Some contaminants of air and their relative sizes (Hinds, 1999)

Nanofiber filter media is preferable for the filtration of smog, fumes, tobacco smoke and viruses. Most of these contaminants by the sizes (see Fig 1.7.) are in the interaction with diffusion, where nanofiber filter media have the best chances to capture those particles (Hung and Leung, 2011). Moreover, the filtration of large particles such as dusts will be a challenge for the nanofiber filter. Despite the effectiveness of filtration, the clogging problem of media will occur under continuous micron particle loading such dusts (Leung and Hung, 2012).

1.2. Filter media and filtration parameters

The most important parameters associated with air filtration are filtration efficiency and pressure drop (Hinds, 1999). The filtration efficiency is the quantitative measurement, which characterizes the ability to remove particles from the air stream flowing through the media. The opposite parameter for filtration efficiency is penetration. Filtration efficiency (η) relates to the fraction of particles removed from the air gas stream and captured by the media, while the penetration (P) is associated with the fraction of particles, which penetrated through the media. After measurement, these parameters can be calculated by using formulas (Hinds, 1999):

$$\eta = \frac{C_{up} - C_{down}}{C_{up}}; \quad (1)$$

$$P = 1 - \eta; \quad (2)$$

where C_{up} and C_{down} are the aerosol concentrations (mg/m^3) or numbers (particles/cm^3) before (upstream) the filter media and after (downstream) the filter media. Efficiency and penetration can be expressed both as friction (-) and percentage (%).

The review of filtration studies revealed that the efficiency of nanofiber filters as the main filtration indicator is more common among the scientists in Europe

(Podgorski et al., 2006; Sambaer et al., 2011) and Chine (Hung and Leung, 2011; Leung and Hung, 2012; Leung et al., 2010; Mao et al., 2012; Wang et al., 2013; Wang et al., 2014), while penetration is more common in the USA (Zhang et al., 2010; Wang et al., 2008a; Wang et al., 2008b) and Japan (Yun et al., 2010). The author of this work focuses on the parameter of efficiency for further analysis of filter media, both theoretically and practically.

Theoretically, efficiency mostly depends on:

- Physical filter media properties such as fiber packing density (α), filter media thickness (Z), mean fiber diameter (d_f) and the morphology of the media. Reduction in fiber diameter leads to enhanced filtration efficiency together with the increased pressure drop, when α of fiber media is kept constant (Hinds, 1999). α together with fiber diameter are the most important characteristics for the fine particle filtration (Wang et al., 2014). α shows the volume of fiber solids in the medium per unit volume of medium. α is the opposite value of porosity ($\varepsilon = 1 - \alpha$), which is the three-dimensional volume void fraction of the medium (Hutten, 2007). Knowing the Z and basis weight (W) of the filter media, which can be easily measured, the α of the nanofiber could be calculated by using the following empirical formula (Leung et al., 2010):

$$\alpha = \frac{fiber\_volume(m^3)}{total\_media\_volume(m^3)} = \frac{W}{\rho \cdot Z}; \qquad (3)$$

where ρ is the density of the fiber material.

Considering the filters with the same fiber diameter and with different α, the highest filtration efficiency and pressure drop are generated from the nanofiber filter having higher α together with higher W and Z (Hung and Leung, 2011).

The effect of physical properties and morphology on filtration performance of nanofiber filters are discussed and described in subchapter 1.4. in more details.

- Filtering particle size and morphology. As mentioned before, the investigations of nanofiber filtration are focused on the particles below 1 µm. Nevertheless, the size range below 1 µm has its unique MPPS range, in which interactions of diffusion and interception has weakest forces for capturing particles. The range of MPPS strongly depends on the fiber diameter: the decreasing fiber diameter transfers MPPS to the smaller range of size (Hinds, 1999). The role of morphology is known from the literature as well. Wang (2013) performs filtration experiments with different morphology of nanoparticles. He has found that the elongated particles, such as carbon nanotubes and nanoparticles agglomerates, have higher filtration efficiency than sphere particles with the same mobility. The main reason is that the elongated particles by the geometric size are bigger than the spheres, thus leading to the higher filtration efficiency when the interception interaction is important. Grinshpun et al., (2014) as well investigated the effects of particle morphology on filtration efficiency. The results showed that the particles from combustion processes have lower filtration efficiency compared to NaCl particles. The biggest difference was

observed between the plastic and NaCl particles, which is the most common challenging particles of filters between scientists and engineers working in the filtration industry. The authors of the mentioned study discussed that the differences in efficiency can be attributed to an interaction between the particles and filter fibers (particle morphology, charges, surface properties etc.).

- Air gas conditions. This includes filtering air temperature, pressure and flow rate. According to filtration standard (EN1822, 2009), the filtration tests of new filter media must be performed under standard air conditions, T=293 K, p= 760 mm Hg. Therefore, the consideration of the effects of the temperature and pressure on filtration performances can be neglected. In this case, the most important indicator is the flow rate, which is defined as the volume of the air passed through the unit of surface area of filter media. The flow rate is known as well as the face velocity expressed in terms of cm/s or m/s. The minimum face velocity for testing HEPA filters must be 5.3 cm/s, according to the filtration standard (EN1822, 2009) requirements. Moreover, face velocity can be several times higher: it depends on the test target. Leung et al., (2010) found that with increasing face velocity from 5 cm/s to 10 cm/s, the filtration efficiency was reduced, especially for the small particles (<100 nm), while for particles larger than 300 nm, the filtration efficiency remained nearly unchanged. The authors argued that the doubling of face velocity is similar to the reducing by a factor of half retention time of particles in filter media. Therefore, the chance for small particles to collide on fibers through diffusion interaction is lower. Wang (2013) obtained similar results, when he found that with increasing filtration velocity (from 2 cm/s to 10 cm/s and then to 20 cm/s), the filtration efficiency for particles below 200-300 nm reduces because of the weaker diffusion interaction. The trend is reversed for particles > 300 nm, because the inertial effect is more important, which increases with the velocity (Wang, 2013). The results of that study suggest that the lower filtration velocity should be used to separate larger particles, and the higher filtration velocity should be used to separate smaller particles. The optimum filtration velocity depends on the targeted particle size and the filter parameters. The author concluded that the optimum filtration velocity depends on the targeted particle size and filter parameters.

Theoretically, the starting point in filtration efficiency is to consider the collection of particles by single fiber. The single fiber efficiency, according to Baron and Willeke (2001), is defined as the ratio of the number of particles striking the fiber to the number which would strike if the streamlines were not diverted around the fiber. The overall or total filtration efficiency of a clean (unused) fiber filter media can be analytically calculated by using formula (Brown, 1993):

$$\eta = 1 - \exp\left(\frac{-4\alpha\eta_f Z}{\pi(1-\alpha)d_f}\right); \qquad (4)$$

where η_f stand for single fiber efficiency, and d_f is the average fiber diameter. As mentioned in subchapter 1.1., for nanofiber filters, the mechanisms of interception and diffusion are more significant than the inertial impaction (Hung and Leung, 2011), then:

$$\eta_f = \eta_D + \eta_R; \tag{5}$$

where η_D and η_R are the single fiber efficiencies due to the diffusion and interception. η_R is expressed as (Brown, 1993):

$$\eta_R = \frac{(1+R)^{-1} - (1+R) + 2(1+1.996Kn)(1+R)\ln(1+R)}{2(-0.75 - 0.5\ln\alpha) + 1.996Kn(-0.5 - \ln\alpha)}; \tag{6}$$

where R is the interception ratio and is equal to the ratio between particle diameter and fiber diameter - d_p/d_f ; Kn is Knudsen number equal to:

$$Kn = \frac{2\lambda}{d_f}; \tag{7}$$

where λ is the mean free path of air gas molecules (molecules under standard conditions is 65.3 nm).

The expression of the efficiency due to the diffusion is (Brown, 1993):

$$\eta_D = 2.27 Ku^{-\frac{1}{3}} Pe^{-\frac{2}{3}} (1 + 0.62 Kn Pe^{\frac{1}{3}} Ku^{-\frac{1}{3}}); \tag{8}$$

where Ku is Kuwabara hydrodynamic factor; Pe is Peclet number; both are expressed in equations (9) and (10) accordingly:

$$Ku = -\frac{1}{2}\ln\alpha - \frac{3}{4} + \alpha - \frac{\alpha^2}{4}; \tag{9}$$

$$Pe = \frac{d_f U_0}{D}; \tag{10}$$

where U_0 is the face velocity, and D is the diffusion coefficient expressed as:

$$D = \frac{k_B T C_S}{3\pi\mu d_p}; \tag{11}$$

where k_B is the Boltzmann constant, T – absolute temperature, μ - air dynamic viscosity, d_p – particle diameter, and C_s is the Cunningham slip correction factor, which, according to Rader (1990), is:

$$C_s = 1 + Kn\left[1.207 + 0.44\exp(-0.78/Kn)\right]. \tag{12}$$

From the expressions given above, it can be seen that the single fiber efficiency due to the interception mostly depends on the interception ratio that represents the ratio between filtering particle size and mean fiber diameter of filter media; the α and the Kn number has an influence on interception as well. Whereas, single fiber efficiency due to the diffusion depends on three dimensionless

parameters: the *Kn* number, the *Pe* number that represents the relative strength between the interception and diffusion interactions and depends on the face velocity itself and the α.

Kn number is very important for the nanofiber filter (Hosseini and Tafreshi, 2010; Sambaer et al., 2011). *Kn* number is defined as the ratio of the molecular mean free path length to a representative fiber diameter, and it classifies the regime of airflow over fibers. The air slip flow regime ($0.001<Kn<0.25$), the continuum flow regime ($Kn<0.001$), transition regime ($0.25<Kn<10$) and molecular ($Kn>10$) flow regime can occur inside the fiber medium. The nanofiber media filter, which has an average fiber diameter, which is approximately higher than 500 nm, belong to the slip flow regime, and the nanofiber filters with diameter lower than 500 nm stands for transition regime. Some scientists (Kirsch and Stechkina, 1978; Hung and Leung, 2011; Wang et al., 2008a) stated that the results when using the slip flow condition may be applied to $Kn\sim1$ (what corresponds to fiber diameter of ~130 nm), named as a large slip by Hung and Leung (2011). Slip flow regime affects the nanofiber filtration in two important ways (Brown, 1993). Firstly, for airflow through nanofiber medium and microfiber medium of equal fiber lengths, the pressure drop through the nanofiber medium will be less. This is because fewer molecules exchange the momentum with the fiber; there is less air drag on fiber. Secondly, the single fiber efficiency due to the diffusion is enhanced of small particles on nanofibers. The streamlines of air gas flow pass much closer to the surface of the nanofiber compared to the microfiber. This provides the improvement of interception interaction of small particles in air gas stream, because more of these particles pass close enough to collide with the nanofiber compared to the microfiber.

Practically, the pressure drop is expressed as the difference between the static pressures measured upstream and downstream of the filter media. The pressure drop based on Kuwabara flow with slip effect is defined analytically (Brown, 1993):

$$\Delta P = \frac{4\mu\alpha Z U_0 (1+1.996Kn)}{0.25 d_f^2 (-0.5\ln\alpha - 0.75 + \alpha - \frac{\alpha^2}{4} + 1.996Kn(-0.5\ln\alpha - 0.25 + \frac{\alpha}{4}))}; \quad (13)$$

It can be seen that the pressure drop mostly depends on α, Z, U_0 and *Kn* number as mentioned above in the discussion of efficiency dependencies. According to Darcy law, there is a linear relationship between the pressure drop and U_0. The steepness of linear relationship depends on the Z of filter and fiber diameter. Hung and Leung (2011) found that the nanofiber filter with larger Z has a higher steepness of linear relationship (pressure drop against U_0) than the nanofiber with moderate or lower Z. If the Z of nanofiber filters will be the same, the higher steepness of linear relationship will have nanofiber filter with smaller fiber diameter.

Finally, for the evaluation of overall performance of the filter, a useful criterion named as the quality factor (*QF*) is used. *QF* reflects the filter quality and is intended to describe the ratio between the filtration efficiency and the pressure drop. According to Hung and Leung (2011), *QF* is regarded as the benefit to cost ratio of a filter, where benefit stand for filtration efficiency, and cost refers to the

pressure drop. Simply, *QF* is a filter quality factor and is expressed by the formula (Hinds, 1999):

$$QF = -\frac{\ln(1-\eta)}{\Delta P}. \qquad (14)$$

According to Wang et al., (2008a), the desirable filters give high efficiency and low pressure drop; thus, the larger values of *QF* indicate better quality of the filters. Nanofiber filter media with high efficiency (>90 %) and rather high-pressure drop (>100 Pa) have a lower value of *QF* in comparison to the nanofiber filter with rather low efficiency together with the low pressure drop. This can be explained by the fact that electrospun nanofiber mat elevates pressure drop without significantly improving the efficiency, which lowers *QF* and leads to worse performance (Leung et al., 2010). The significance is more noticeable when the nanofiber filter media have higher basis weight or thickness. Moreover, the nanofiber filters (with lower basis weight or thickness), which have high *QF* (as a result of the combination of low filtration efficiency and low-pressure drop) have no practical applications notwithstanding that its performance by *QF* is high.

1.3. The electrospinning and properties of nanofiber media

1.3.1 The principle of electrospinning

The main techniques for nanofiber based material production are multicomponent fiber spinning, centrifugal spinning, modular meltblowing, pressurised gyration process, solvent-free (melt) electrospinning and electrospinning (Agarwal et al., 2013; Chang et al., 2014; Hassan et al., 2013; Lu et al., 2013; Mahalingam and Edirisinghe, 2013; Nagy et al., 2013; Ward, 2005). The latter is the most popular technique due to its simplicity and inexpensive instrumental setup (Bhardwaj and Kundu, 2010; Pham et al., 2006; Wang et al., 2012). There are some varieties of electrospinning designs, but typically, the basic electrospinning equipment consist of a high voltage power supply, a syringe pump with a flat tip needle and a conducting collector (Rogina, 2014). This type of electrospinning is known as the needle electrospinning as well (Li et al., 2014; Vahtrus et al., 2015). Electrospinning is an electro-hydrodynamic process, which begins with the preparation of polymer solution. Then, the syringe of the pump is filled by the polymer solution, which is used as spinning material. With increasing voltage, the polymer solution droplet at the needle tip is electrified by the electrostatic forces, which are formed between the needle and the conducting collector. When the high voltage overcomes the solution surface tension, the droplet is deformed into a cone shape named Taylor cone (Li and Xia, 2004; Taylor, 1969). This induces the ejection of solution droplet to form a charged jet. This jet is eventually stretched into long filaments, which are travelling to the collector. In this travel, solvent evaporation leads to the solidification of the filaments into fibers (Niu and Lin, 2012). Electrospun fibers are collected on the collector as randomly oriented or parallel-aligned mats (Beachley and Wen, 2009).

There are two different types of needle electrospinning setup, vertical and horizontal (Bhardwaj and Kundu, 2010). The typical set up of electrospinning devices in vertical and horizontal position is shown in Fig. 1.8.a and 1.8.b, respectively.

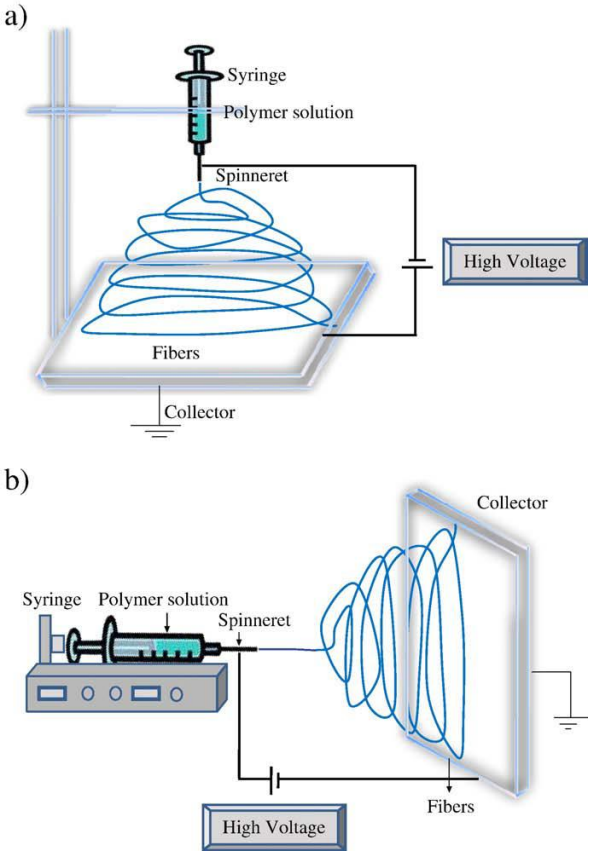

Fig. 1.8. The principle diagram of the vertical electrospinning (a) and the horizontal electrospinning (b) (Bhardwaj and Kundu, 2010)

The main parameters, which affect the fiber diameter and morphology of electrospun fibers, are the polymer solution parameters, processing (electrospinning) conditions and ambient conditions (Teo and Ramakrishna, 2006). The most import factor in solution parameters is a polymer solution concentration in the chosen solvent or solvent mixture for dissolving that polymer (Greish et al., 2010; Li et al., 2013; Zander, 2013; Zheng et al., 2012). Solution concentration, which is strongly proportional to the viscosity of the solution, has significant influence on the fiber diameter (Bhardwaj and Kundu, 2010). It has been observed that in low polymer concentrations, only the beads are formed on the collectors, whereas the increase in polymer concentration leads to the beaded fiber production, and finally, in the following increase, the fibers are formed. The increasing polymer solution concentration leads to the thicker fiber deposition in electrospinning. Practically, the formation of fibers in electrospinning has a broad polymer solution concentrations

range, but there is the upper polymer concentration after which the electrospinning process is impossible. After that, the upper concentration, the entanglements of the polymer chains are restricted, and the deposition of fibers is repressed. At this concentration point, the electric field is not able to overcome the interactions between the polymer chains, because they are very strong. In lower polymer solution concentrations, which are responsible for the formation of beaded fibers or beads, there are not enough entanglements between the polymer chains. As a result, the fibers are not formed, because the interaction, which keeps the polymer chains together, is too weak. Zheng et al., (2012) have investigated polystyrene (PS) in order to study the formation of fibers from different solvents (tetrahydrofuran (THF) and *N, N*-dimethylformamide (DMF) and concentrations (5-30 % (w/v)). They found that the beads of average size of 10 μm were produced from 5 % (w/v) concentration of PS in THF, whereas bowl-like beads with size of 10-20 μm occurred from 10 % PS/THF solution. When the concentration increased to 20 %, the beaded fiber (bead size ranging from 10 to 30 μm, and the fibers thickness of 1-2 μm and the width of 2-5 μm) structure occurred. Finally, only the ribbon like fibers with the thickness of 1-2 μm and the width of 5-10 μm were produced from 30 % PS/THF solution. Slightly different results were observed by using the PS/DMF solution, which is not volatile as THF. Electrospinning with this solution was able to form the beaded fibers from 10 % concentration with fiber diameter of 100-300 nm and the size of beads 4-10 μm. As the concentration increased to 20 % PS/DMF, mostly the fibers with the diameter of 300-900 nm were composed, whereas, when the concentration was increased to 30 %, the uniform fibers with the diameter around 1.5-2.5 μm were produced. The similar tendency was observed with other polymers from the other studies: the increase in cellulose acetate (CA) concentration from 10 to 20 wt% has influenced the increase in fiber diameter in a range of 200-800 nm (Greish et al., 2010); the increase in the concentration of PEO solution from 8 to 10 wt% leads to the increase in the fiber diameter from 85 to 115 nm (Li et al., 2013); the fiber diameter has increased from 553 to 1071 nm for 15-25 wt% polyamide 6 solutions (Chowdhury and Stylios, 2010).

Ambient parameters such as humidity and temperature can influence the process of electrospinning as well. By increasing the temperature of polymer solution, the viscosity of the polymer solution decreases, whereas the solution conductivity increases. All these trends lead to the deposition of smaller fibers (Bhardwaj and Kundu, 2010). Zheng et al., (2012) have observed that at low humidity (<10 %), the electrospun fibers have smooth surface, while at high humidity (>50 %), the nanopores on the surface of the fibers and network structure inside the fibers have occurred. However, the most of the researchers use of higher/lower temperature and humidity for special purpose and investigations. Normally, the temperature and humidity are kept at ~18-25 °C and ~30-40 % in most of the studies.

Fundamentally, as mentioned above, the electrospinning process is influenced by the electrospinning conditions, which are described in more details:

- Applied voltage. Direct current (DC) voltage supply is used in electrospinning in most cases; however, it is as well possible to apply

alternating current (AC) potential (Andrady, 2008). Usually, it is enough to use a DC voltage in the range of several tens of kiloVates to produce fibers in the electrospinning. The voltage expressed in kV is a crucial parameter in electrospinning. In every research associated with the experiment of electrospinning, it is indicated, used or applied voltage in kV (Bhardwaj and Kundu, 2010). Sometimes, the term electric field expressed in kV/cm (applied voltage over spinning distance (as well known as the tip-to-collector distance) is used (Yang et al., 2015; Zhang et al, 2010). The applied voltage affects the fiber diameter, but the influence of each case is very individual and depends on various other polymer solutions and electrospinning parameters. It has been observed that the increasing voltage from 10 to 20 kV in PS electrospinning cause the fiber diameter reduction from 223 to 173 nm (Subramanian et al., 2010). As the voltage increases, the electrostatic forces acting on the solution droplet increase as well, which provides an additional force to overcome the viscoelastic and surface tension forces exerted by the solution (Subramanian et al., 2010). This induces the increase of the elongation of the polymer chains in the jet and produces smaller fibers. The similar tendency (when the voltage is increased, fiber diameter decreases) was reported by Chowdhury and Stylios (2010); Liu and Wang (2013); Rodoplu and Mutlu (2012). However, the higher voltage may cause a higher mass flow resulting in thicker fibers. Jacobs et al., (2010) as well investigated the influence of the applied voltage on the morphology and diameter of electrospun poly ethylene oxide (PEO) fibers. They found that the electrospinning at 5 kV produced irregular beaded fibers instead of the fiber formation. As the voltage increased from 10 to 17.5 kV, the thicker fibers with fewer beads were produced. Further increasing the applied voltage to 20 kV was responsible for the smaller fiber formation, whereas the ‘‘bead-on-string’’ morphology with the smallest fibers was observed at 25 kV. Typically, it is enough to apply 10-30 kV for fiber production in the needle electrospinning depending on the certain polymer or its solution and research targets.

- Feed rate. The feed rate of the polymer solution in the electrospinning is ensured by a syringe pump with a needle or just capillary tube. Basically, in vertical electrospinning systems, more droplets on the collectors are produced compared to the horizontal electrospinning devices (Bhardwaj and Kundu, 2010). Accordingly, the syringe pump is responsible for stable and continuous feeding of polymer. The needle of the syringe is connected to one of the electrodes from the DC power supply. The feed rate of the solution from the syringe is an important parameter because it influences the jet velocity and the material transfer rate (Bhardwaj and Kundu, 2010). It has been shown that different feed rates are used for productions of fibers from various types of polymer. Even in the case of a certain polymer, but dissolved in different mixture of solvents, the feed rate can be different. For example, several studies investigated the electrospinning of cellulose acetate (CA) fibers from the different solutions: Greish et al., (2010) and

Tian et al., (2011) used 4 mL/h of feed rate (for solution containing acetone and N,N-dimethylacetamide (DMAc) solvents at a volume ratio of 2:1); whereas Han et al., (2008) used 3 mL/h of feed rate (for the solution containing acetic acid/water at a ratio 75:25 by weight), and Celebioglu and Uyar (2011) used 1 mL/h of feed rate (for the solution containing dichloromethane (DCM)/acetone in various proportions). Thus, the feed rate is a unique for different polymers and their solvent systems, but every polymer system has the optimal range of feed rate, which ensures formation of uniform fibers. Thus, very low and high feed rates are not describable. According to Kattamuri and Sung (2004), at very low feed rates, it is difficult to maintain a continuous jet, while at very high feed rates, the polymer jet is ejected too fast, and as a result, the fibers with regular structure are not generated. Zargham et al., (2012) obtained similar results when they found that very low feed rates (0.1 mL/h) lead to the formation of small droplets at the needle in the electrospinning of polyamide 6 (PA 6), while at high feed rates (1 mL/h and 1.5 mL/h), a large semi-spherical droplets were formed at the needle, and as a result, the unspun droplets were formed on the collector. The authors concluded that the feed rate of 0.5 mL/h, which was proportional to the electrospinning speed, was responsible for the formation of a stable Taylor cone, less instabilities and the narrowest fiber diameter distribution with uniform fiber morphology, whereas the largest fiber diameters with irregular (with defects such as branched or splitted fibers) fiber morphology were obtained at high flow rates.

- Collector. The nature of the collector significantly affects the morphology of electrospun fibers (Kumbar et al., 2008). In the most cases, the collector is a conductor grounded by collecting plate (metallic screen, wire mesh, plate, aluminium foil or rotating wheel), which utilizes electric field (Bhardwaj and Kundu, 2010; Li and Wang, 2013). The morphology of randomly oriented fiber is generated by using simple static collecting surface (Beachley and Wen, 2009), because fibers on such simple collector are deposited as a random mass due to the bending instability of charged jet (Bhardwaj and Kundu, 2010). The aligned fibers are formed as a result of the presence of a rotating collector (Beachley and Wen, 2009). Moreover, a rotating collector gives additional time for solvent evaporation. The higher rotation speed of rotating collector, the greater alignment of fibers with narrower distribution of fiber diameter are achieved. Very aligned fibers are produced by using rotation speed over one thousand rpm (Liu et al., 2013; Mathew et al., 2006). Everyone can consider that the morphology of random deposited fibers is more attractive for the filtration application due the high porosity (Gupta et al., 2009), but uniformity of fiber layer in this system is worse than in the rotating system.
- Electrospinning distance. This comprehends to the distance of the electric field between the needle tip of the syringe and the collector, which is as well-known as a working distance, spinning distance, collecting distance or

tip to collector distance (Liu et al., 2013; Zander, 2013). The latter definition is used commonly. The tip to collector distance has an influence on fiber diameter and morphology, but it is not as significant as other parameters discussed above (Bhardwaj and Kundu, 2010). However, the increasing tip to collector distance may increase the evaporation of solvent, leading to smaller fibers keeping the voltage as a constant (Heikkila and Harlin, 2008). Moreover, when the distance is too large, no fibers are deposited. Decreasing the distance between the tip and collector (increasing the electric field strength) leads to the deposition of wetter fibers, because the jet has not enough time for the solvent evaporation. As a result, larger fibers or, in some cases, the beaded fibers are formed (Mazoochi et al., 2012). For example, Chowdhury and Stylios (2010) demonstrated that the electrospinning of PA 6 at the tip to collector distances of 5, 8 and 11 cm leads to the formation of fibers in diameters of 1257, 1002 and 936 nm, respectively. However, it has been reported that the increase in the distance leads to the increase of fiber diameter instead due to the weakened field strength (Bosworth and Downes, 2012). A certain polymer solution has its optimal electrospinning parameters including the tip to collector distance, which has a specific range to be able to produce fibers. Typically, the tip to collector distance varies between ~10 and ~20 cm.

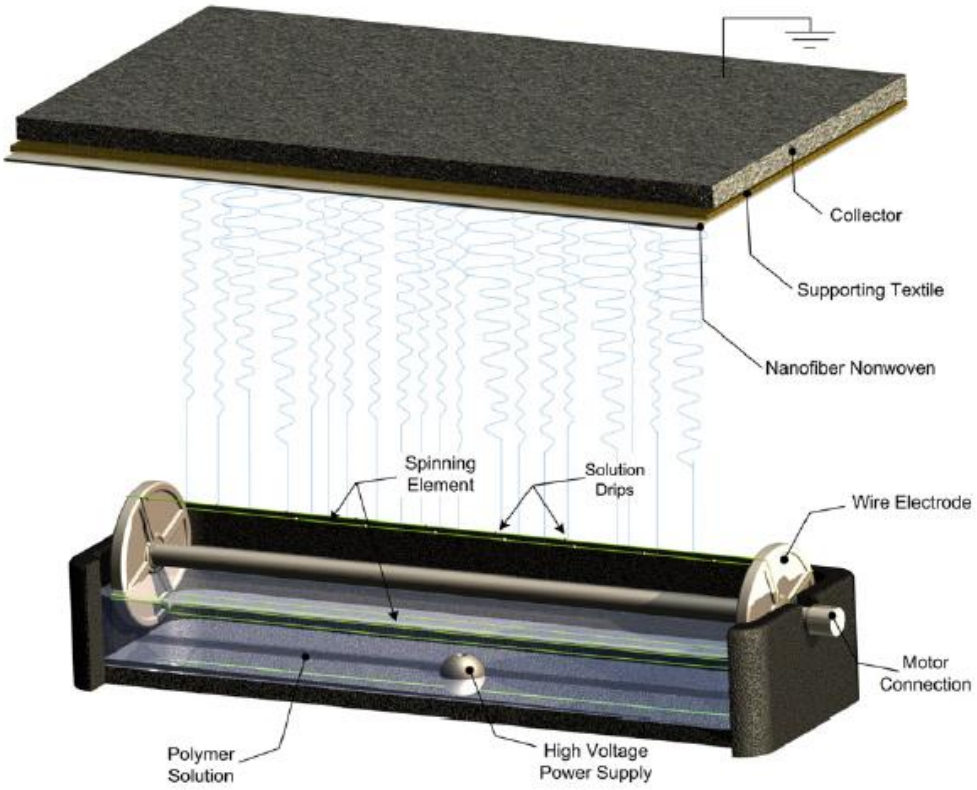

Fig. 1.9. The principle diagram of needleless electrospinning (Sambaer et al., 2011)

Typically, the needle electrospinning presented above has a smaller fiber production rate together with the low consumption of materials, which is more suitable for laboratory scale experiments (Wang et al., 2012). For industrial applications, for higher fibers production rates, from open solution surface, the needleless (as well known as the roller) electrospinning (see Fig. 1.9.) method is applied (Forward and Rutledge, 2012; Jirsak et al., 2010). Without higher production rates, which depend on the fibers generator (cylinder with rounded rim, disc and ball) shape and dimension, this technique is as well characterized by the continuous mass production and ease of upkeep (Kostakova et al., 2009; Niu et al., 2012). Several tens to hundred jets are generated from a free surface of polymer solution held in bath in needleless electrospinning instead of jet generation at the needle tip in needle electrospinning (Li et al., 2014). Thus, syringes and needles are not needed there. However, this method has disadvantages too: the high consumption of materials for experimenting, the diameter of the produced electrospun fiber is thicker, and the fibers have wider distribution (Sasithorn and Martinová, 2014). The applied higher voltage and/or the smaller electrospinning distances are required to overcome the polymer solution surface tension and additional gravity forces, because the jets in roller electrospinning must flight from the bottom to the top. As a result, the higher concentrations of the polymer solution are difficult to spin, whereas in needle, electrospinning is impossible. However, the electrospinnable polymer concentration depends on the certain polymer and its origin (Petrik and Maly, 2009). The principal differences between two electrospinning methods are summarized in Table 1.1., according to Wang et al., (2012); Sasithorn and Martinová, (2014); Niu et al., (2012); Zhou et al., (2010); Holopainen et al., (2014).

Several researchers as well proposed the modified setup of the needle electrospinning to enhance the productivity and covering an area (Ding et al., 2004; Varabhas et al., 2008, Zhang et al., 2011; Zhou et al., 2009). This includes the increase of the number of needles, i.e., jets (from 2 to 16) by a technique known as the multi-needle. This technique can be divided into multi-jets from single needle; multi-jets from multiple needles (Nayak et al., 2011). Despite higher production rate, this technique had problems as well. Multi-jets from single needle tended to clog, because it is quite difficult to ensure the distribution of the flow from the syringe into the different needles. Hence, a regular cleaning system must be ensured for each needle during the fiber production (Niu and Lin, 2012). Multi-jets from multiple needles must be separated by a certain distance (1-3.2 cm), because each of the jet interacts with the neighbouring jets, repelling each other because of the same polarity electric charge (Varesano et al., 2009). As a result, the separate covered areas are deposited on the collector. The Moving support, which has fixed syringes with needles, along the collector is used to combine the separate deposition areas (Ding et al., 2004; Sun et al., 2010). The usage of the multiple needle technique allows the formation of blends mats that are consisted of two or more polymers characterized by different properties as well.

Table 1.1. The principal differences between needle and needleless electrospinning techniques

Technique	Needle (see Fig.1.8.)	Needleless* (see Fig. 1.9.)
Main differences	The polymer jet is travelling in horizontal or vertical (from top to bottom) direction from needle to collector	The polymer jets are formed from a widely open liquid surface, and the directory of travelling are from bottom to top
	The fiber diameter is smaller	The fiber diameter is thicker
	Small fiber production rate (up to 0.41 g/h for silk fibers, 0.3 g/h for polyvinyl alcohol (PVA) fibers)	High fiber production rate (up to 2.05 g/h for silk fibers, 3.1-8.6 g/h for PVA fibers, ~9 g/h for PAN fibers)
	The low consumption of materials for experimenting (min 10 mL solution)	The high consumption of materials for experimenting (min 200 mL solution)*
	The electrospinning duration is the function of the thickness of fiber media	The thickness of fiber media is controlled by the speed of substrate (0.13 m/min-1.57 m/min)*
	Usually, lower spinnable voltage (10-30 kV) is enough	Higher spinnable voltage (30-80 kV)
	Spinning distance of the unit is longer	Spinning distance of the unit is shorter
	Wider spinnable concentration range of solutions	Narrower spinnable concentration range of solutions

* NanoSpider (NS LAB 500). More information is available from www.elmarco.com

1.3.2. Polymeric materials suitable for the production of nanofiber filtration media

At present, more than 200 different kinds of polymers have been electrospun (Bhardwaj and Kundu, 2010). They can be divided in synthetic polymers and natural polymers. The latter normally offer better biocompatibility and lower immunogenicity, compared to the synthetic polymers, which have other advantages over the natural polymers, such as necessary mechanical properties and desired degradation rate (Bhardwaj and Kundu, 2010; Hakkarainen et al., 2002). The electrospinning, apart from the neat single polymer system, is as well possible with copolymers, polymer blends, composites, single polymer systems containing additives and even with inorganic materials (by the combination of electrospinning and sol–gel methods with calcination (Mao et al., 2012; Heikkila and Harlin, 2009; Munj et al., 2014; Shahi et al., 2011; Thammawong et al., 2014).

The used polymeric materials for production (includes needle and needleless electrospinning techniques) of nanofiber media are summarized in Table 1.2. Together with the list of the used polymers, additional information of solution concentrations and electrospinning conditions are presented. The latter information will be used as well in subchapter 1.3.3. as the initial and additional information for

evaluation of nanofiber media properties and filtration parameters from the same studies.

Most of electrospun polymers fiber medium is rather soft; therefore, the rigid substrate (supporting structure) with sufficient mechanical strength is used, on which the fibers are deposited (Leung et al., 2010). The substrate was a microfiber medium (Hung and Leung, 2011; Leung et al., 2010; Leung and Hung, 2012), nonwoven substrate (Wang et al., 2014), filter paper (Wang et al., 2013), polyester fabric (Sambaer et al., 2011), activated carbon fiber (Zhang et al., 2010), polypropylene substrate (Li et al., 2012; Shahrabi et al., 2014). The authors of the mentioned studies stated that the substrate must have negligible filtration efficiency and pressure drop compared to the nanofiber media.

Over the last 6 years (time period of 2009-2015), most of the studies which deal with the filtration performance of nanofiber media filter use thermoplastic polymers. The common electrospinning conditions were applied for these polymers with the exception of several trends (as discussed in subchapter 1.3.3.): lower spinnable voltage < 30 kV in needle electrospinning, higher spinnable voltage > 70 kV in needleless electrospinning; different polymers had a different feed rate in needle electrospinning: PA≤0.3 mL/h, PAN≥1 mL/h etc. However, in the most of studies, the arguments for choosing a certain polymer for filtration applications are lacking. Therefore, the author of the thesis performs an additional review of the characteristics of used polymeric materials as fiber media. Despite the main characteristics, in order to capture the aerosol particles from the air, the nanofiber media filters must have a rich mechanical and antiwear properties as well (Wang et al., 2013)

Some polymers have unsuitable properties to be used as materials for filter media. For example, polyethylene oxide (PEO) and polyvinyl alcohol (PVA) are water-soluble polymers (Chen et al., 2015; Nagy et al., 2010). Fiber mats from PS are brittle; therefore, they have weak mechanical properties (Feng and Shen, 2010). Electrospun PEO fibers are not as brittle as PS, but the mechanical properties presented by Bianco et al., (2013) are rather poor in terms of tensile modulus (4±2 MPa), ultimate tensile stress (0.20±0.03 MPa) and strain at failure (15±4 %). Instead of using pristine PEO fibers, it was proposed to use PEO blends with poly(3-hydroxybutyrate-co-3-hydroxyvalerate) (PHBV) to enhance the mechanical properties, because PHBV electrospun fibers has tensile modulus of 80±15 MPa (Bianco et al., 2013). PVA differently than PEO has higher elasticity and hydrophilic characteristics. Thus, the mechanical properties of electrospun are higher: tensile modulus up to 60 MPa (Li et al., 2014), tensile strength in the range of 4 -20 MPa (Jeung et al., 2007; Li et al., 2010; Li et al., 2014). Some researchers have found that the mechanical properties of PVA fibers can be reinforced several times by inserting filamentous nanocellulose fibrils or multi-walled carbon nanotubes into PVA forming composites (Jeung et al., 2007, Li et al., 2014). Nevertheless, despite that, both PEO and PVA belong to the polymer group, which represents “green electrospinning” from aqueous solution avoiding harmful organic solvents (Chen et al., 2015); the application of both polymers in filtration field are rather limited due to their solubility in water.

Table 1.2. Electrospun nanofiber for air filtration applications I: the used polymeric materials, electrospinning conditions

Study	Polymers; solution concentrations	Electrospinning parameters
Zhang et al., 2009	PA 6 (MW: 63,000 g/mol), 10, 12, 15 wt% in formic acid	Voltage – 15 kV, Distance – 15 cm, Feed rate – 0.06 mL/h, Collector - stationary
Zhang et al., 2010	PAN (MW: 150,000), 6 % w/v in DMF	Voltage – 15 kV, Distance – 20 cm, Feed rate – 1 mL/h, Collector – stationary, Collection time – 5 and 15 min
Yun et al., 2010	PAN (MW: 150kDa) Polymethylmethaacrylate (PMMA) (MW: 90 kDa), 10 wt% and 25 wt% in DMF	Voltage – 13 (for PAN) and 9 (for PMMA) kV, Distance – 15 cm, Feed rate – 2.4 mL/h, Collector – rotating cylinder, Collection time – 20 and 40 min
Leung et al., 2010	PEO (MW: 600,000 g/mol), 5 % wt% in isopropyl alcohol and water (8/2 v/v).	Voltage – 20 kV, Distance – 14 cm, Feed rate – 0.36 mL/h, Collector – rotating cylinder
Hung and Leung, 2011	PA 6; 12, 20 and 24 wt% in formic acid	*Needleless electrospinning: Voltage – 80 kV, Distance – 19 cm, Collector – moving substrate*
Sambaer et al., 2011	Polyurethane (PU), 13 wt% in DMF	*Needleless electrospinning: Voltage – 75 kV, Distance – 18 cm, Collector – moving substrate 0.16 m/min*
Li et al., 2012	PVA (MW: ~121,000), 6-10 wt% in water	*Needleless electrospinning: Voltage – 70 kV, Distance – 12 cm, Collector – moving substrate*
Wang et al., 2013	PVC/PU (8/2 w/w), 8 wt% in tetrahydrofurane/DMF (1/9 w/w)	Voltage – 28 kV, Distance – 20 cm, Feed rate – 2.5 mL/h, Collector – rotating cylinder, Collection time – 180 min
Wang et al., 2014	PAN containing 8 wt% nanoparticles of SiO_2, 12 wt% in DMF	Voltage – 30 kV, Distance – 15 cm, Feed rate – 1.5 mL/h, Collector – rotating cylinder
Shahrabi et al., 2014	PA 66, concentration is not specified, solvent formic acid	Voltage – 25 kV, Distance – 15 cm, Feed rate – 0.3 mL/h, Collection time – 30, 60 and 90 min

PA has a superior fiber forming ability in electrospinning; it is biodegradable and biocompatible synthetic polymer with good mechanical properties which are further enhanced by the hydrogen bonds (Baraka et al., 2009; Heikilla et al., 2008; Pant et al., 2010; Pant et al., 2011; Pant et al., 2012). PA 6 was one of the first polymers to be electrospun, and the potential usage of PA fibers nowadays is not decreasing due to its attractive diameter and properties (Bagheri et al., 2012; Guerrini et al., 2009; Nirmala et al., 2011; Schueren et al., 2010). PA can yield very small fiber diameter < 150nm with narrow diameter distribution, especially PA 6/6.

The mechanical properties of PA depend on the amorphous structure and crystallinity (Lin et al., 2012). In the amorphous region, in the absence of moisture, PA chains are cross-linked to form networks by intra-chain and interchain hydrogen bonds. The absorption of moisture breaks the webs. Nevertheless, even moisture PA fibers have good mechanical properties, such as high tensile modulus in the range of 699-5000 MPa (Bazbouz and Stylios, 2010; Lin et al., 2012; Lingaiah et al., 2008), high-tensile strength 120-304 MPa (Bazbouz and Stylios, 2010; Marsano et al., 2010) and elongation 300±50 % (Marsano et al., 2010). It was reported that the electrospun fibers from the homopolymer PA 6 and the condensation PA 6/6 were characterized by similar mechanical behaviour, although a small difference in repeat-unit structure leads to a difference in the degree of hydrogen bonding interactions (Lin et al., 2012). The filtration industry considers fibers produced from PA as having good-excellent chemical resistance to various biological and oxidizing agents, acids and solvents with exception of mineral acids (PA chemical resistance to mineral acid is defined as poor) (Sutherland and Purchas, 2002).

PAN is another widely used polymer for air filtration application due to the chemical stability and excellent weatherability (Nie et al., 2013; Wang et al., 2014). According to Sutherland and Purchas (2002), PAN fibers are defined by good-excellent chemical resistant to biological and oxidizing agents, mineral and organic acids and solvents. PAN fibers are characterized as both strong and tough (Papkov et al., 2013). Recent study (Papkov et al., 2013) has demonstrated improvements in tensile modulus and strength of electrospun PAN fibers with a decreasing fiber diameter. The authors found that the reduction in fiber diameter from 2.8 μm to ~100 nm leads to the simultaneous enhancement in tensile modulus from 0.36 to 48 GPa, tensile strength from 15 to 1750 MPa, and the toughness from 0.25 to 605 MPa with the largest values were fixed for the nanofibers smaller than 250 nm. The similar findings of mechanical properties of PAN fibers in terms of tensile modulus (3-13.3 GPa) and tensile strength (0.3-870 MPa) were found by Mataram et al., (2010) and Qin et al., (2011). Qin et al., found that initial treatment of PAN fibers by heating and stretching appropriately in nitrogen makes the nitrile groups partially cyclized and enhances the molecular orientation. Finally, fully stabilized PAN fibers were obtained in the reaction with air with a higher preferred orientation. These obtained PAN fiber, known as carbon fibers, had higher density, smaller interlayer spacing and better preferred orientation, which provided considerable increases in tensile modulus more than 10 times, and in tensile strength, it was approximately 3 times greater. While, Mataram et al., (2010) reported that the mechanical properties of electrospun PAN fibers can be increased several times, according to the enhancement of silica (SiO_2) nanoparticles content at 1 wt% in PAN/SiO_2 composite. The composite fibers formed from PAN/SiO_2 were as well tested and used for air filtration applications (Wang et al., 2014). The authors of a recent study found that the incorporation of SiO_2 nanoparticles into electrospun PAN fibers creates hierarchical roughness on the nanofiber surfaces, which exhibit great impact on the morphology, porous structure and filtration performance of the resultant media filters.

PU fibers are interesting in engineering material fields because of its properties of both rubber and plastics, including excellent abrasion resistance and the possibility of significantly improving resistance against mechanical deformation. (Chen et al., 2006; Lee et al., 2003). Several studies reported that mechanical properties of PU electrospun fibers are slightly lower compared to PAN or PA. PU fibers had tensile modulus in the range of 0.62-7 MPa, tensile strength 7.04-40 MPa, elongation at break 300-1210 % (Chen et al., 2006, Lee et al., 2003; Sen et al., 2004). PU composites with single walled carbon tubes (SWNT) or MWNT are able to enhance mechanical properties. It was found that, compared to pure PU fibers, the tensile modulus and the tensile strength of SWNT-PU composites (1:100 wt%) increases by 46-104 % and 300 %, respectively, depending on the preparation degree of SWNT (Sen et al., 2004). Chen et al., (2006) reported that increasing the concentration of nanotubes from 0 to 17.7 wt% in MWNT-PU composite leads to the enhancement of tensile modulus by 27 times. While 9.3 wt% of MWNT in PU exhibited the highest increase in tensile strength, i.e., 2.4 times greater than that of pure PU fiber. Both works written by Sen et al., (2004) and Chen et al., (2006) indicated that better mechanical properties for the SWNT or MWNT in PU composites could be due to the improved dispersion of the nanotubes. Lee et al., (2003) investigated the mechanical behaviour of PVC/PU fibers blends. They found that pure PU had a low tensile modulus (0.62 MPa), while pure PVC fibers had low tensile strength (0.9 MPa) and elongation behaviour (153 %) due to the non-bonded structure of PVC fiber mats. Whereas a distinct elastic region was formed before what seems to be a plastic or elastomeric behaviour with an increased tensile modulus, strength and elongation for 75/25 and 50/50 PVC/PU fibers blends (Lee et al., 2003). As a result, the highest tensile modules (11.8 MPa) were exhibited by 50/50 PVC/PU fibers blend compared to the initial tensile modulus of PU (0.62 MPa) and PVC (3.75 MPa).

PMMA, a well-known, transparent thermoplastic, has previously been used for adsorption, ionic conductivities and sensing application in composites (Bae et al., 2013; Khan et al., 2014; Matabola et al., 2011; Zhang et al., 2014) due to the amorphous PMMA with sufficient amount of molecular orientation (Chen et al., 2014). Together with the high ionic conductivity, electrospun PMMA fibers are defined by high electrolyte uptake and good chemical stability (Chen et al., 2014). It has been reported that pristine PMMA fibers have more moderate mechanical properties in terms of tensile modulus and tensile strength compared to PAN fibers. Tensile modulus were in the range of 0.6-1.49 GPa and tensile strength – 16.8-33 MPa (Andersson et al., 2014; Li et al., 2013). Moreover, the mechanical properties of PMMA electrospun fibers could be doubled with PMMA composites made from using electrospun graphene-incorporated-PA 6 nanofibers as the reinforcement (Li et al., 2013).

A literature review revealed that the most attractive polymers for air filtration applications, according to their mechanical properties, are PAN and PA fiber media. These polymers have highest tensile modulus and tensile strength and are characterized as insoluble in water. PAN, PA and PU composites with SiO_2 nanoparticles or various nanotubes are suitable for the filtration process as well,

since the composites offer additional advantages in the morphology of fiber media surface and mechanical properties. To the best of the author's knowledge, natural based electrospun polymers have not been widely used for filtration applications. The potential possibility of the usage of natural based polymers such as CA in the filtration field seems attractive, because CA is a cellulose derivative polymer of an environment benign nature (Tian et al., 2011). Moreover, according to Greish et al., (2010), the electrospun fibers from CA are characterized by a good chemical resistance, thermal stability and biodegradability. Tensile modulus of electrospun CA fibers (i.e. ~247MPa) is not very high as in the PAN or PA fiber media, but quite enough to be used in practical application of filtration processes (Gopiraman et al., 2013).

1.3.3. Properties and filtration parameters of the nanofiber filtration media

Table 1.3. summarizes the filtration parameters together with the characteristics of fiber diameter of electrospun nanofiber media for MPPS at face velocity 5-5.3 cm/s obtained by the different authors. The electrospinning conditions of presented studies are given in Table 1.2. Only the parameters of nanofiber media with the best filtration performance are presented. Some results were interpolated directly from the graphs; thus, caution should be exercised when comparing the results due the bias.

Numerous experimental studies were carried out to examine the filtration performance of electrospun fibers for various purposes. One of the purposes was to achieve high filtration efficiency and *QF*. Considering the nanofiber filter with high filtration efficiency seems attractive due to the very small fiber diameter, regardless the pressure drops. However, the combination of efficiency and pressure drop can be defined by two alternatives: the pressure drop together with high efficiency (>90 %) is rather low (<100 Pa), and the pressure drop together with high efficiency (>90 %) is rather high (>100 Pa). Practically, in nanofiber filtration studies, there is an impossible combination between the high efficiency and rather low-pressure drop. If nanofiber filter is characterized by high efficiency, it absolutely has rather higher pressure drop in most of the cases (see Table 1.3. for studies of Zhang et al., 2009; Leung et al., 2010; Sambaer et al., 2011), except for a few exceptions. One of the expectations is multi-ply technology, which is one of the techniques to enhance *QF* (see Table 1.3. for Li et al., 2012; Zhang et al., 2010; Wang et al., 2014). Nanofibers filters with multi-ply structure, which are produced by stacking up nanofiber media layers into integral multi-layer filter, are expected to improve the filtration performance with respect to the higher efficiency together with a lower pressure drop. Leung et al., (2010) argued that the improvements in *QF* by using multi-ply layers become more significant at higher basis weight of nanofiber media. The multi-ply technique can be regarded as an alternative to adjust α and Z under fixed basis weight what provides higher filtration efficiency and lower pressure drop (Leung et al., 2010). The recent study of Wang et al., (2014) demonstrated a fascinating filtration performance (QF=0.077 Pa^{-1}) of nanofiber media composed of

17 layers. Their used nanofiber filter media (PAN/SiO_2) with roughness surface as well contributed to the excellent performance. While Yun et al., (2010) found that the modification of the internal structure of electrospun nanofiber by using microspheres was able to enhance *QF*, compared to the morphology structure of nanofiber. The enhancement of filtration performance of both beaded nanofiber and composite particle/nanofiber filters is explained by the fact that the insertion of microspheres into nanofibers resulted in wider physical separation of nanofiber media layers. As a result, the distance between nanofiber increased, and the volume fraction of the structure decreased.

The effects of various electrospinning parameters (voltage, polymer concentration, collection time, tip-to-collector distance etc.) as well as nanofiber filter characteristics (packing density - α, basis weight - *W*, thickness - *Z*, fiber diameter etc.) on filtration performance were extensively studied as well. Zhang et al., (2009) found that the electrospun nanofiber media filter produced from higher polymer concentration (from 10 to 15wt% of PA 6) and under larger tip-to-collector distance (from 15 to 20 cm) and higher feed rate (from 0.6 to 3 ml/h) are responsible for higher filtration efficiency and *QF*. According to Hung and Leung (2011), the reduction of nanofiber diameter from 185 (filter M1) to 94 (filter S) nm with the same W=0.0423 g/m^2 (electrospun from 20 and 12 wt% PA 6 solution, respectively) enhances filtration efficiency but elevates the pressure drop at the same time. MPPS shits from 120 nm for M1 to 80 nm for S. They noticed that smaller fibers are responsible for facilitating the filtration of NaCl aerosol particles in the range of 50-500 nm through improved diffusion and interception mechanisms. The improvement of interception is larger than of diffusion, as indicated by shifting down of the MPPS. For nanofiber filter S, QF was higher for capturing 100-380 nm particles compared to M1, and otherwise, OF was lower for 50-90 nm particles, respectively. Leung et al., (2010) studied the effect of face velocity, packing density and thickness on filtration performance of nanofiber filters. One of the findings was that MPPS decreases (from ~140 nm to ~90 nm) with increasing α (from ~0.005 to 0.035) for electrospun nanofiber filter with the same fiber diameter. Moreover, the effect of *Z* on MPPS in nanofiber filter is less important than that of α. There are dependencies between *W* and *Z*; *W* and α are not strongly expressed as a linear. α increases with *W*, but the increase rate drops subsequently after W=0.4 g/m^2; *Z* starts to increase as well after W=0.4 g/m^2. Another important finding is that the filtration efficiency decreases with the face velocity (from 5 to 10 cm/s), and the reduction becomes significant for smaller particles (<100 nm). It is explained by reduced retention time of particles on nanofiber media; thus, there is the lower opportunity for particles to collide on nanofiber through Brownian motion. Sambaer et al., (2011) investigated the effect of air velocity, viscosity, temperature and pressure between the particles and fiber media theoretically through the 3D structure model and experiment as well. It has been observed that an increase in face velocity (from 2 to 8.55 cm/s), viscosity (from 1.9 10^{-5} to 7.6 10^{-5} Pa s) and pressure (from 0.05 to 0.3 MPa) leads to efficiency decrease due to the reduced Brownian motion intensity. Whereas the increase in air temperature (from 100 to 1000 K) leads to efficiency enhancement due to the reduced particle slip effect and increased Brownian motion.

Table 1.3. Electrospun nanofiber for air filtration applications II: the filtration properties for most penetrating particle size (300 nm)

Study	Filter name	Fiber diameter, nm	Quality factor, Pa^{-1}	Filtration efficiency, %	Pressure drop, Pa
Zhang et al., 2009	15wt% 12wt% 10wt%	110-150 70-100 60-90	0.028 ~0.02 ~0.02	~97 ~90.5 ~87	~122.7 ~114.7 ~96.9
Zhang et al., 2010	PAN5 PAN15 PAN5x3 PAN15x2	224	0.037 0.023 0.063 0.025	47.7 89.8 92.05 97.93	18 98 41 152
Yun et al., 2010	NF4 NF5 BF4 BF5	420 420 390 390	The values are uncertain, do not match with ΔP	~28.5 ~67.2 ~48.3 ~81.2	
Leung et al., 2010	N9S N8S N7S N3S N3Sx2 N3Sx3	208	0.016 0.017 0.018 0.028 0.027 0.026	~92.5 ~90 ~83 ~33 ~57 ~70	161.2 131.8 99.4 13.2 ~31.3 ~46.3
Hung and Leung, 2011	S M4 L	94 185 220	0.039 0.022 0.022	~56 ~80 ~75	20.9 74 62.2
Sambaer et al., 2011*	PU	293	0.007	~87	316
Li et al., 2012**	N1 N2 N3 N4 N5 N1x3	90	~0.047 ~0.055 ~0.045 ~0.037 ~0.035 ~0.061	92.61 96.44 96.63 96.98 95.95 99.95	~55 ~60 ~74 ~95 ~92 ~120
Wang et al., 2013**	PVC/PU(8wt%)	~800	0.0368	99.5	144
Wang et al., 2014****	PAN/SNP-8x17	578	0.077	99.989	117
Shahrabi et al., 2014*****	C3 C6 C9	89 97 103	0.290 0.331 0.292	94.48 98.66 99.31	10 13 17

*Face velocity was 5.7 cm/s. Under 5-5.3 cm/s, the face velocity *QF* will be higher.
**Filtration tests were performed with monodisperse ~75 nm NaCl particles. *QF* will be lower for filtration tests with 300 nm particles.
***Value of *QF* for 300-500 nm particles. *QF* will be lower only for 300 nm particles.
**** Value of *QF* for 300-500 nm particles. *QF* will be lower only for 300 nm particles.
*****Face velocity was 0.21 cm/s. Under 5-5.3 cm/s, the face velocity *QF* will be lower.

Wang et al., (2013) reported high *QF* (0.0368 Pa^{-1}) of electrospun nanofiber media filter produced from PVC/PU 8/2 w/w blends. The morphology of the tortuous structure of blended nanofibers played an important role in the final properties fiber media, including air permeability (154.1 mm/s), tensile strength (9.9 MPa) and abrasion resistant (134 cycles). Their last study (Wang et al., 2014) as well deals with the development of fiber media of blends (PAN/SiO_2) in the formation of skeletal frame-worked media with rough surface as mentioned above.

The study of Shahrabi et al., (2014) is interesting, because in this study, as a test aerosol was used the atmospheric particles. Together with the atmospheric particles, which are defined as non-uniform, dioctyl phthalate as uniform particles were used to evaluate the filtration efficiency of the nanofiber filter. The results showed that the efficiency for dioctyl phthalate particles was less than for the atmospheric particles. Moreover, at longer electrospinning (collection) time, the difference between efficiencies was at the lowest level. Together with increasing collection time, the fiber diameter increases as well as filtration efficiency increases, especially for smaller particle sizes (see Table 1.3.).

It is worth to note that the nanofiber media filters have increased in pressure drop much more rapidly compared to the microfiber filter in the usage stage (Leung and Hung, 2012). It is explained that microfiber filter is thicker and has higher dust holding capacity under continuous loading of aerosol particles compared to the nanofiber media filters. The clogging of nanofiber media filter is a problem, since it is working under high aerosol concentrations, and nanofiber filter must be replaced by other new, when the deposited mass of aerosol particles reach several grams per square meter on fiber media surface. When deposited mass was $2g/m^2$, the pressure drops were 150-270 Pa of nanofiber filters with corresponding diameters of 98 and 300 nm (Leung and Hung, 2012).

1.4. The summary of the literature review

The literature review revealed that the effects of various parameters and media properties on air filtration performance are quite well examined; however, there are no studies specifically focused on the assessment of filtration characteristics of various polymeric materials. With this in mind, it would be useful to perform experimental study with comparison of nanofibers produced from various polymeric materials for their suitability and performance to be used as the air filters based on the comparison of filtration properties.

Based on analysis of recent studies presented in the literature review, the principal diagram of linkages between solution parameters, electrospinning parameters, nanofiber filter media characteristics of filtration parameters is proposed in Fig. 1.10. The diagram comprises dependence between various sub-parameters and sub-characteristics. Polymer solution parameters combined with voltage, nature of collector and feed rate from electrospinning area are the main contributors to fiber diameter and morphology of filter media. Collection time and tip to collector distance parameters in electrospinning have the greatest influence on the basis weight and thickness characteristics, which directly affect the packing density in filter media. While the filtration parameters mainly depend on fiber diameter,

morphology and packing density. The review presented in this thesis as well contributes to the better understanding of the production and usage of nanofiber filters.

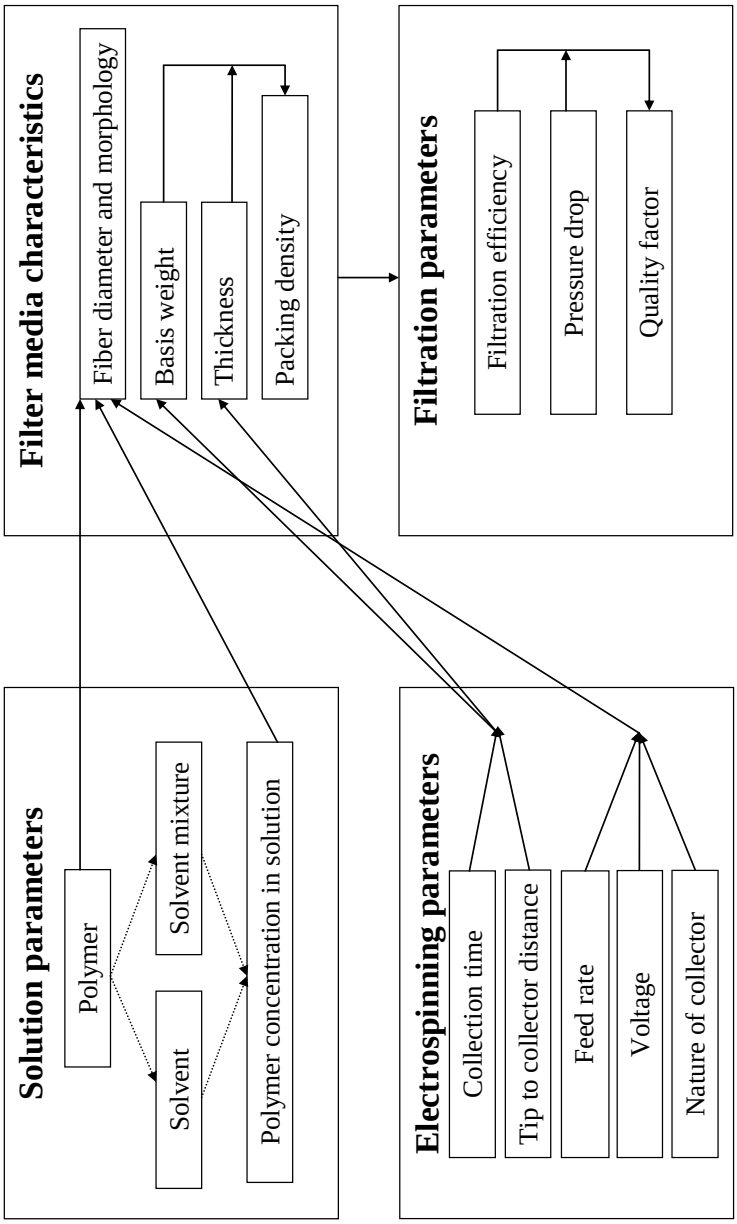

Fig. 1.10. The principal diagram of the factors having effect on the characteristics of the filter media

The following recommendations can be drawn in terms of electrospun nanofibers for air filtration applications:

1. It is recommended to use nanofiber media filters in applications where the concentration of particles is comparatively low (between 1,000 and 50,000 particles/cm^3), otherwise the pressure drop will increase, and the filter media will be clogged. The diameter of the vast majority of particles should be <1 μm.
2. The face velocity should range between 0.02 and 0.1 m/s, otherwise the quality factor will decrease dramatically, especially for smaller particles (<100 nm).
3. The substrate (supporting structure) used for collection of deposited elementary fibers must be strong and tough, but at the same time, it must be permeable with a negligible decrease in filtration efficiency (<10 %) and/or pressure drop (< 5 Pa).
4. Nanofiber media filters could be used in the final stages of filtration, for example: clean room environments, low face velocity ventilation systems as a supplement to microfiber filters and specific applications of chemical engineering.

2. EXPERIMENTAL

2.1. Materials used for the production and testing of nanofibers media

The materials used in the experiment can be classified into polymers, solvents and filter testing materials. Polymers and solvents were used for the preparation of polymer solutions, which further were employed in electrospinning for the formation of nanofiber. Electrospun nanofiber was further tested in an experimental filtration stand with testing materials, i.e., challenging aerosol particles, which were generated by nebulizer. The materials, their properties (analytic grade, MW etc.) and subchapter where they were used are listed in Table 2.1. All the materials were purchased from Sigma-Aldrich and were used without any purification.

Table 2.1. The list of materials used in the experimental of electrospinning and filter media testing

Material	Properties	Subchapter
Polymers		
Cellulose acetate (CA)	MW ~30,000 by GPC. 39.8 wt. % acetyl. Relative density 1.3 g/mL at 25 °C	3.1. and 3.3.
Polyamide 6, poly(hexano-6-lactam (PA 6)	MW not provided. Relative density 1.084 g/mL at 25 °C	3.2. and 3.3.
Polyamide 6/6, Poly[imino(1,6-dioxohexamethylene (PA 6/6)	262.35 g/mol. Relative density 1.18 g/mL at 25 °C	3.2. and 3.3.
Polyacrylonitrile (PAN)	MW 150,000. Relative density 1.184 g/mL at 25 °C	3.3.
Polyvinyl acetate, poly (1-acetyloxiethene (PVAc)	MW ~100,000 by GPC. Relative density 1.18 g/mL at 25 °C	3.3.
Solvents		
Acetone	min. concentration 99.8 %	3.1. and 3.3.
Dichloromethane (DCM)	min. concentration 99.8 %	3.1., 3.2. and 3.3.
N,*N*-dimethylformamide (DMF)	min. concentration 99.8 %	3.1. and 3.3.
Acetic acid	min. concentration 99 %	3.1., 3.2. and 3.3.
Formic acid	min. concentration 85 % min. concentration 98 %	3.2. and 3.3.
Test aerosols		
Sodium chloride (NaCl)	min. concentration 99 %	3.3.
Polystyrene latex (PSL) suspension	0.1 μm mean particle size 0.3 μm mean particle size	3.3.

2.2. Experimental electrospinning system for nanofiber media fabrication

Polymer solutions were prepared by dissolving a specific polymer in the characteristic solvent or solvent mixture. The solutions were prepared by mechanical stirring at the room temperature. The used polymer solutions for different parts of the research of the thesis are presented in the following subchapters: 2.2.1., 2.2.2., 2.2.3.

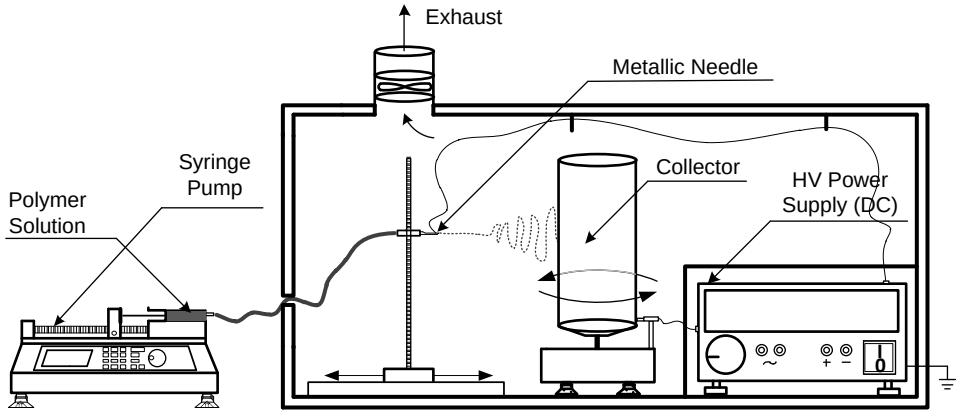

Fig. 2.1. Schematic view of the experimental electrospinning system

A single needle system was used in the electrospinning experiments. The electrospinning system (see Fig. 2.1.) consisted of a high voltage DC power supply based on the "Flyback" principle (Alaraj et al., 2014; Arshak and Almukhtar, 2000). The grounded electrode was connected to the collector drum, while the high voltage electrode was connected to the needle of the syringe. The mixed polymer solutions were loaded into a syringe equipped with a needle, fixed horizontally on the syringe pump (LSP01-1A, Baoding Longer Precision Pump Co., Ltd., China). Electrospun fibers were collected on a vertically positioned cylindrical collector coated with the supporting substrate and rotating at a linear speed of 0.025 m/s (rotation frequency of 6 rpm). The electrospinning was carried out in an enclosed Plexiglas chamber at ambient conditions (~19-21 °C and ~34-42 % relative humidity) for all the experiments. Collected samples of the electrospun nanofibers were dried in a vacuum at room temperature for several hours.

The electrospinning parameters (voltage, tip to collector distance, feed rate and collection time) as well as the supporting substrates used in this thesis for different part of the researches are given in the following subchapters.

2.2.1. Fabrication of the cellulose acetate nanofiber media

The cylindrical-collector was coated with aluminium foil substrate due its conductivity. Moreover, the aluminium foil as a conductivity material has an advantage for better observation of nanofiber mats by microscope.

Homogeneous solutions were obtained by dissolving CA in an acetone/DCM/DMF ternary solvent mixture in room temperature. A full-factorial

experiment design was applied, including acetone/DCM/DMF ratios of 1/1/1 and 2/1/1 (v/v/v) as well as CA concentrations of 9, 10, 11, 12 % (w/v). The conductivity measurements of prepared CA solutions were performed before electrospinning by using conductivity meter (HI 8733, Hanna Instruments, USA) at 20 °C.

The electrospinning parameters were as follows: voltage = 18 kV, feed rate = 2.8 mL/h and tip to collector distance (TTCD) = 11 cm.

2.2.2. Fabrication of the polyamide nanofiber media

The polyester fabric (17 g/m^2) was selected as a supporting substrate on the collector. This type of substrate allowed performing measurements of thickness and basis weight due its flexibility, easy severability of layers between the pristine substrate and the nanofiber media.

The polymer solutions were obtained by dissolving PA 6 or PA 6/6 in formic acid, formic acid (FA)/acetic acid (AA) 3:2 (v/v) or FA/DCM 3:2 and 3:1 (v/v) at room temperature. The PA6/6 concentrations in the solutions were 8, 11 and 14 % (w/v), while PA 6 concentrations were 20, 24 and 28 % (w/v). The concentration ranges that were chosen for both PA species ensured the formation of well-defined nanofibers.

The electrospinning process parameters used for PA 6/6 were as follows: voltage of 12 and 20 kV, feed rate of 0.25 mL/h and TTCD of 6 and 12 cm. The electrospinning process parameters for PA 6 were voltage of 12 and 20 kV, feed rate of 0.25 mL/h and TTCD of 7 and 14 cm.

2.2.3. Experimental design of the nanofiber media

The mathematical design of the experiments presented in subchapter 3.2. was based on the D-optimal-interaction model developed within MODDE 7 software (Umetrics AB, Sweden). Each experiment for PA 6 and PA 6/6 was conducted with the predefined combination of variables that included the concentration of the solution, the nature of the solvent, the deposition voltage, the tip-to-collector distance and the collection time. Once all the responses (fiber diameter, basis weight, thickness and solidity) of the experiments were obtained, the Partial Least Squares (PLS) method was applied to develop a polynomial model relating the factors to the responses. PLS deals with all the factors simultaneously considering their covariances. The advantage of this model is a reliable interpretation and prediction of the interaction between the experimental factors and responses.

The electrospinning of PA fibers was carried out *via* 34 controlled experiments as recommended by D-optimal-interaction model, 17 experiments for each grade of PA. Seven different combinations of solution concentrations and solvents were applied for each PA species. Two separate models, one for the PA 6/6 and one for the PA 6, were developed. Goodness of fit (R^2) and goodness of prediction (Q^2) parameters were estimated as measures for the accuracy of the model.

2.2.4. Fabrication of the polyamide, polyvinyl acetate, polyacrylonitrile and cellulose acetate nanofiber media for filtration applications

The fiberglass mesh surface (substrate) having a structure of the square pore network of 1x1 mm was used to collect the nanofibers. The substrate of fiberglass with the basis weight of ~120 g/m^2 was characterized by a negligible pressure drop ΔP=0.3 Pa and the filtration efficiency (300 nm particles) of 0.2 % at a face velocity of 5.3 cm/s.

Table 2.2. The characteristics of polymer solutions and electrospinning parameters

ID	Polymer	Solvent	Concentration, % (w/v)	Voltage, kV	TTCD, cm	Feed rate, mL/h	Electro-spinning duration, min
PA6/6_120s	Polyamide 6/6	FA	9.0	20	16	0.25	120
PA6/6_120l	Polyamide 6/6	FA	14.0	20	16	0.25	120
PA6/6_160l	Polyamide 6/6	FA	14.0	20	16	0.25	160
PA6_300	Polyamide 6	FA	26.0	20	16	0.25	300
PVAc_30	Polyvinyl acetate	DMF/AA (10/1 v/v)	37.5	24	20	0.5	30
PVAc_40	Polyvinyl acetate	DMF/AA (10/1 v/v)	37.5	24	20	0.5	40
PVAc_60	Polyvinyl acetate	DMF/AA (10/1 v/v)	37.5	24	20	0.5	60
PVAc_80	Polyvinyl acetate	DMF/AA (10/1 v/v)	37.5	24	20	0.5	80
PAN_40_6	Polyacrylonitrile	DMF	6.0	19	20	0.8	40
PAN_40_8	Polyacrylonitrile	DMF	8.0	19	20	0.8	40
PAN_60	Polyacrylonitrile	DMF	8.0	19	20	0.8	60
PAN_80	Polyacrylonitrile	DMF	8.0	19	20	0.8	80
CA_40	Cellulose acetate	Acetone/DCM/DMF (2/1/1 v/v/v)	11.0	18	16	3	40
CA_70	Cellulose acetate	Acetone/DCM/DMF (2/1/1 v/v/v)	11.0	18	16	3	70

Polymer solutions were prepared by dissolving PA6/6 or PA6 in FA, PVAc in DMF/AA (10/1 v/v), PAN in DMF, while CA was added in the solvent mixture of acetone/DCM/DMF (2/1/1 v/v/v). After numerous trials, the following concentrations of solutions were found as best suitable for the electrospinning: PA6/6 was 9 and 14 % (w/v), PA6 26 % (w/v), PVAc 37.5 % (w/v), PAN 6 and 8 % (w/v) and CA 11 % (w/v).

The electrospinning process parameters used for PA6/6, PA6, PVAc, PAN and CA nanofiber mats formation are presented in the Table 2.2.

2.3. Characterization of the electrospun nanofiber media

The morphology of fiber networks and corresponding diameters were investigated by using a scanning electron microscopy (SEM) and atomic force microscopy (AFM). Hitachi S-4800 microscope (Japan) equipped with a cold field

emitter was operating at 2 kV accelerating voltage, while Quanta 200 FEG (USA) was operating at 10-20 kV accelerating voltage. No specific sample preparation was performed before imaging. AFM was performed by using Asylum Research MFP-3D instrument (USA) in alternating current (AC) mode. Mikromasch NSC-15 silicon cantilevers with Al coated backside, typical resonant frequency of 325 kHz and force constant of 40 N/m were used in the experiment. The samples for AFM analysis were electrospun on the Si wafer surface attached to the collector.

The basis weight (the mass of the nanofibers per unit filter area in g/m^2) of nanofiber media was controlled by the duration of electrospinning process and was defined by using microbalances (MXA-5, Radwag, Poland). The thickness of the nanofiber filter mat was measured in the centre of the nanofiber media by using a digital micrometer with a measurement resolution of 1 μm. The measurements of basis weight and thickness were performed at 5 different samples from two different mats of electrospinning. The packing density of nanofiber media was estimated by using formula (3).

The average diameter of the fibers was determined by analysing the SEM images with ImageJ (NIH, USA) image analysis software. In case of each sample, the fiber diameters were measured at 50-100 different points.

2.4. Experimental electrospun nanofiber media filtration performance testing system

The experimental setup shown in Fig. 2.2. was used to measure the filtration efficiency and pressure drop across the filter sample. The air compressor provided dry and clean air through the three-filter system to Collison nebulizer (Model CN 24 J, BGI Inc., USA), where monodisperse PSL and polydisperse NaCl aerosol particles were generated. The monodisperse PSL particles (diameter = 100 and 300 nm) were suspended in deionized water (DIW) (0.2 mL of PSL suspension in 100 mL DIW). The concentration of NaCl by weight in DIW was 0.1 %. After nebulisation, the generated aerosol was dried by the diffusion dryer packed with the silica gel and was flown to the dilution chamber. After passing the dilution chamber, the airflow with aerosol split into two paths. In one path, the airflow passed through the aerosol charge equalizer (based on the DC corona discharge) (Alonso et al., 2006; Intra and Tippayawong, 2011) and was directed to the tube with the installed filter sample. The flow rate was 3.23 L/min corresponding to the face velocity of 5.3 cm/s in case of 36 mm filter. The diameter of sampling probes upstream and downstream around the filter was 20 mm. The airflow from the dilution chamber was directed to HEPA filter and flowmeter for balancing flow rates of the entire filtration system. The pressure drop before and after the filtration media was measured by a pressure sensor (Model P300-5-in-D, Pace Scientific Inc., USA). The upstream and downstream concentrations of aerosols were measured by ELPI+ (Electrical Low Pressure Impactor, Dekati Ltd., Finland). ELPI+ enables the measurement of real-time particle size distribution and concentration in the size range of 6 nm – 10 μm with a 10 Hz sampling rate.

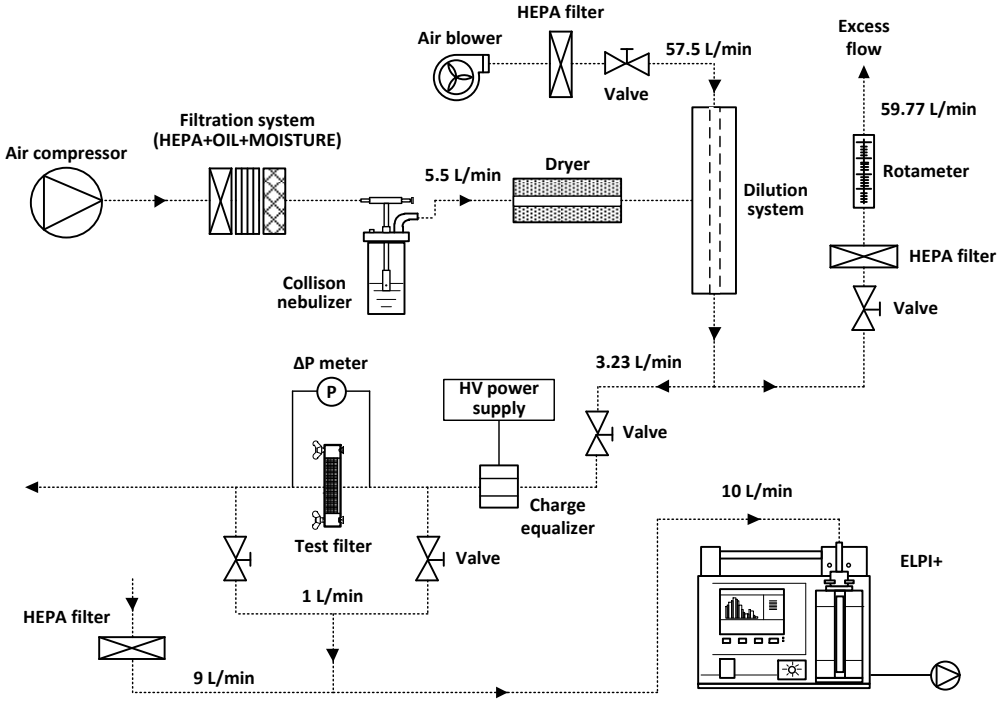

Fig. 2.2. The experimental set-up for filtration efficiency and pressure drop measurements

Nanofiber media filters having high filtration efficiency at a low-pressure drop are the most desirable in filtration. Both aspects are considered in the quality factor (*QF*) of the filter as well referred to as a figure of merit of the filter, which is often used to evaluate the filtration performance of filters. *QF* was estimated by using formula (14).

The tested corresponding gas flow regimes of nanofiber media were estimated by using Knudsen number in the formula (7).

3. RESULTS AND DISCUSSIONS

3.1. Optimization of the preparation conditions for the formation of cellulose acetate nanofibers

The potential possibility of the usage of natural based polymers such as CA in the filtration field seems attractive, because CA is a cellulose derivative polymer of an environment benign nature (Tian et al., 2011). Moreover, according to Greish et al., (2010) the electrospun fibers from CA are characterized by a good chemical resistance, thermal stability and biodegradability.

It has been demonstrated that the solvent systems used for CA fiber production have a significant influence on the morphology and diameter of fibers (Celebioglu and Uyar, 2011; Han et al., 2008; Tungprapa et al., 2007). Traditional single solvent systems are not suitable for uniform CA fiber formation. Using single solvent systems such as *N*,*N*-dimethylformamide (DMF), dichlormethane (DCM), formic acid, methanol, chloroform and pyridine mainly produce discrete beads, while the acetone solvent in electrospinning forms short and beaded fibers (Tungprapa et al., 2007). As a result, the binary solvent systems are used in CA electrospinning to obtain uniform fibers below diameter of 1000 nm. The most appropriate solvent system for electrospinning of CA fibers was shown to be a mixture of acetone/N,N-dimethylacetamide (DMAc) (Hong et al., 2013; Liu and Hsieh, 2002; Tian et al., 2011; Tsioptsias et al., 2011). Binary solvent systems of successful uniform CA fibers electrospinning are mixtures of acetone/DMAc (Greish et al., 2010; Tungprapa et al., 2007), acetone/DCM (Celebioglu and Uyar, 2011), methanol/DCM (Tungprapa et al., 2007) and acetic acid/water (Han et al., 2008). In most cases, the successful electrospinnability of CA fibers from binary solvent systems was defined by the difference in the boiling points and dielectric constants of both solvents. Prolonged utilization of the solvent system containing volatile compounds causes clogging of the spinneret during the electrospinning process, especially in a low humidity environment (Bhardwaj and Kundu, 2010; Wang et al., 2012). A binary system of acetone/DCM (boiling point 40 °C and 56 °C, respectively) is a typical example of such solvent system.

In this thesis, there was developed a new ternary solvent system (acetone/DCM/DMF) for continuous electrospinning of CA nanofibers introducing DMF (boiling point 154 °C) as a widely used solvent to the mixture of acetone and DCM to reduce the overall volatility of the system. The influence of the CA concentration on the average diameter and morphology of the electrospun nanofibers was investigated.

In the case of a ternary solvent system of acetone/DCM/DMF at a ratio of 1/1/1 (v/v/v), the electrospun fibers showed beaded fibers with droplets and stick together morphology. This ternary mixture contained 1/3 part by volume of DMF solvent, which is characterized by high boiling point, while the ternary solvent system at ratio 2/1/1 (v/v/v) had 1/4 part by volume of DMF solvent. The increased amount of DMF solvent in the ternary system of 1/1/1 (v/v/v) had an impact on the overall boiling point of the mixture. When the electrospinning is performed from

solvents with higher boiling point value, the ejected charged jet does not have enough time to dry during its time of flight. As a result, the droplets and stick-together morphology of fibers were fabricated.

Using a solvent system of acetone/DCM/DMF 2/1/1, the electrospinning was possible starting with the CA concentration higher than 9 % (w/v). In case of concentration lower than 9 % (w/v), the fibers were not formed due to the jet breaking up into the droplets. Electrospinning of the 9 and 10 % (w/v) CA (Fig. 3.1. a and b) resulted in the formation of beaded fibers. The electrospun mat of the 11 % (w/v) CA showed rather uniform structure with the exceptions of several defected fibers (Fig. 3.1. c). The smooth fibers were obtained from 12 % w/v solution (Fig. 3.1. d). The respective diameter distributions of fibers are presented on the right side of Fig. 3.1. Properties of the electrospun CA fibers obtained from the ternary solvent mixture are presented in the Table 3.1.

The comparative analysis of electrospun CA fiber diameters showed that the CA solution concentrations have an effect on the fiber diameter range. It has been determined that the diameters of fibers did not follow the normal (Gaussian) distribution (Statistica, StatSoft Inc., USA) ($p<0.05$ based on Shapiro-Wilk's W test) (see histograms in Fig 3.1). Moreover, the analysis has clearly shown that an increase of CA solution concentration has direct influence on the diameter of electrospun fibers (linear $R^2=0.966$), whereas the concentration increase has indicated a decline of CA solution conductivity (linear $R^2=0.965$) (see Table 3.1.).

Table 3.1. Properties of the electrospun CA fibers obtained from the acetone/DCM/DMF ternary solvent system

Parameter	Concentration of CA in ternary solution, % w/v			
	9 %	10 %	11 %	12 %
Conductivity of the solution, μS/cm	3.50	3.40	3.35	3.30
Mean fiber diameter, nm	152	179	241	264
Standard deviation of diameter, nm	57	62	92	97
Median fiber diameter, nm	143	165	232	251
25th percentile diameter, nm	116	127	172	199
75th percentile diameter, nm	178	214	299	319

The findings from the other studies that are using various solvent systems for electrospinning CA fibers are presented in Table 3.2. Han et al., (2008) reported that the low diameter (up to 200 nm), smooth CA fibers could be formed from acetic acid/water solvent system (ratio of 70/30 and 75/25 w/w). Respectively, Tungprapa et al., (2007) found that the low diameter CA fibers could as well be formed from acetone/DMAc solvent system (ratio of 1/1 v/v). While the largest smooth fibers of CA by diameter over 1000 nm could be obtained by using the higher amount of DCM solvent part of the solvent systems. Despite the broader diameter of CA fibers from DCM/acetone solvent system (ratio of 3/1 and 9/1), these fibers are practically important, because of its porous structure inside the fibers (Celebioglu and Uyar, 2011). These properties would be useful for the filtration application due to high surface to volume ratio. However, the morphology of beaded fibers of CA that is

shown in Fig. 3.1. (a-b) as well would be useful for the filtration application, as the beaded fiber mats decrease the volume fraction and increase the effective fiber surface area (Yun et al., 2010).

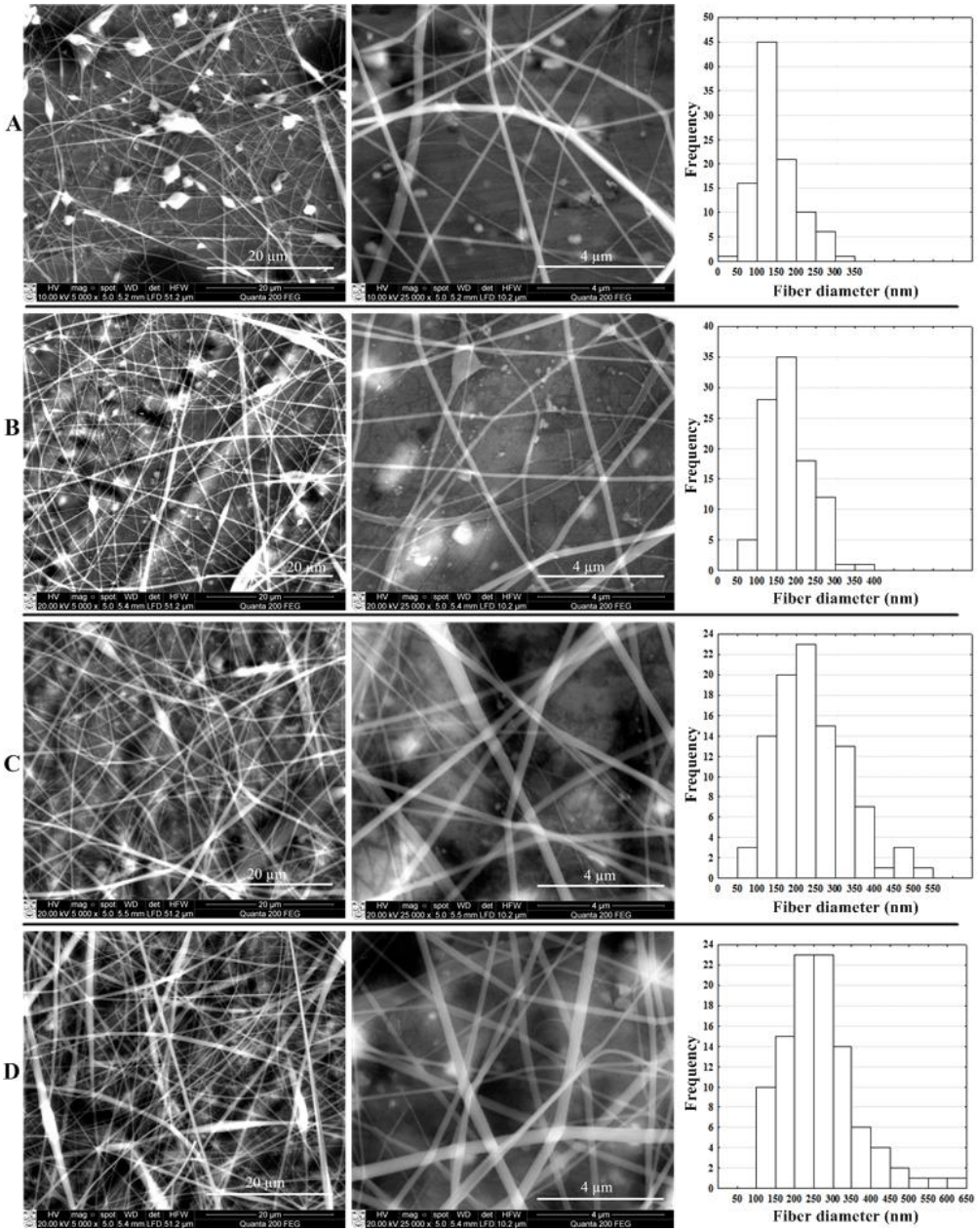

Fig. 3.1. SEM images of the electrospun CA nanofibers obtained from the acetone/DCM/DMF ternary solvent system and fiber diameter distribution histograms: CA concentrations (a) 9 % w/v, (b) 10 % w/v, (c) 11 % w/v, (d) 12 % w/v

Table 3.2. The comparison of various CA solution parameters and the resulting electrospun fibers

Research	Electrospinning parameters	Concentration of the CA and solvent system	Fiber diameter, nm
Celebioglu and Uyar, (2011)	Voltage(V)=15 kV, feed rate (fr)=1 mL/h, TTCD=10 cm (22 °C and 30 % relative humidity (RH))	10 % w/v in DCM/acetone 1/1 v/v	300-1000
		7.5 % w/v in DCM/acetone 2/1 v/v	500-1500
		10 % w/v in DCM/acetone 2/1 v/v	750-1350
		7.5 % w/v in DCM/acetone 3/1 v/v	750-2500
		10 % w/v in DCM/acetone 3/1 v/v	1000-2500
		5 % w/v in DCM/acetone 9/1 v/v	1500-3500
		7.5 % w/v in DCM/acetone 9/1 v/v	3500-7000
Han et al., (2008)	V=25 kV, fr=3 mL/h, TTCD=10 cm (25 °C)	17 wt.% in acetic acid/water 70/30 w/w	160
		17 wt.% in acetic acid/water 75/25 w/w	180
		17 wt.% in acetic acid/water 80/20 w/w	~350
		17 wt.% in acetic acid/water 85/15 w/w	~400
		17 wt.% in acetic acid/water 90/10 w/w	~600
		17 wt.% in acetic acid/water 95/5 w/w	1280
Tungpraparat al., (2007)	V=12 kV, TTCD=15 cm	16 % w/v in acetone/DMAc 1/1 v/v	160
		16 % w/w in acetone/DMAc 3/1 v/v	260
		14 % w/v in acetone/DMAc 2/1 v/v	230
		16 % w/v in acetone/DMAc 2/1 v/v	260
		18 % w/v in acetone/DMAc 2/1 v/v	330
		20 % w/v in acetone/DMAc 2/1 v/v	370
		8 % w/v in DCM/methanol 4/1 v/v	1100
		10 % w/v in DCM/methanol 4/1 v/v	1580
		12 % w/v in DCM/methanol 4/1 v/v	1230
Present work	V=18 kV, fr=2.8 mL/h, TTCD=11 cm (20 °C and 40 % RH)	11 % w/v in acetone/DCM/DMF 2/1/1 v/v/v	241
		12 % w/v in acetone/DCM/DMF 2/1/1 v/v/v	264

It can be concluded that the smooth CA fibers could be obtained from the acetone/DCM/DMF solvent system (ratio 2/1/1 v/v/v) with comparatively low concentrations of CA solutions resulting in a mean fiber diameter of 241-264 nm. It should be pointed out that in all the described solvent systems, acetone is an essential component in the electrospinning of CA fibers.

3.2. The effects of the polymer concentration and electrospinning parameters on the characteristics of electrospun polyamide nanofiber media

Electrospun nanofibers from the PA already found a number of applications which includes protective textile, sensors, photovoltaic cells, drug delivery, catalysis and fuel cells (Yan et al., 2015; Nirmala et al., 2014; Schoenmaker et al., 2012; Pang et al., 2014; Pant et al., 2013; Panthi et al., 2013). However, the discussion of their applications for filtration purposes is rather limited (Hung and Leung, 2011; Shahrabi et al., 2014; Zhang et al., 2009). Recent reports on the properties of electrospun nylon-6 nanofibers showed PA as a particularly attractive material for

the filtration applications (Barakat et al., 2009; Pant et al., 2010). Therefore, the research presented in this subchapter was conducted with the comprehensive design and characterization of the electrospun PA 6 and PA 6/6 nanofiber media suitable for the air filtration applications. In this thesis, there was employed a principal component analysis modelling to systematically investigate the effects of the fiber deposition parameters, such as polymer solution composition and electrospinning conditions, on the filtration properties of the obtained nanofibers (fiber diameter, basis weight, thickness and packing density). In this thesis, there derived response surfaces of the nanofiber media that allow determining the set of parameters necessary to obtain specific nanofiber characteristics for a particular filtering application. Finally, based on the modelling results, the author selected the best fiber deposition parameters, fabricated nanofiber filter media (mats) and characterized their filtration properties.

3.2.1. The characteristics of the electrospun polyamide 6 and polyamide 6/6 nanofiber media

Morphology and fiber diameter of the electrospun fibers was obtained from the SEM images shown in Fig. 3.2., whereas the basis weight and thickness have derived from the experimental measurements, while the solidity values were estimated by using formula (3). The composition of the initial PA solutions, electrospinning process parameters and the resulting nanofiber media characteristics relevant to the air filtration are presented in Table 3.3. The fibers of PA 6/6 were electrospun from the polymer concentration ranges from 8 to 14 % (w/v), while the fibers of PA 6 were electrospun at the concentrations ranges from 20 to 28 % (w/v). The compositional concentration of the precursor solutions appeared to be the main parameter influencing the fiber diameter, as discussed in the later subsection (3.2.2.). The selected ranges of the concentrations resulted in a varying fiber diameter with the corresponding values ranging from 60 to 376 nm for PA 6/6 and 99 to 236 nm for PA 6. PA 6/6 revealed a wider electrospinnable range in comparison to PA 6. This agrees with the previously reported data on the electrospinning of PA 6/6 (Chowdhury and Stylios, 2010) and PA 6 (Heikkila and Harlin, 2008).

The values of the calculated basis weight were in the range of 0.12 to 1.84 g/m^2 for PA 6/6 and 0.11 to 1.07 g/m^2 for PA 6, while the thickness values were 6 to 16 μm for PA 6/6 and 5-14 μm for PA 6, respectively. An apparent dependence of the basis weight and thickness on the collection time can be inferred. However, as discussed in the subsection 3.2.2., the collection time was not the only factor affecting the above mentioned nanofiber mat parameters. The packing density increased simultaneously with the basis weight in most cases, but the increase rate dropped after the basis weight value of 0.6 g/m^2 was reached (exp. no. 15 and 17 were not considered).

Table 3.3. Properties of PA solutions, electrospinning process parameters and the resulting nanofiber characteristics

Exp no.*	Solution parameters		Electro-spinning parameters				Characteristics of the produced nanofibers			
	Concentration [%] (w/v)	Solvent system	Voltage [kV]	TTCD [cm]	Collection time [min]	Morphology**	Fiber diameter [nm]	Basis weight [g/m^2]	Thickness [μm]	Packing density
1	8	FA	20	6	20	UF	68±10	1.01±0.11	15	0.059
2	8	FA	12	6	5	UF	67±12	0.25±0.05	8	0.027
3	8	FA	20	12	5	UF	60±11	0.12±0.02	6	0.018
4	8	FA	12	12	20	UF	66+9	0.29±0.09	8	0.032
5	8	FA	20	12	20	UF	62±8	0.36±0.04	9	0.035
6	11	FA	20	6	5	UF+FSN	132±38	0.34±0.09	8	0.037
7	11	FA	20	12	20	UF+FSN	137±28	0.38±0.06	9	0.037
8	11	FA	12	6	5	UF+FSN	184±53	0.27±0.02	8	0.030
9	11	FA	12	12	20	UF+FSN	160±34	0.32±0.08	8	0.035
10	14	FA	20	6	5	F+FSN	347±106	0.42±0.08	10	0.037
11	14	FA	12	12	5	F	376±118	0.16±0.08	6	0.023
12	14	FA	12	6	20	F+SN	349±125	0.94±0.07	15	0.055
13	14	FA	20	12	20	F+SN	351±110	0.62±0.09	10	0.055
14	8	FA/AA3:2	20	12	20	UF	95±17	0.63±0.10	10	0.054
15	11	FA/AA3:2	12	6	20	UF	197±31	1.84±0.11	16	0.101
16	8	FA/DCM3:2	20	12	20	F+ST+SN	511±253	0.62±0.05	10	0.054
17	11	FA/DCM3:2	12	6	20	F+ST+SN	-	1.29±0.44	11	0.103
18	20	FA	20	7	20	UF	135±39	0.89±0.11	14	0.059
19	20	FA	12	7	5	UF	99±29	0.27±0.09	7	0.036
20	20	FA	20	14	5	F	103±44	0.11±0.03	5	0.020
21	20	FA	12	14	20	UF	101±30	0.23±0.03	9	0.024
22	20	FA	20	14	20	UF	106±28	0.38±0.07	11	0.032
23	24	FA	20	7	5	UF+FSN	200±49	0.32±0.11	10	0.030
24	24	FA	20	14	20	UF+FSN	184±41	0.43±0.06	11	0.036
25	24	FA	12	7	5	UF	144±38	0.38±0.04	10	0.035
26	24	FA	12	14	20	UF+FSN	169±49	0.32±0.10	9.5	0.031
27	28	FA	20	7	5	UF+FSN	236±23	0.47±0.14	11	0.039
28	28	FA	12	14	5	F	223±69	0.21±0.09	6	0.032
29	28	FA	12	7	20	F+SN	215±75	1.07±0.17	14	0.070
30	28	FA	20	14	20	UF+SN	228±51	0.48±0.09	11	0.403
31	20	FA/AA3:2	20	14	20	UF	90±10	0.31±0.04	10	0.029
32	24	FA/AA3:2	12	7	20	UF+FSN	144±39	0.58±0.05	10	0.054
33	20	FA/DCM3:1	20	14	20	UF+FSN	94±18	0.34±0.03	9	0.035
34	24	FA/DCM3:1	12	7	20	F+SN	192±73	1.02±0.22	14	0.067

* Exp. no. 1-17 - experiments with PA 6/6 solutions, exp. no. 18-34 – experiments with PA 6 solutions. ** F – fibers; UF – uniform fibers; ST – stick together fibers; SN – spider-net structure; FSN – fragmented spider-net structure.

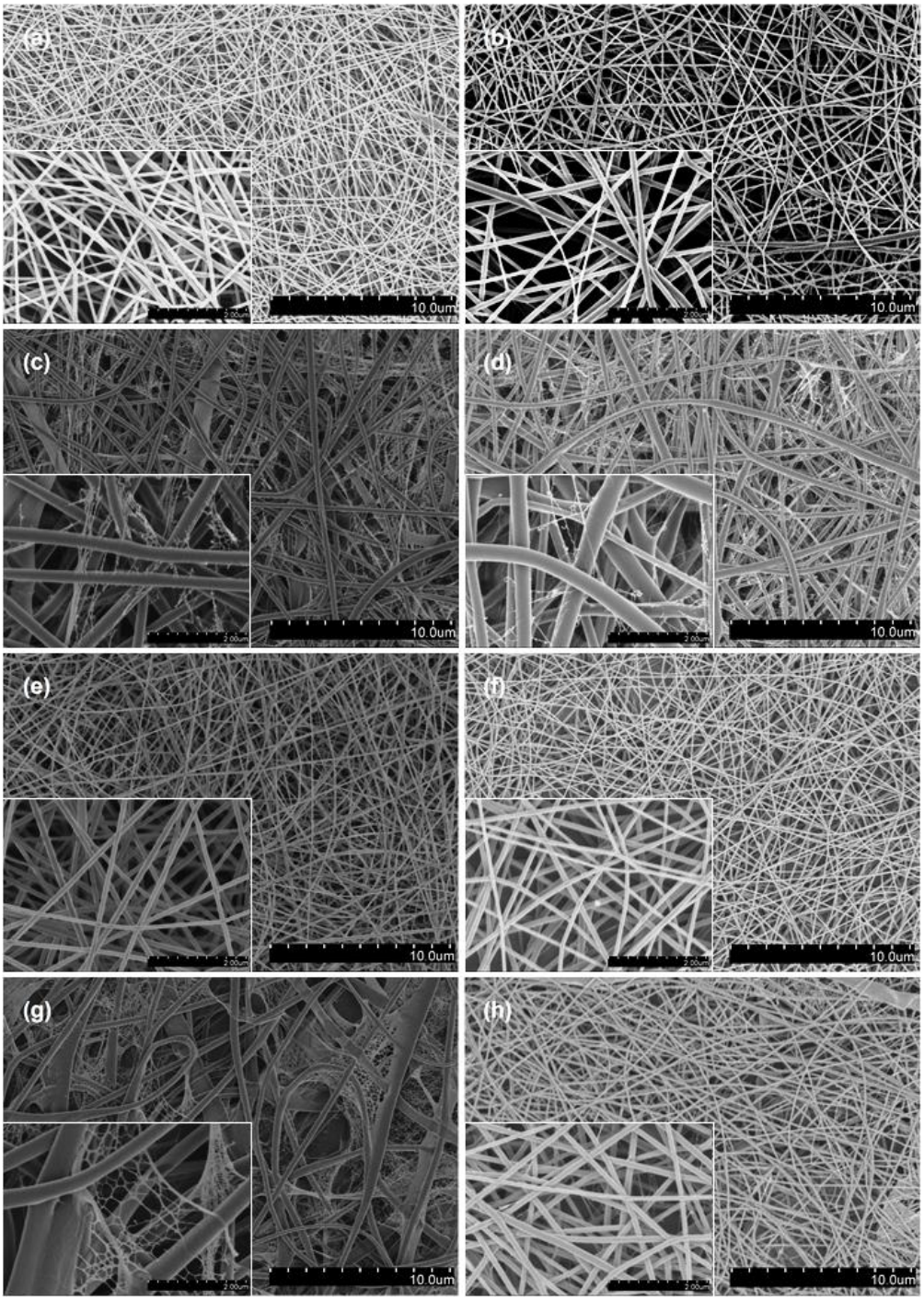

Fig. 3.2. SEM images of the PA nanofibers deposited using (a) PA 6/6 8 % w/v in FA, (b) PA6 20 % w/v in FA, (c) PA 6/6 14 % w/v in FA, (d) PA 6 28 % w/v in FA, (e) PA 6/6 8 % w/v in FA/AA 3:2 v/v, (f) PA 6 20 % in FA/AA 3:2 v/v, (g) PA 6/6 8 % w/v in FA/DCM 3:2 v/v, (h) PA 6 20 % w/w in FA/DCM 3:1 v/v

The electrospinning technique can form various nanofiber structures depending on the solvent system and the polymer concentration. The representative SEM images of PA 6/6 and PA 6 fibers are shown in Fig. 3.2. Based on the structural differences, the electrospun PA mats were grouped into three basic types of morphologies: fibers (F), uniform fibers (UF) and stick-together fibers (ST). The morphology of F was characterized by the wider distribution of fiber diameter within the electrospun mat (standard deviation of fiber diameter (SD)/fiber diameter (FD) > 0.3), while the UF morphology of the electrospun mat can be characterized as smooth with a narrower distribution of the fiber diameters (SD/FD < 0.3). Due to the residual solvent deposited on the collector, the structure of the coalesced fibers can be observed in the ST morphology samples.

In most cases, UF morphology was observed for lower to middle range of polymer concentrations, e.g., 8, 11 % w/v for PA 6/6 and 20, 24 % w/v for PA 6, respectively. Only in case of PA 6 with polymer concentration of 28 % w/v, the UF morphology was observed (experiments no. 27, 30 in Table 3.3.). It is worth noting that FA/AA solvent mixture in ratio of 3:2 v/v for both grades of polyamides contributed to the especially smooth and uniform fibers (Fig. 3.2. e, f).

The detailed analysis of the SEM images revealed the presence of the nano scale fibers in the range of few tens of nanometers known as the spider-net like (SN) fibers (Fig. 3.2. c, d, g) (Barakat et al., 2009; Pant et al., 2010). It has been shown that the SN structures yield the improved mechanical properties of PA mats (Barakat et al., 2009). The formation of the SN structure may be explained by the formation of the hydrogen bonds between the main polyamide chains of the amide groups (CO-NH) and oligomeric, monomeric ionic species ($-CONH_2-^+$) (Pant et al., 2010). The presence of the oligomeric and monomeric ions in solution is due to the formic acid, which is capable of attacking the lactam to produce a series of short oligomers and monomers (Pant et al., 2010). In this thesis, it was proposed that these additional SN structures could be advantageous for the air filtration applications due to the formation of a denser structure of filtering layer, thus increasing the filtration efficiency due to the particle interception mechanism. Thus, the formation of the spider-net like morphology is desirable in case of the application of a nanofiber layer for filtration.

The SN structures were observed in the electrospun nanofibers obtained from both polyamides. However, not all the experiments were successful in yielding the SN morphology (see Table 3.3.). It can be seen that the polymer concentration was one of the main factors influencing the formation of SN structures. These structures were observed in the higher polymer concentrations of both polyamides, e.g., 14 % w/v for PA 6/6 and 28 % w/v for PA6 solutions in FA (see exp. no. 12, 13, 29, 30). In the case of PA solutions in FA/DCM as a solvent, SN or fragmented spider-net (FSN) structures for lower and middle range of concentrations were observed (see exp. no. 16, 17, 33, 34). The formation of SN structure in exp. no. 16 can be explained by the increased flow of PA solution. The prolonged utilization of the solvent system containing the volatile compounds, such as DCM with the boiling point of 39 °C, causes clogging of the nozzle during the electrospinning process, especially in a low humidity environment (Bhardwaj and Kundu, 2010). The

clogging of the nozzle was as well observed in the study. In order to avoid clogging, the feed rates of the solutions with DCM were increased two-fold, which in turn produced moister nanofibers. Moister nanofibers of electrospun mats exp. no. 16 and 17 were thicker and were characterized by the stick-together morphology. The effective distance between the short oligomeric and monomeric ionic species and amide groups were shorter in such morphology. Therefore, the probability of the hydrogen bond formation mechanism was more viable. Another parameter influencing the formation of the SN structure was the collection time of the nanofiber mat. Only the nanofiber mats with 20 min collection time demonstrated the SN structure (exp. no. 12, 13, 16, 17, 29, 30, 34).

The increased collection time and polymer concentration of PA as well as the presence of DCM were the main factors influencing the formation of SN structure, while the lower voltage (12 kV) and shorter collection time (5 min) were the factors having no effect on the formation SN structures (exp. no. 11, 25, 28). The findings of the thesis agree with the results that were reported previously (Pant et al., 2010) and could be explained by the fact that the lower voltages invoke less ionization of the polyamide solution, resulting in the absence of SN structures. It was demonstrated that the formation of the multi-layer SN structures could be increased by using inorganic salts (NaCl, KBr and $CaCl_2$) for PA 6 and PVA electrospun nanofiber mats (Barakat et al., 2009).

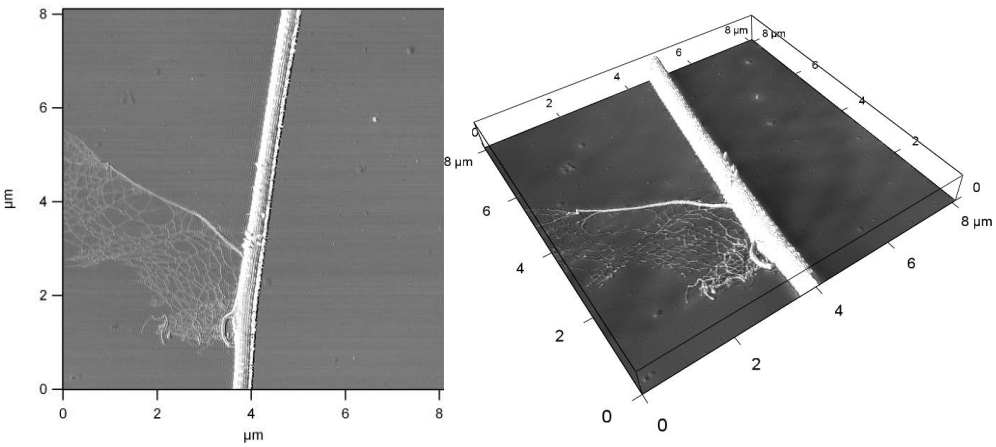

Fig. 3.3. Two-dimensional and three-dimensional AFM images of a single polyamide fiber and the spider-net like (SN) structure

The AFM analysis allowed a more detailed analysis of the formed SN structure. Fig. 3.3. shows single fiber and the attached SN structure of PA 6/6 (exp. no. 16). The width and the height of a single fiber was 465 nm and 220 nm, while the width and height measurements of SN fibers ranged between 9-28 nm and 7-15 nm, respectively.

3.2.2. Partial Least Squares regression analysis of the nanofiber media characteristics

The data collected during the experimental runs were fitted to the PLS model with the aim to establish a relationship between the factors (voltage, tip-to-collector distance, collecting time, solvent system and concentration of solution) and their responses (fiber diameter, basis weight and thickness) of the obtained nanospun fibers. The packing density was not included in the modelling, since it is a function of the fiber basis weight and thickness of the fiber media (Formula 3). The calculated values of the packing density for the samples obtained in this work are presented in Table 3.3. The developed models were rather accurate, as indicated by their high values of R^2 (higher than 0.90 for all the filtering parameters), while the Q^2 values ranged from 0.62 to 0.71.

The results of the effects modelling of polymer solution and electrospinning parameters on PA 6 and PA 6/6 nanofiber media characteristics are presented in Fig. 3.4. The positive values stand for the factors positively affecting the responses, while the negative values represent factors reducing the values of the responses. The error-bars represent the confidence intervals indicating the uncertainty of each factor. The factors were considered statistically insignificant if their confidence intervals included zero.

The analysis of the experimental results agrees with the previous data (Beachley and Wen, 2009; Guerrini et al., 2009; Pant et al., 2012) where the polymer concentration had a substantial impact on the fiber diameter (see Fig. 3.4. a, d). Lower polymer concentrations influenced a greater mobility of the polymer chains and larger instabilities of the polymer jet during the electrospinning. This induced greater stretching of the polymer jet resulting in the lower nanofiber diameters. Higher polymer concentrations caused a restricted movement of the polymer chain, and the jet of polymer was stabilized (Heikkila and Harlin, 2008).

Another factor having great influence on the fiber diameter was the presence of DCM in solvent systems (Fig. 3.4. a). For PA 6/6, a rapid evaporation of DCM from FA/DCM 3:2 v/v system (exp. no. 16 and 17) obstructed the continuous flow of the polymer solution to the nozzle. After the increase of the feed rate of FA/DCM 3:2 v/v, the fiber diameter increased. However, a stick-together morphology became noticeable. In contrast, when PA 6 nanofibers were electrospun with FA/DCM 3:1 v/v solvent system (exp. no. 33 and 34), the influence of DCM solvent on the fiber diameter was found to be negligible. FA/AA 3:2 (v/v) solvent system demonstrated an inverse effect on the fiber diameter (see Fig. 3.4. a, d).

The effects of TTCD and the deposition voltage on the resulting nanofiber diameter were analysed for each concentration of the polymer solution by using experimental data shown in Table 3.3. For PA 6/6, the TTCD had no significant effect on the fiber diameter, whereas an increase in the voltage resulted in a decrease of the fiber diameter. On a contrary to PA 6, a higher voltage (20 kV) combined with a shorter TTCD (7 cm) resulted in the increase of PA 6 fiber diameter. A stronger electric field (kV/cm) was responsible for the formation of thicker electrospun PA 6 fibers, whereas the smallest fibers were obtained at medium values of the electric field. In case of the higher voltage, the jet induced by higher

electrostatic forces and higher repulsive forces favoured the deposition of smaller fibers (Heikkila and Harlin, 2008). However, the higher voltage may cause a higher mass flow resulting in larger fibers. A shorter TTCD caused a deposition of a moister jet and resulted in the coalescence of the fibers leading to a thicker fiber mat, while the longer TTCD enhanced the evaporation of solvent leading to smaller fibers. Similar findings were as well reported previously (Heikkila and Harlin, 2008).

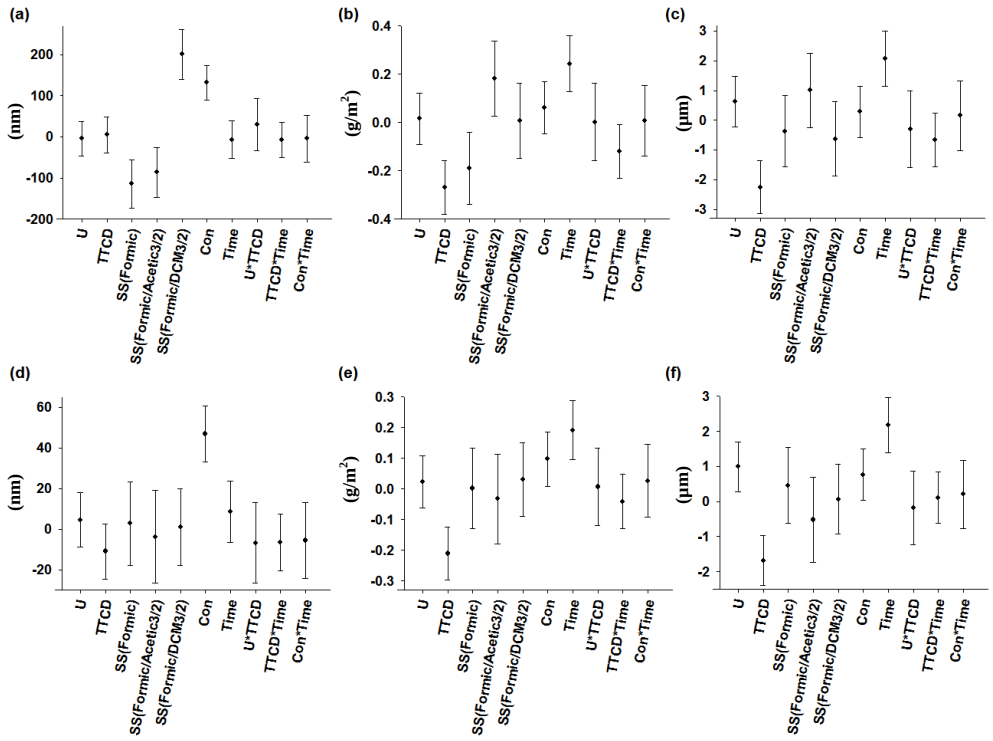

Fig. 3.4. The inputs of polymer solution concentration and electrospinning parameters on air filtration essential nanofiber media characteristics: (a) PA 6/6 fiber diameter, (b) PA 6/6 basis weight, (c) PA 6/6 thickness, (d) PA 6 fiber diameter, (e) PA 6 basis weight, (f) PA 6 thickness. U – voltage, TTCD – tip-to-collector distance, SS – solvent system, Con – concentration

The effect of TTCD and the collection time on the basis weight and the thickness of the nanofibers are presented in Fig. 3.4. b, e and Fig. 3.4. c, f. TTCD had a slightly larger effect on the basis weight and thickness of PA 6/6 fibers with the corresponding negative responses of -0.27 g/m^2 and -2.26 µm, respectively; the collection time had a positive modelled response on the basis weight of PA 6/6 fibers with the corresponding value of 0.24 g/m^2, while the collection time had as well a positive modelled response on the thickness of PA 6 fibers with the value of

2.17 μm. The modelling results clearly showed that the basis weight and thickness of the fibers were dependent not only on the collection time but on the TTCD as well.

3.2.3. Prediction and optimization of the polymer solution and electrospinning parameters

Prediction of PA 6 and PA 6/6 fiber diameter and basis weight through the optimization of the polymer solution and electrospinning parameters provide the prerequisites for the practical usage of the nanofibers for the larger scale air filtration applications. Based on the results of the complex experimental design data, the response surface plots for obtaining nanofiber media with desirable fiber characteristics were derived (see Fig. 3.5.).

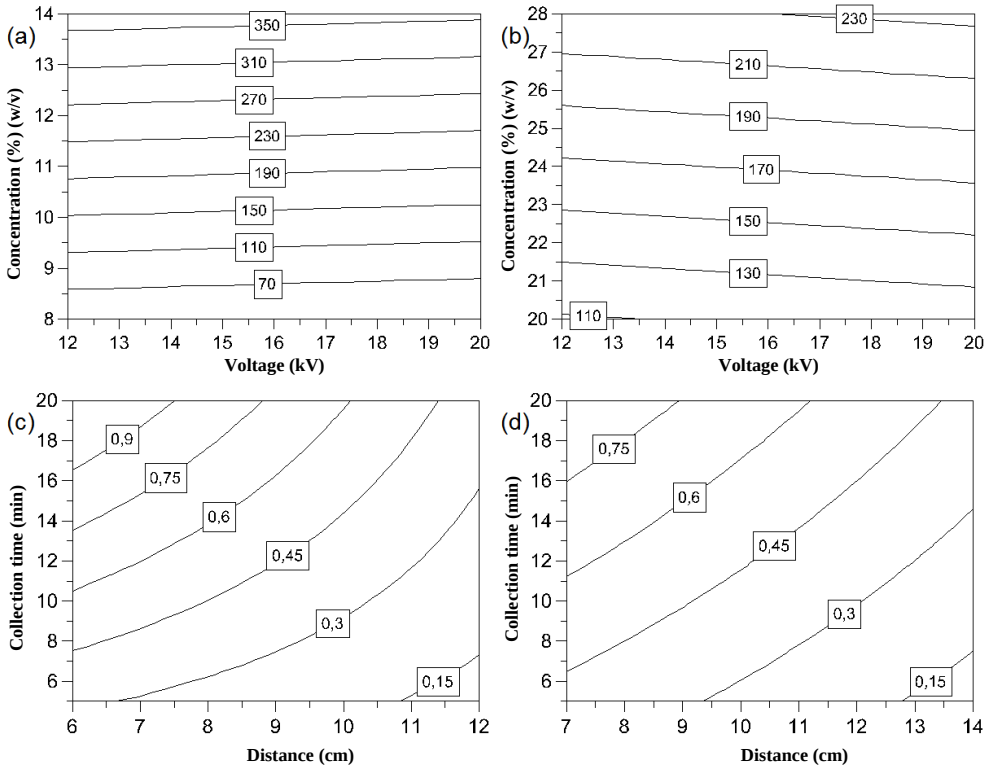

Fig. 3.5. Response surface plots for the prediction of fiber diameter and basis weight through the optimization of the polymer solution and electrospinning parameters: (a) PA 6/6 fiber diameter (TTCD – 9 cm, solvent system – FA, collection time – 12.5 min), (b) PA 6 fiber diameter (TTCD – 10.5 cm, solvent system – FA, collection time – 12.5 min), (c) PA 6/6 basis weight (voltage – 16 kV, concentration – 11 %, solvent system – FA), (d) PA 6 basis weight (voltage – 16 kV, concentration – 24 %, solvent system – FA)

The PLS analysis showed that the fiber diameters of both PA materials were influenced mostly by a single factor, a precursor concentration, while the other factors were almost negligible. However, the voltage was as well chosen as an

important factor for the nanofiber characteristics prediction due to the experimental trends observed for both PA precursors at every used concentration, as discussed in section 3.2.2.

The representative parameters of filtering material productivity are its basis weight and thickness. It has been shown that both parameters mostly depend on the collection time and TTCD and had only minor differences between them in models shown in Fig. 3.5. (b, c for basis weight; e, f for thickness). Basis weight was picked for the filtering media property prediction as a more reliable one due the higher precision measurements obtained in this work.

In order to form nanofibers with the desired diameter (see Fig. 3.5. a) for PA 6/6 and Fig. 3.5. b for PA 6, the determined values of the polymer concentration and electrospinning voltage may be obtained from the data shown in Fig. 3.5. At the same time, the other parameters (TTCD– 9 cm (for PA 6/6), 10.5 cm (for PA 6), solvent system – FA, collection time – 12.5 min) should be maintained constant. Additionally, the deposition parameters, i.e., collection time and the TTCD, of fibers with the specific basis weight (see Fig. 3.5. c for PA 6/6 and Fig. 3.5. d for PA 6) may be as well determined from Fig. 3.5., keeping the other parameters (voltage – 16 kV; concentration – 11 % (for PA 6/6), 24 % (for PA 6); solvent system – FA) constant.

Finally, the size of particles that are filtered is another important parameter in the development of filtration media. It was proposed that for larger particles (100 nm and above), the nanofiber filters with smaller fiber size (150 nm and below), larger packing density (approximately 0.1) and basis weight could be considered (Wang et al., 2008b). For smaller particles (100 nm and below), the filters with larger fiber size (500 nm and above), smaller packing density (approximately 0.01) and the basis weight are suggested (Wang et al., 2008b). From the modelling data presented in Fig. 3.5., it is apparent that for the larger particle filtration, the desirable smaller fiber diameter (150 nm and below) and larger basis weight could be obtained by using high voltage above 16 kV for PA 6/6 and low voltage of less than 16 kV for PA 6. Additionally, low solution concentrations of PA 6/6 less than 10 % w/v and less than 22.5 % w/v for PA 6 as well as a high collection time for both PA precursors (above 16 min) combined with a short TTCD of ~6 cm and ~7 cm for PA 6/6 and PA 6, respectively, should be used to obtain the filtering material mats necessary for larger particle filtration. For smaller particle filtration, the desirable larger fiber diameter of 500 nm and above could not be produced by using the data obtained *via* modelling in Fig. 3.5., but it can be produced by using FA/DCM solvent system for PA 6/6 at higher concentration ranges (see Table 3.3., exp. no. 16). Another alternative is to use other polymers such as PMMA that are able to generate fibers *via* electrospinning with diameters up to several micrometres, especially when mixed with the volatile solvents (Qian et al., 2010).

3.3. The comparison of the filtration properties of electrospun polyamide, polyvinyl acetate, polyacrylonitrile and cellulose acetate nanofiber media

The nanofiber media produced from different polymers *via* electrospinning were examined for the removal of aerosol particles from the airflow. From the literature analysis given in subsection 1.3.2. and the results delivered in subsections 3.1. and 3.2., PA 6/6, PA 6, CA and PAN were selected for the further comparative studies. Additionally, polyvinyl acetate (PVAc) was included in the research, because the PVAc is characterized by adhesive properties and is insoluble in water, but it is slightly hydrophilic and is able to absorb water to some extent (Park et al., 2008). Based on the literature analysis and discussion presented in subsections 1.3.3. and 1.4., it is useful to perform the comparative work of electrospun nanofibers produced from various polymeric materials for their suitability and performance to be used as the air filters. Among PA 6, PA 6/6 and PAN nanofiber media filters, the application of electrospun PVAc and CA nanofiber media as the air filters is reported for the first time.

3.3.1. The characteristics of the electrospun nanofiber media

The representative SEM images of nanofiber media electrospun from the four polymeric materials are shown in Fig. 3.6. The morphology of the nanofiber media as well as the range of fiber diameter has derived from the SEM images, while the basis weight was estimated by the experimental measurements. The morphological characterization, range of fiber diameter and the basis weight for each fiber medium are presented in Table 3.4. Three different morphological formations: fibers, uniform fibers (smooth) and beaded fibers (having micro and nano sized embedded beads along the fiber axis) were defined. In order to distinguish between the fibers and uniform fibers, the methodology described in subsection 3.2.1. was used. In case the ratio of the standard deviation of the fiber diameter to the mean of the fiber diameter (SD)/(FD) was > 0.3, this fiber media morphology was considered not uniform, while the SD/FD ratio < 0.3 indicated a uniform (smooth) fiber media. The ratio of SD/FD defined as a coefficient of variation (CV) is as well given in Table 3.4.

The formation of beaded fibers can be explained by the increased molecular entanglement of the polymer chains, which is high enough to prevent a complete breakup of the charged jet; at the same time, it is not high enough to suppress the occurrence of the capillary instability (Somvipart et al., 2013). A desired polymer concentration (in the lower range of spinnable concentration for most polymers) (Cramariuc et al., 2013; Munir et al., 2009; Somvipart et al., 2013) as well as a higher voltage (for smaller electrospinning distances) (Cramariuc et al., 2013) are the key parameters in the formation of beaded fibers. At higher polymer concentrations, the regular fibers are produced because the viscoelastic forces from the entanglement become predominant and suppress the prevalence of the capillary instability (Cui et al., 2007; Somvipart et al., 2013).

Table 3.4. The characteristics of produced nanofibers

ID	Morphology	Fiber diameter, nm	Coefficient of variation	Basis weight, g/m^2
PA6/6_120s	Uniform fibers	149±34	0.23	1.36±0.25
PA6/6_120l	Fibers	362±131	0.36	1.55±0.27
PA6/6_160l	Fibers	373±119	0.32	2.07±0.30
PA6_300	Fibers	326±100	0.31	4.56±0.28
PVAc_30	Beaded fibers*	331±94	0.28	6.45±0.31
PVAc_40	Beaded fibers*	298±101	0.34	8.09±0.90
PVAc_60	Beaded fibers*	235±65	0.28	11.34±0.40
PVAc_80	Beaded fibers*	399±109	0.27	12.03±0.76
PAN_40_6	Beaded fibers*	292±101	0.35	3.36±0.41
PAN_40_8	Uniform fibers	512±35	0.07	3.88±0.32
PAN_60	Uniform fibers	437±60	0.14	4.37±0.23
PAN_80	Uniform fibers	535±55	0.10	5.26±0.31
CA_40	Fibers	350±129	0.37	8.89±0.52
CA_70	Fibers	363±131	0.36	23.67±1.04

*The morphology of beaded fibers has been directly derived from the SEM images, not from the values of the variation coefficient

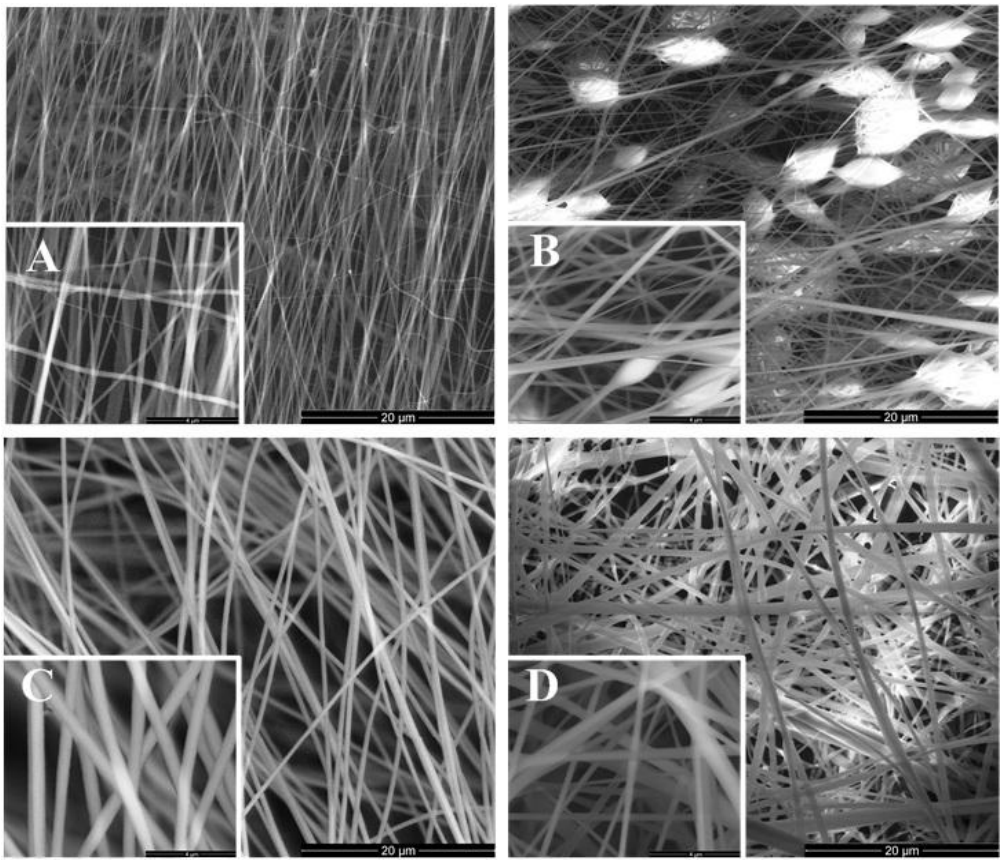

Fig. 3.6. SEM images of the electrospun nanofibers media filters: (a) PA6/6_120s, (b) PVAc_60, (c) PAN_80, (d) CA_70

All the electrospun PVAc fiber mats showed the morphology of beaded fibers (see Fig. 3.6. b). The concentration of PVAc solution was the highest compared to the other polymers (see Table 2.2.); moreover, the PVAc polymer used in this study had a relatively lower molecular weight compared to the other PVAc polymers available on the market. The PVAc fiber media was formed by using the highest (24 kV) fixed voltage (see Table 2.2.). The formation of beaded fibers was observed in PAN_40_6 mats as well. The concentration of polymer solution was the lowest amongst all the PAN mats. The average diameter of the fiber beads varied from 1 to 5 μm. The PVAc_60 mats were characterized by the largest number of beaded fibers with the mean diameter of beads of 3.28 μm, while the PVAc_80 specimens indicated a smaller amount of beads with the mean diameter of 2.99 μm. Due to the lower collection time in the electrospinning process, the fiber media PVAc_30, PVAc_40 and PAN40_6 had the lowest amount of beaded fibers.

As seen in Fig. 3.6. a, the fiber media formed from 9 % (w/v) PA6/6 solution exhibited smooth fibers with the mean diameter of 149 nm. PA6/6_120s nanofiber mats were characterized by the smallest fiber diameter among all the nanofiber mats. PAN nanofiber media PAN_40_8, PAN_60 and PAN_80 (see Fig. 3.6. c) as well exhibited continuous smooth fibers with uniform orientation. The mean fiber diameter varied between 437-535 nm and was the highest among the all analysed media, while the fiber diameter of the another nanofiber media (PA6/6_l, PA6_300, PVAc's and CA's) ranged between 235 nm (PVAc_60) and 399 nm (PVAc_80).

The basis weight of nanofiber media filters increases with the electrospinning duration. Thus, the mats with longer electrospinning deposition time had the larger basis weight. The largest basis weight was observed in CA medium, which could be considered as a function of the electrospinning duration combined with the polymer solution feed rate (see Table 2.2.). Accordingly, CA_70 nanofiber medium had the largest basis weight of 23.67 g/m^2, while PA6/6_120s exhibited the lowest basis weight - 1.36 g/m^2.

3.3.2. Filtration efficiency of the polystyrene latex aerosol particles

The results of filtration testing using 100 and 300 nm PSL particles are presented in Table 3.5. The SEM image of filtered PVAc_60 nanofiber media filter with captured 100 and 300 nm PSL particles is presented in Fig. 3.7.

The filtration tests included single nanofiber media and multi-ply nanofiber media (indicated as x2 and x3). The multi-ply nanofiber media has been proposed in previous studies as well (Leung et al., 2010; Zhang et al., 2010). Filters with the multi-ply structure are expected to improve the filtration performance with respect to the higher efficiency together with a lower pressure drop.

Electrospun PVAc and PAN nanofiber media had higher filtration efficiency than PA6/6, PA6 and CA media. PVAc80 fiber media achieved the highest filtration efficiency: for 100 nm particles, it was 99.57 %, and for 300 nm particles, it was 97.38 %. The filtration efficiency of PAN80 media for 100 nm particles was 98.01 %, while PAN40_8x3 for 300 nm particles showed 96.02 % efficiency. A relatively large pressure drop accompanied these high filtration efficiencies: PVAc80 – 132.83 Pa, PAN80 – 90.37 Pa and PAN40_8x3 – 99.80 Pa. Despite the longer deposition

time of PA mats and higher feed rate of CA mats in electrospinning process, which were responsible for the largest basis weight, the nanofiber media from PA6/6, PA6 and CA indicated lower than 91 % filtration efficiency and a pressure drop > 100 Pa. Such differences in filtration performance can be explained by the different morphologies of nanofiber media. Filters produced from PVAc were related to the enrichment of media with the volume fraction of beaded fibers (discussed in the subsection 3.3.1.). The beaded fibers are responsible for better physical separation of the nanofiber layers and the increase of the distance between nanofibers, which as well increases the air permeability together with the filtration performance (Yun et al., 2010). While a good filtration performance of PAN nanofiber media filters can be explained by the porous PAN fibers (Yu et al., 2010; Nataraj et al., 2012) and very smooth, continuous orientated fibers with narrow diameter distributions (Chen and Yu, 2010; Ji and Zhang, 2008) as presented in this thesis (see Fig. 3.6. c and Table 3.4.). Moreover, PAN nanofibers cause a gas flow slip regime (values of Knudsen number are in this regime or very close), which contributes to such good filtration performance. The fiber diameters of electrospun nanofiber media presented in this thesis varied between 149-535 nm, accordingly, and *Kn* ranged between 0.890-0.249. Only for PAN_80 nanofiber mats, the airflow conditions reached the slip flow regime with the *Kn* of 0.249; other nanofiber media was exposed to the transition regime of the airflow. The transition regime under $Kn<1$ has a synonymous name as well, i.e., a large slip (Hung and Leung, 2011). Despite the lack of comprehensive theoretical predictions on the filtration performance of electrospun fibers in moderate slip regime (Ahn et al., 2006; Hung and Leung, 2011), the nanofiber media tested in this thesis demonstrated a good filtration capability.

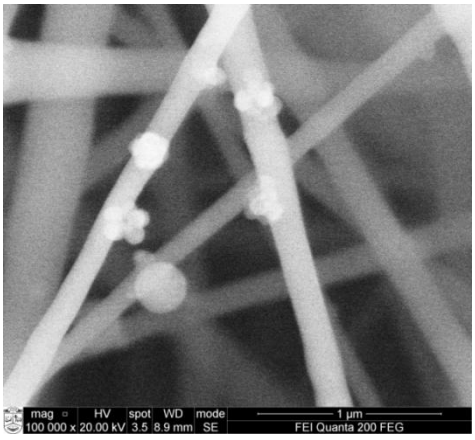

Fig. 3.7. The SEM image of the filtered PVAc_60 nanofiber media filter with captured PSL particles

The comparison of filtration efficiency and pressure drop from the other studies is summarized in Table 1.3.

Table 3.5. Filtration properties of the nanofiber media (mean±standard deviation)

ID	Pressure drop, Pa	Filtration efficiency, %, at		Quality factor, (Pa^{-1}), at	
		100 nm	300 nm	100 nm	300 nm
PA6/6_120s	50.77±3.67	62.02±3.17	72.30±2.75	0.019	0.025
PA6/6_120sx2	94.13±2.74	82.83±2.31	87.6±2.01	0.019	0.022
PA6/6_120sx3	125.50±3.32	85.36±2.72	90.17±1.89	0.015	0.019
PA6/6_120l	5.10±2.01	24.33±3.34	22.22±3.89	0.055	0.049
PA6/6_120lx2	9.60±2.22	26.43±3.05	24.22±3.54	0.032	0.029
PA6/6_120lx3	14.02±2.39	32.16±2.56	32.02±2.89	0.028	0.028
PA6/6_160l	18.70±1.70	25.79±0.13	26.69±0.05	0.016	0.017
PA6_300	148.00±17.19	84.73±1.94	89.24±1.38	0.013	0.015
PVAc_30	4.93±1.31	21.51±0.53	21.16±2.18	0.049	0.047
PVAc_30x2	8.80±1.98	26.62±1.24	23.61±1.87	0.035	0.031
PVAc_30x3	15.20±2.01	36.29±1.67	31.81±1.48	0.030	0.025
PVAc_40	21.68±4.92	39.73±6.51	43.20±6.57	0.023	0.026
PVAc_60	80.57±16.03	98.79±0.37	96.79±0.49	0.055	0.042
PVAc_80	132.83±15.49	99.57±0.31	97.38±0.16	0.041	0.027
PAN_40_6	21.37±1.25	55.94±2.17	59.92±2.30	0.038	0.043
PAN_40_6x2	42.40±2.10	80.90±1.45	83.36±1.98	0.039	0.042
PAN_40_6x3	60.00±2.45	86.61±1.23	88.27±1.55	0.034	0.036
PAN_40_8	33.77±8.39	77.64±6.27	79.49±6.75	0.044	0.047
PAN_40_8x2	64.01±4.21	94.29±2.52	91.89±3.01	0.045	0.039
PAN_40_8x3	99.80±2.10	95.91±1.20	96.02±1.34	0.032	0.032
PAN_60	64.60±1.54	94.24±0.90	91.96±0.94	0.044	0.039
PAN_80	90.37±2.57	98.01±0.47	95.83±0.35	0.043	0.035
CA_40	6.57±0.25	24.47±1.77	24.18±2.61	0.043	0.042
CA_40x2	13.6±2.43	44.30±1.57	30.74±1.76	0.043	0.027
CA_40x3	20.2±2.78	55.51±1.42	50.79±1.36	0.040	0.035
CA_70	49.03±1.21	62.91±0.59	60.22±2.16	0.020	0.019
CA_70x2	105.99±2.49	85.83±1.24	84.40±1.80	0.018	0.018
CA_70x3	139.90±3.81	88.64±1.00	88.59±0.92	0.016	0.016

It is important to note that nearly all the nanofiber mats had a better filtration efficiency for 100 nm PSL particles than for 300 nm particles. A few exceptions were observed with PA6/6_120s and PA6_300 nanofiber media: PA6/6_120s had ~10.3 % higher efficiency for 300 nm particles than 100 nm particles, and PA6_300 had ~4.5 % higher efficiency for 300 nm particles than 100 nm. The PA6/6_120s nanofiber medium was characterized by a fiber diameter of 149 nm and is expected to have most penetrating particle size (MPPS) in the range between 150 and 100 nm. Thus, the particles of a larger diameter (300 nm) should be primarily trapped by the interception and to some extent inertial impaction mechanisms. The result obtained in this thesis correspond to the findings of other authors (Wang et al., 2008a) and support the idea that nanofiber media with a low fiber diameter (<200 nm) are more suitable for the filtration of bigger particles, while the filter media with comparatively high fiber diameter (>500 nm) are more suitable for the filtration of smaller particles (~100 nm). The decreasing fiber diameter and increasing basis weight of nanofiber filters transfers the MPPS to the smaller range of sizes (Hinds, 1999; Leung et al., 2010; Wang et al., 2008a).

3.3.3. Quality factors of one-ply and multiply nanofiber media

The filtration *QF*s have derived from the experimental results of filtration efficiency and pressure drop and are presented in Table 3.5.

The comparison of single-ply to multi-ply nanofiber mats of the same medium showed that only some of the multi-layer media increased their *QF*. The relationships between the basis weight and *QF* for separation of 100 and 300 nm PSL particles are presented in Fig. 3.8. The *QF*s of multi-ply mats from CA and PA_6/6l dramatically decreased with the growth of basis weight, while the decrease of *QF*s of PAN mats was rather moderate. The multi-ply structures of PA6/6_120sx2, PA6/6_120sx3 compared to a single-ply PA6/6_120 mats decreased *QF*s as well. The same could be said about PA6/6_120lx and PVAc_30x single-ply media. While the nanofiber media produced from PAN and CA polymers were able to improve *QF* in multi-ply formations, the PAN_40_6x2 nanofiber media for 100nm particles showed slightly higher *QF* = 0.039 Pa^{-1} compared to *QF* = 0.038 Pa^{-1} of PAN_40_6 (not presented in Fig. 3.8.), the PAN_40_8x2 compared to PAN_40_8 for 100 nm particles (accordingly, QF = 0.045 and 0.044 Pa^{-1}), the CA_40x2 compared to CA_40 for 100 nm particles (accordingly, *QF* = 0.0430 and 0.0427 Pa^{-1}), and CA_40x3 compared to CA_40x2 for 300 nm particles (accordingly, *QF* = 0.035 vs. 0.027 Pa^{-1}). These nanofiber media were characterized by 40 min (shorter compared to the other specimen) deposition time.

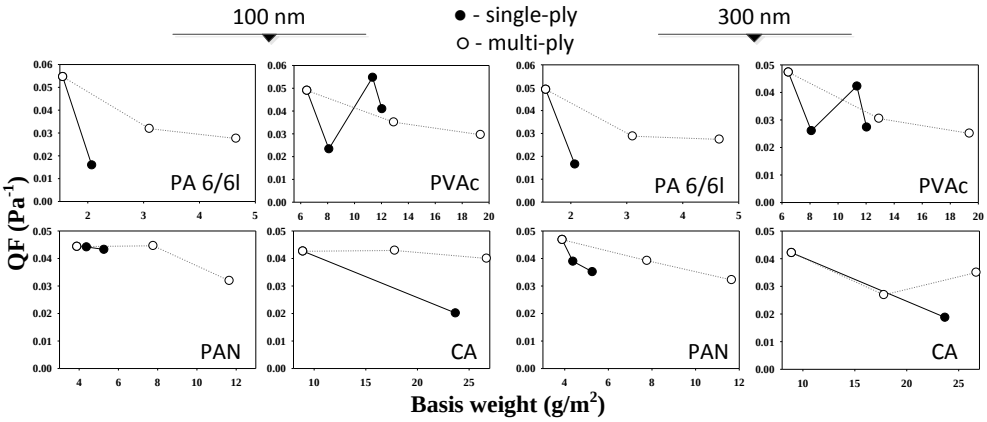

Fig. 3.8. The relationships between the filtration quality factors and basis weight of single-ply and multi-ply nanofiber media using 100 and 300 nm PSL particles

The exception of the QF value in the single-ply form was PVAc nanofiber media filter. In case of the basis weight of 11.34 g/m2, the PVAc nanofiber media filter (i.e. PVAc_60, the second filled dot from the right in Fig. 3.8._PVAc) was able to improve QF in comparison to the previous value of PVAc single filter with a lower basis weight. The lowest fiber diameter (235 nm), higher amount of beads and the optimal collection time in electrospinning of PVAc_60 nanofiber media filter were the main contributors of this phenomenon.

The findings of this thesis show that the *QF* of multi-ply nanofiber media with shorter electrospinning time (i.e. lower basis weight) can increase by the negligible margin or even slightly decrease when filtering 100 and 300 nm particles. This corresponds with the findings of the other authors (Leung et al., 2010; Zhang et al., 2010). Leung et al., (2010) showed that N3S one-ply nanofiber media for 100 and 300 nm particles had the highest filtration *QF* in comparison to two or three-ply layers. The authors argued that the improvements in *QF* by using multi-ply layers become more significant at higher basis weight of the nanofiber media. Zhang et al., (2010) as well investigated the filtration performance of multi-ply nanofiber structures. They found that the multi-ply nanofiber media filter with very low deposition (5 min) time had almost double better *QF* than the one-ply, while other multi-ply nanofiber filter with longer deposition time (15 min) showed only slightly better *QF* than the multi-ply. However, the nanofiber media filters in that study were characterized by the lower uniformity due to the absence of rotating drum system in electrospinning.

Table 1.3. summarizes the *QF* together with the other filtration properties for 300 nm particle size (characterized as MPPS for HEPA filters by the European Standard EN1822-1) obtained by different authors. Only characteristics of nanofiber media with the best filtration performance are presented.

Comparing the results obtained in this thesis with the results presented in Table 1.3., considering both high efficiency and *QF*, the attention should be drawn to the nanofiber media filters of PAN_60, PAN_80, PAN_40_8x3 (Table 3.5.), PVAc_60 and PVAc_80. The PVAc_60 had the highest *QF* (0.042 Pa^{-1}) and the second high efficiency (96.79 % at 300 nm) from this group filters due to the morphology of beaded fiber, which was characterized by the smallest fiber diameter (see Table 3.4.) and larger beads than in other nanofiber media filters. Such great structure was responsible for the richer volume fraction with deeper physical separation of the nanofibers (Yun et al., 2010) compared to the PVAc_80 nanofiber media filter. The PVAc_80 nanofiber media filter, despite the larger fiber diameter (see Table 3.4.) and larger beads, showed the highest efficiency (97.38 %) among all the filters presented in this thesis, when filtering 300 nm PSL particles.

3.3.4. Comparison of the filtration efficiency of polystyrene latex monodispersed and sodium chloride poly-dispersed aerosols

Based on the results obtained from the filtration performance with PSL particles, the authors selected the specimens with the highest filtration efficiency and QF and performed additional filtration efficiency tests with NaCl particles ranging in diameter between 6 and 1000 nm. The representative nanofiber mats from PAN_60, PAN_80, PVAc_60 and PVAc_80 were analysed for the filtration efficiency. The results shown in Fig. 3.9. demonstrate that the PVAc_80 nanofiber medium achieved the highest filtration efficiency (98.09-99.99 %) for 30-300 nm particles, while PAN_80 nanofiber medium indicated the highest filtration efficiency (~98.50 %-99.99 %) for 300-600 nm particles. All the selected specimens showed very good filtration results (~100 %) for the particles larger than 600 nm.

MPPS determines the particle size, at which the filter media is least efficient (Lalagiri et al., 2013). Theoretically, the MPPS is a region of minimum filtration efficiency somewhere between 50-500 nm (Hinds, 1999; Park et al., 2011). Particles in this range are too large to be effectively pushed around by the diffusion and too small to be effectively captured by the interception or impaction. In contrast, the diffusion dominates for the particles smaller than 100 nm, and the particles above 500-600 nm may be captured by interception and inertial impaction. The MPPS of PVAc_60, PAN_80 nanofiber media ranged between 200 and 300 nm, while for PVAc_80, the MPPS was shifted towards 300 nm size, whereas MPPS PAN_60 indicated MPPS below 200 nm (as well see Table 3.4. for fiber diameter and basis weight comparison). According to filtration theories (Hinds, 1999; Leung et al., 2010; Wang et al., 2008a), the decreasing fiber diameter and increasing packing density of filters transfers the MPPS to the smaller range of sizes.

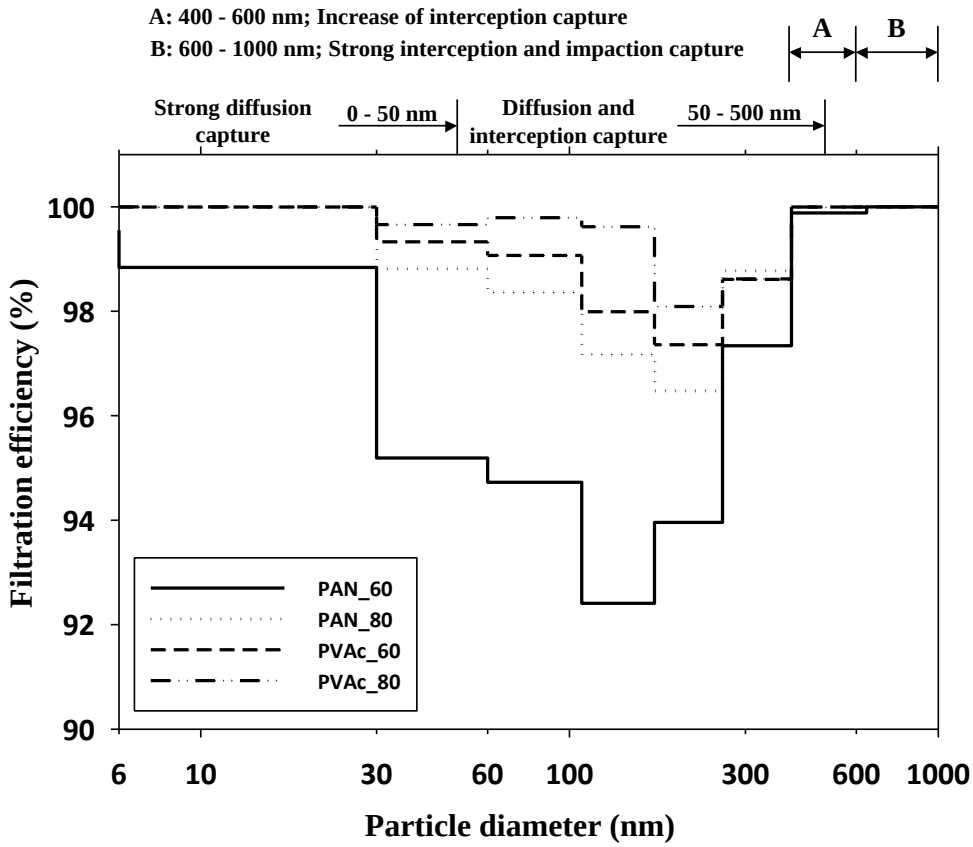

Fig. 3.9. The relationship between the filtration efficiencies (%) and size of NaCl aerosol particles (nm) at 5.3 cm/s face velocity

It is interesting to note that the nanofiber filters tested for NaCl aerosol particles showed slightly higher filtration efficiency compared to the respective fiber

mats analysed for the PSL particles separation (the same size of particles and fixed average pressure drop values). The filtration efficiency when separating 100 and 300 nm NaCl particles was on average ~0.65 % higher than separating the same size PSL particles (differences are statistically insignificant according to Mann-Whitney U test ($p>0.05$)). Irregular NaCl particles of larger density may have a larger aerodynamic diameter as compared to their physical diameter (DeCarlo et al., 2004). This leads to the greater capture efficiency for 100 nm NaCl particles, due to the stronger diffusion interaction with the fiber. At the same time, ELPI may have attributed NaCl particles smaller than 100 nm by physical diameter to channel No. 5 ($d50=0.094$ μm). The aerodynamic particles size distributions can be slightly underestimated, because there is a relatively wide cutoff aerodynamic diameter of the stages in ELPI (Järvinen et al., 2014). Thus, some uncertainty is introduced when counting particles, which by diameter are very close to 100 nm or 300 nm. Particles of NaCl are as well less penetrating than the spherical plastic ones (Grinshpun et al., 2014). The same study reports that the penetration of particles from combustion processes was significantly higher than that of NaCl particles, and the biggest difference was observed between the plastic and NaCl particles. The authors of the mentioned study discussed that the differences in efficiency can be attributed to the interaction between the particles and filter fibers (particle morphology, charges, surface properties etc.). PSL particles (dynamic shape factor (DSF) ~1) are ideal spheres, as opposed to the variously shaped NaCl particles, which may be nearly spherical (DSF – ~1.02), cubes (DSF – 1.065 – 1.17) and agglomerates (DSF – 1.3 - 1.4) as a result of coagulation (Zelenyuk et al., 2006). Nearly cubical are the smaller particles with more rounded edges and cubic particles or agglomerates with higher DSF associated with a larger fraction of rectangular prisms. These types of particles have higher chance to collide with the fiber media, which in turn may result in better filtration efficiency.

4. CONCULSIONS

1. The regular electrospun cellulose acetate fibers were prepared from a novel ternary acetone/*N*,*N*-dimethylformamide/dichloromethane solvent system with an optimized ratio of 2/1/1 v/v/v. The electrospinning of the 11 and 12 % (w/v) cellulose acetate solutions have resulted in a uniform morphology of the nanofiber media with the mean fiber diameter of 241-264 nm.
2. The experimental results showed that the polyamide 6/6 had a wider distribution of the fiber diameter (60-376 nm) compared to the polyamide 6 (90-236 nm). The increase of polymer concentration was responsible for the increase of fiber diameter: the marginal diameters of polyamide 6/6 were received for 8 and 14 % w/v of polymer concentration, while for polyamide 6/6, the marginal diameters were obtained for 20 to 28 % w/v polymer concentration solutions. The collection time as well as tip-to-collector distance had more significant effect on the basis weight of the nanofibrous materials from polyamide 6/6; the increase of collection time by 15 min in average raised the basis weight by 0.24 g/m^2, while the increase of distance by 6 cm decreased the basis weight values on average by -0.27 g/m^2.
3. The comparative filtration properties of the single-ply polyamide 6, polyamide 6/6, polyvinyl acetate, polyacrylonitrile and cellulose acetate nanofiber media mats indicated that polyvinyl acetate and polyacrylonitrile media have the highest filtration efficiencies and quality factors. Due to the unique morphology of the beaded nanofibers, the polyvinyl acetate media were characterized by the ultimate values of quality factors and filtration efficiencies: 0.0548 Pa^{-1} (98.79 %) for 100 nm particles and 0.0423 Pa^{-1} (96.79 %) for 300 nm particles, accordingly.
4. The comparison of single-ply to multi-ply nanofiber mats of the same medium showed that only some polyacrylonitrile and cellulose acetate of the multi-layer media increased their quality factor compared to the single-ply form. The increase interval was between 0.0003 and 0.008 Pa^{-1}.
5. The comparison of filtration efficiency of polystyrene latex and sodium chloride aerosol particles showed moderate difference. The filtration efficiency of 100 and 300 nm sodium chloride particles was on average ~ 0.65 % higher compared to the same size polystyrene latex particles.

REFERENCES

1. AGARWAL, S. et al. Functional Materials by Electrospinning of Polymers. *Progress in Polymer Science*, 2013, 38(6), 963-991. ISSN 0079-6700.
2. AHN, Y. C. et al. Development of High Efficiency Nanofilters Made of Nanofibers. *Current Applied Physics*, 2006, 6(6), 1030-1035. ISSN 1567-1739.
3. ALARAJ, M. et al. Microbial Fuel Cell Energy Harvesting Using Synchronous Flyback Converter. *Journal of Power Sources*, 2014, 247, 636-642. ISSN 0378-7753.
4. ALONSO, M. et al. The Measurement of Charging Efficiencies and Losses of Aerosol Nanoparticles in a Corona Charger. *Journal of Electrostatics*, 2006, 64(3-4), 203-214. ISSN 0304-3886.
5. ANDERSSON, R. L. Micromechanics of Ultra-Toughened Electrospun PMMA/PEO Fibres as Revealed by In-Situ Tensile Testing in an Electron Microscope. *Scientific Reports*, 2014, 4(6335), 1-8. ISSN 2045-2322.
6. ANDRADY, A. L. *Science and Technology of Polymer Nanofibers*. John Wiley and Sons: Hoboken, 2008.
7. ARSHAK, K. I. and B. ALMUKHTAR. The Design and Development of a Novel Flyback Planar Transformer for High Frequency Switch Mode DC–DC Converter Applications. *Microelectronics Journal*, 2000, 31, 929-935. ISSN 0026-2692.
8. ASKARI, M. et al. Fabrication of High Performance Chitosan/Polyvinyl Alcohol Nanofibrous Mat with Controlled Morphology and Optimised Diameter. *The Canadian Journal of Chemical Engineering*, 2014, 92(6), 1008-1015. ISSN 1939-019X.
9. BAE, H. S. et al. Fabrication of Highly Porous PMMA Electrospun Fibers and Their Application in the Removal of Phenol and Iodine. *Journal of Polymer Research*, 2013, 20(158), 1-7. ISSN 1022-9760.
10. BAGHERI, H. et al. Novel Polyamide-Based Nanofibers Prepared by Electrospinning Technique for Headspace Solid-Phase Microextraction of Phenol and Chlorophenols from Environmental Samples. *Analytica Chimica Acta*, 2012, 716, 34-39. ISSN 0003-2670.
11. BARAKAT, N. A. M. et al. Spider-Net within the N6, PVA and PU Electrospun Nanofiber Mats Using Salt Addition: Novel Strategy in the Electrospinning Process. *Polymer*, 2009, 50(18), 4389-4396. ISSN 0032-3861.
12. BARHATE, R. S. et al. Porous Nano- and Microfibrous Polymeric Membrane Material for Catalytic Support. *Chemical Engineering Research and Design*, 2011, 89(6), 621-630. ISSN 0263-8762.
13. BARHATE, R. S. and S. RAMAKRISHNA. Nanofibrous Filtering Media: Filtration Problems and Solutions from Tiny Materials. *Journal of Membrane Science*, 2007, 296, 1-8. ISSN 0376-7388.
14. BARON, P. A. and K. WILLEKE. *Aerosol Measurement: Principles, Techniques and Applications*. John Wiley and Sons: New York, 2001.
15. BAZBOUZ, M. B. and G. K. STYLIOS. The Tensile Properties of Electrospun Nylon 6 Single Nanofibers. *Journal of Polymer Science Part B: Polymer Physics*, 2010, 48(15), 1719-1731. ISSN 1099-0488.

16. BEACHLEY, V. and X. WEN. Effect of Electrospinning Parameters on the Nanofiber Diameter and Length. *Materials Science and Engineering: C Materials for Biological Applications*, 2009, 29(3), 663-668. ISSN 0928-4931.
17. BHARDWAJ, N. and S. C. KUNDU. Electrospinning: a Fascinating Fiber Fabrication Technique. *Biotechnology Advances*, 2010, 28(3), 325-347. ISSN 0734-9750.
18. BIANCO, A. et al. Electrospun PHBV/PEO Co-Solution Blends: Microstructure, Thermal and Mechanical Properties. *Materials Science and Engineering C*, 2013, 33, 1067-1077. ISSN 0928-4931.
19. BOSS, M. J. and D. W. DAY. *Building Vulnerability Assessments: Industrial Hygiene and Engineering Concepts*. CRC Press, Taylor and Francis Group, 2009. ISBN 13:978-1-4200-7483-3.
20. BOSWORTH, L. and S. DOWNES. Acetone, a Sustainable Solvent for Electrospinning Poly(ε-Caprolactone) Fibres: Effect of Varying Parameters and Solution Concentrations on Fibre Diameter. *Journal of Polymers and the Environment*, 2012, 20(3), 879-886. ISSN 1566-2543.
21. BROWN, R. C. *Air Filtration: An Integrated Approach to the Theory and Applications of Fibrous Filters*. Elsevier Science: Oxford, 1993.
22. BUTLER, I. *Nonwoven Fabrics Handbook*, INDA: Cary, 1999.
23. CELEBIOGLU, A. and T. UYAR. Electrospun Porous Cellulose Acetate Fibers from Volatile Solvent Mixture. *Materials Letters*, 2011, 6, 2291-2294. ISSN 0167-577X.
24. CHANG, W. M. et al. The Combination of Electrospinning and Forcespinning: Effects on a Viscoelastic Jet and a Single Nanofiber. *Chemical Engineering Journal*, 2014, 244, 540-551. ISSN 1385-8947.
25. CHEN, H. M. and D. G. YU. An Elevated Temperature Electrospinning Process for Preparing Acyclovir-Loaded PAN Ultrafine Fibers. *Journal of Materials Processing Technology*, 2010, 210(12), 1551-1555. ISSN 0924-0136.
26. CHEN, Y. et al. Measurements of Emission Factors of PM2.5, OC, EC, and BC for Household Stoves of Coal Combustion in China. *Atmospheric Environment*, 2015, 109, 190-196. ISSN 1352-2310.
27. CHEN, S. et al. Nanostructure Science and Technology. In *Electrospun Nanofibers for Energy and Environmental Applications* edited by Ding, B. and J. Yu. Spinger, Heidelberg. 2014. pp. 91-110. ISBN 978-3-642-54159-9.
28. CHEN, W. et al. Carbon Nanotube-Reinforced Polyurethane Composite Fibers. *Composites Science and Technology*, 2006, 66, 3029-3034. ISSN 0266-3538.
29. CHEN, W. et al. Dexamethasone Loaded Core–Shell SF/PEO Nanofibers via Green Electrospinning Reduced Endothelial Cells Inflammatory Damage. *Colloids and Surfaces B: Biointerfaces*, 2015, 126, 561-568. ISSN 0927-7765.
30. CHOWDHURY, M. and G. STYLIOS. Effect of Experimental Parameters on the Morphology of Electrospun Nylon 6 Fibres. *International Journal of Basic and Applied Sciences*, 2010, 10(6), 70-78. ISSN 2077-1223.
31. CHUANFANG, Y. Aerosol Filtration Application Using Fibrous Media - An Industrial Perspective. *Chinese Journal of Chemical Engineering*, 2012, 20(1), 1-9. ISSN 1004-9541.

32. COLVILE, R. N. et al. The Transport Sector as a Source of Air Pollution. *Atmospheric Environment*, 2001, 35(9), 1537-1565. ISSN 1352-2310.

33. CRAMARIUC, B. et al. Fiber Diameter in Electrospinning Process. *Journal of Electrostatics*, 2013, 71(3), 189-198. ISSN 0304-3886.

34. CUI, W. et al. Investigation on Process Parameters of Electrospinning System through Orthogonal Experimental Design. *Journal of Applied Polymer Science*, 2007, 103(5), 3105-3112. ISSN 1097-4628.

35. DECARLO, P. F. et al. Particle Morphology and Density Characterization by Combined Mobility and Aerodynamic Diameter Measurements. Part 1: Theory. *Aerosol Science and Technology*, 2004, 38, 1185-1205. ISSN 0278-6826.

36. DING, B. et al. Fabrication of Blend Biodegradable Nanofibrous Nonwoven Mats via Multi-Jet Electrospinning. *Polymer*, 2004, 45, 1895-1902. ISSN 0032-3861.

37. European Standards for Efficient Particulate Air Filters (EPA), High Efficiency Particulate Air Filters (HEPA) and Ultra Low Penetration Air Filters (ULPA) Used in the Field of Ventilation and Air Conditioning and for Technical Processes, EN 1822-1-5:2009, High Efficiency Air Filters (EPA, HEPA and ULPA).

38. FENG, S. and X. SHEN. Electrospinning and Mechanical Properties of Polystyrene and Styrene-Isoprene-Styrene Block Copolymer Blend Nanofibres. *Journal of Macromolecular Science, Part B*, 2010, 49(2), 345-354. ISSN 0022-2348.

39. FISK, W. J. et al. Performance and Costs of Particle Air Filtration Technologies. *Indoor Air*, 2002, 12(4), 223-234. ISSN 1600-0668.

40. FORD, R. G. Method Developed for Mass Production of Nanofibers. *MRS BULLETIN*, 2011, 36, 249. ISSN 0883-7694.

41. FORWARD, K. M. and G. C. RUTLEDGE. Free Surface Electrospinning from a Wire Electrode. *Chemical Engineering Journal*, 2012, 183, 492-503. ISSN 1385-8947.

42. GOPIRAMAN, M. et al. Structural and Mechanical Properties of Cellulose Acetate/Graphene Hybrid Nanofibers: Spectroscopic Investigations. *eXPRESS Polymer Letters*, 2013, 7(6), 554-563. ISSN 1788-618X.

43. GREISH, E. Y. et al. Effects of Thermal and Chemical Treatments on the Structural Stability of Cellulose Acetate Nanofibers. *Carbohydrate Polymers*, 2010, 82, 569-577. ISSN 0144-8617.

44. GRINSHPUN, S. A. et al. Do Aerosol Filters Certified Based on Testing with NaCl Challenge Provide the Targeted Protection against Combustion Aerosols? In *Aerosol Technology, June 16-18, Karlsruhe, Germany, 2014*. p. T290A14.

45. GUERRINI, L. M. et al. Electrospinning and Characterization of Polyamide 66 Nanofibers with Different Molecular Weights. *Materials Research*, 2009, 12(2), 181-190. ISSN 1516-1439.

46. HAKKARAINEN, M. Aliphatic Polyesters: Abiotic and Biotic Degradation and Degradation Products. *Advances in Polymer Science*, 2002, 157, 113-138. ISSN 0065-3195.

47. HAN, S. O. et al. Electrospinning of Cellulose Acetate Nanofibers Using a Mixed Solvent of Acetic Acid/Water: Effects of Solvent Composition on the Fiber Diameter. *Materials Letters*, 2008, 62, 759-762. ISSN 0167-577X.

48. HASSAN, M. A. Fabrication of Nanofiber Meltblown Membranes and Their Filtration Properties. *Journal of Membrane Science*, 2013, 427, 336-344. ISSN 0376-7388.

49. HEIKKILA, P. and A. HARLIN. Electrospinning of Polyacrylonitrile (PAN) Solution: Effect of Conductive Additive and Filler on the Process. *eXPRESS Polymer Letters*, 2009, 3(7), 437-445. ISSN 1788-618X.

50. HEIKKILA, P. and A. HARLIN. Parameter Study of Electrospinning of Polyamide-6. *European Polymer Journal*, 2008, 44(10), 3067-3079. ISSN 0014-3057.

51. HEIKKILA, P. et al. Electrospinning of Polyamides with Different Chain Compositions for Filtration Application. *Polymer Engineering and Science*, 2008, 48(6), 1168-1176. ISSN 1548-2634.

52. HINDS, W. C. *Aerosol Technology: Properties, Behavior, and Measurement of Airborne Particles*. John Wiley and Sons: New York, 1999.

53. HOLOPAINEN, J. et al. Needleless Electrospinning with Twisted Wire Spinneret. *Nanotechnology*, 2015, 26, 1-8. ISSN 1361-6528.

54. HONG, C. H. et al. Electroactive Bio-Composite Actuators Based on Cellulose Acetate Nanofibers with Specially Chopped Polyaniline Nanoparticles through Electrospinning. *Composites Science and Technology*, 2013, 87, 135-141. ISSN 0266-3538.

55. HOSSEINI, S. A. and H. V. TAFRESHI. Modelling Permeability of 3-D Nanofiber Media in Slip Flow Regime. *Chemical Engineering Science*, 2010, 65(6), 2249-2254. ISSN 0009-2509.

56. HUNG, C. H. and W. W. F. LEUNG. Filtration of Nano-Aerosol Using Nanofiber Filter under Low Peclet Number and Transitional Flow Regime. *Separation and Purification Technology*, 2011, 79(1), 34-42. ISSN 1383-5866.

57. HUTTEN, I. *Handbook of Non-Woven Filter Media*. Elsevier Science and Technology Books, 2007. ISBN: 1856174417.

58. INTRA, P. and N. TIPPAYAWONG. An Overview of Unipolar Charger Developments for Nanoparticle Charging. *Aerosol and Air Quality Research*, 2011, 11, 187-209. ISSN 1680-8584.

59. ISO, Nanotechnologies – Terminology and Definitions for Nano-objects, Nanoparticles, Nanofibre and Nanoplate, ISO/TS 12805:2011(en).

60. YAN, X. Y. et al. Dual-Functional OPH-Immobilized Polyamide Nanofibrous Membrane for Effective Organophosphorus Toxic Agents Protection. *Biochemical Engineering Journal*, 2015, 98, 47-55. ISSN 1369-703X.

61. YANG, T. L. et al. Synthesis and Fabrication of Silver Nanowires Embedded in PVP Fibers by Near-Field Electrospinning Process. *Optical Materials*, 2015, 39, 118-124. ISSN 0925-3467.

62. YU, X. et al. Preparation of Porous Polyacrylonitrile Fibers by Electrospinning a Ternary System of PAN/DMF/H2O. *Materials Letters*, 2010, 64(22), 2407-2409. ISSN 0167-577X.

63. YUN, K. M. et al. Morphology Optimization of Polymer Nanofiber for Applications in Aerosol Particle Filtration. *Separation and Purification Technology*, 2010, 75(3), 340-345. ISSN 1383-5866.

64. JACOBS, V. et al. The Influence of Electrospinning Parameters on the Structural Morphology and Diameter of Electrospun Nanofibers. *Journal of Applied Polymer Science*, 2010, 115, 3130-3136. ISSN 1097-4628.

65. JÄRVINEN, A. et al. Calibration of the New Electrical Low Pressure Impactor (ELPI+). *Journal of Aerosol Science*, 2014, 69, 150-159. ISSN 0021-8502.

66. JEONG, J. S. et al. Mechanical Properties of Electrospun PVA/MWNTs Composite Nanofibers. *Thin Solid Films*, 2007, 515, 5136–5141. ISSN 0040-6090.

67. JI, L. and X. ZHANG. Ultrafine Polyacrylonitrile/Silica Composite Fibers via Electrospinning. *Materials Letters*, 2008, 62(14), 2161-2164. ISSN 0167-577X.

68. JIRSAK, O. et al. Polyamic Acid Nanofibers Produced by Needleless Electrospinning. *Journal of Nanomaterials*, 2010, Article ID 842831, 1-6. ISSN 1687-4110.

69. KATTAMURI, N. and C. SUNG. Uniform Polycarbonate Nanofibers Produced by Electrospinning. *NSTI- Nano Science and Technology Institute*, 2004, 3, 425-428. ISBN 0-9728422-9-2.

70. KHAN, W. S. et al. Enhancing Thermal and Ionic Conductivities of Electrospun PAN and PMMA Nanofibers by Graphene Nanoflake Additions for Battery-Separator Applications. *International Journal of Energy Research*, 2014, 38(15), 2044-2051. ISSN 1099-114X.

71. KIBBLE, A. and R. HARRISON. Point Sources of Air Pollution. *Occupational Medicine*, 2005, 55, 425-431. ISSN 0962-7480.

72. KIRSCH, A. A. and I. B. STECHKINA. The Theory of Aerosol Filtration with Fibrous Filters. In *Fundamentals of Aerosol Science* edited by D. T. Shaw. Wiley: New York, 1978.

73. KOSTAKOVA, E. et al. Composite Nanofibers Produced by Modified Needleless Electrospinning. *Materials Letters*, 2009, 63, 2419-2422. ISSN 0167-577X.

74. KUMBAR, S. G. Recent Patents on Electrospun Biomedical Nanostructures: An Overview. *Recent Patents on Biomedical Engineering*, 2008, 1, 68-78. ISSN 1874-7647.

75. LALAGIRI, M. et al. Filtration Efficiency of Submicrometer Filters. *Industrial and Engineering Chemistry Research*, 2013, 52(46), 16513-16518. ISSN 0888-5885.

76. LEE, K. H. et al. Mechanical Behavior of Electrospun Fiber Mats of Poly(vinyl chloride)/Polyurethane Polyblends. *Journal of Polymer Science: Part B: Polymer Physics*, 2003, 41, 1256-1262. ISSN 1099-0488.

77. LEE, K. W., and B. Y. H. LIU. On the Minimum Efficiency and Most Penetrating Particle Size for Fibrous Filters. *Journal of the Air Pollution Control Association*, 1980, 30, 377-381. ISSN 0002-2470.

78. LEUNG, W. W. F. and C. H. HUNG. Skin Effect in Nanofiber Filtration of Submicron Aerosols. *Separation and Purification Technology*, 2012, 92, 174-180. ISSN 1383-5866.

79. LEUNG, W. W. F. et al. Effect of Face Velocity, Nanofiber Packing Density and Thickness on Filtration Performance of Filters with Nanofibers Coated on a Substrate. *Separation and Purification Technology*, 2010, 71(1), 30-37. ISSN 1383-5866.

80. LI, B. et al. Transparent PMMA-Based Nanocomposite Using Electrospun Graphene-Incorporated PA-6 Nanofibers as the Reinforcement. *Composites Science and Technology*, 2013, 89, 134-141. ISSN 0266-3538.

81. LI, D. and Y. XIA. Electrospinning of Nanofibers: Reinventing the Wheel. *Advanced Materials*, 2004, 16(14), 1151-1170. ISSN 1521-4095.

82. LI, D. et al. Three-Dimensional Polycaprolactone Scaffold via Needleless Electrospinning Promotes Cell Proliferation and Infiltration. *Colloids and Surfaces B: Biointerfaces*, 2014, 121, 432-443. ISSN 0927-7765.

83. LI, J. et al. Needleless Electro-Spun Nanofibers Used for Filtration of Small Particles. *eXPRESS Polymer Letters*, 2013, 7(8), 683-689. ISSN 1788-618X.

84. LI, N. et al. Preparation and Properties of PVDF/PVA Hollow Fiber Membranes. *Desalination*, 2010, 250, 530-537. ISSN 0011-9164.

85. LI, W. et al. Enhanced Thermal and Mechanical Properties of PVA Composites Formed with Filamentous Nanocellulose Fibrils. *Carbohydrate Polymers*, 2014, 113, 403-410. ISSN 0144-8617.

86. LI, Z. and C. WANG. *One-Dimensional Nanostructures. Electrospinning Technique and Unique Nanofibers*. Springer books, series: SpringerBriefs in Materials, 2013. ISBN 978-3-642-36427-3.

87. LIN, Y. et al. Mechanical Properties of Polymer Nanofibers Revealed by Interaction with Streams of Air. *Polymer*, 2012, 53, 782-790. ISSN 0032-3861.

88. LINGAIAH, S. et al. Electrospinning of Nylon-66 Polymer Nanofabrics. In *Proceedings of the 49th Aiaa/Asme/Asce/Ahs/Asc Structures, Structural Dynamics, and Materials Conference, Schaumburg, Ill, USA, April 2008*. pp.1-13.

89. LIU, H. and Y. L. HSIEH. Ultrafine Fibrous Cellulose Membranes from Electrospinning of Cellulose Acetate. *Journal of Polymer Science Part B: Polymer Physics*, 2002, 40(18), 2119-2129. ISSN 1099-0488.

90. LIU, S. L. et al. Assembly of Oriented Ultrafine Polymer Fibers by Centrifugal Electrospinning. *Journal of Nanomaterials*, 2013, Article ID 713275, 1-9. ISSN 1687-4110.

91. LU, Y. et al. Parameter Study and Characterization for Polyacrylonitrile Nanofibers Fabricated via Centrifugal Spinning Process. *European Polymer Journal*, 2013, 49(12), 3834-3845. ISSN 0014-3057.

92. MAHALINGAM, S. and M. EDIRISINGHE. Forming of Polymer Nanofibers by a Pressurised Gyration Process. *Macromolecular Rapid Communications*, 2013, 34, (14), 1134-1139. ISSN 1521-3927.

93. MAO, X. et al. Silica Nanofibrous Membranes with Robust Flexibility and Thermal Stability for High-Efficiency Fine Particulate Filtration. *RSC Advances*, 2012, 2, 12216-12223. ISSN 2046-2069.

94. MARSANO, E. Polyamide 6 Nanofibrous Nonwovens via Electrospinning. *Journal of Applied Polymer Science*, 2010, 117(3), 1754-1765. ISSN 1097-4628.

95. MATABOLA, K. P. et al. Studies on Single Polymer Composites of Poly(Methyl Methacrylate) Reinforced with Electrospun Nanofibers with a Focus on Their Dynamic Mechanical Properties. *eXPRESS Polymer Letters*, 2011, 5(7), 635-642. ISSN 1788-618X.

96. MATARAM, A. et al. Characterization and Mechanical Properties of Polyacrylonitrile/Silica Composite Fibers Prepared via Dry-Jet Wet Spinning Process. *Materials Letters*, 2010, 64, 1875-1878. ISSN 0167-577X.

97. MATHEW, G. et al. Preparation and Anisotropic Mechanical Behavior of Highly-Oriented Electrospun Poly(Butylene Terephthalate) Fibers. *Journal of Applied Polymer Science*, 2006, 101, 2017-2021. ISSN 1097-4628.

98. MAZE, B. et al. A Simulation of Unsteady-State Filtration via Nanofiber Media at Reduced Operating Pressures. *Journal of Aerosol Science*, 2007, 38(5), 550-571. ISSN 0021-8502.

99. MAZOOCHI, T. et al. Investigation on the Morphological Characteristics of Nanofiberous Membrane as Electrospun in the Different Processing Parameters. *International Journal of Industrial Chemistry*, 2012, 3(2), 1-8. ISSN 2228-5970.

100. MUNIR, M. M. et al. Scaling Law on Particle-To-Fiber Formation during Electrospinning. *Polymer*, 2009, 50(20), 4935-4943. ISSN 0032-3861.

101. MUNJ, H. R. et al. Biocompatible Electrospun Polymer Blends for Biomedical Applications. *Journal of Biomedical Materials Research Part B: Applied Biomaterials*, 2014, 102(7), 1517-1527. ISSN 1552-4981.

102. NAGY, Z. K. et al. Electrospun Water Soluble Polymer Mat for Ultrafast Release of Donepezil HCl. *eXPRESS Polymer Letters*, 2010, 4(12), 763-772. ISSN 1788-618X.

103. NAGY, Z. K. et al. Solvent-Free Melt Electrospinning for Preparation of Fast Dissolving Drug Delivery System and Comparison with Solvent-Based Electrospun and Melt Extruded Systems. *Journal of Pharmaceutical Sciences*, 2013, 102(2), 508-517. ISSN 1520-6017.

104. NAYAK, R. et al. Recent Advances in Nanofibre Fabrication Techniques. *Textile Research Journal*, 2011, 82(2), 129-147. ISSN 0040-5175.

105. NATARAJ, S. K. et al. Polyacrylonitrile-Based Nanofibers—a State-Of-The-Art Review. *Progress in Polymer Science*, 2012, 37(3), 487-513. ISSN 0079-6700.

106. NIE, G. et al. Fabrication of Polyacrylonitrile/CuS Composite Nanofibers and Their Recycled Application in Catalysis for Dye Degradation. *Applied Surface Science*, 2013, 284, 595-600. ISSN 0169-4332.

107. NIRMALA, R. et al. Preparation and Characterization of Electrospun Ultrafine Polyamide-6 Nanofibers. *Polymer International*, 2011, 60, 1475-1480. ISSN 1097-0126.

108. NIRMALA, R. et al. Recent Progress on the Fabrication of Ultrafine Polyamide-6 Based Nanofibers via Electrospinning: A Topical Review. *Nano-Micro Letters*, 2014, 6(2), 89-107. ISSN 2311-6706.

109. NIU, H. and T. LIN. Fiber Generators in Needleless Electrospinning. *Journal of Nanomaterials*, 2012, Article ID 725950, 1-13. ISSN 1687-4110.

110. NIU, X. et al. Needleless Electrospinning: Influences of Fibre Generator Geometry. *The Journal of the Textile Institute*, 2012, 103(7), 787-794. ISSN 0040-5000.

111. OH, G. Y. et al. Adsorption of Toluene on Carbon Nanofibers Prepared by Electrospinning. *Science of Total Environmental*, 2008, 393(2-3), 341-347. ISSN 0048-9697.

112. PANG, Z. et al. Fabrication of PA6/TiO2/PANI Composite Nanofibers by Electrospinning–Electrospraying for Ammonia Sensor. *Colloids and Surfaces A: Physicochemical and Engineering Aspects*, 2014, 461, 113-118. ISSN 0927-7757.

113. PANT, B. et al. Characterization and Antibacterial Properties of Ag NPs Loaded Nylon-6 Nanocomposite Prepared by One-Step Electrospinning Process. *Colloids and Surfaces A: Physicochemical and Engineering Aspects*, 2012, 395, 94-99. ISSN 0927-7757.

114. PANT, H. R. et al. Effect of Successive Electrospinning and the Strength of Hydrogen Bond on the Morphology of Electrospun Nylon-6 Nanofibers. *Colloids and Surfaces A: Physicochemical and Engineering Aspects*, 2010, 370(1-3), 87-94. ISSN 0927-7757.

115. PANT, H. R. et al. Electrospun Nylon-6 Spider-Net like Nanofiber Mat Containing TiO(2) Nanoparticles: A Multifunctional Nanocomposite Textile Material. *Journal of Hazardous Materials*, 2011, 185(1), 124-130. ISSN 0304-3894.

116. PANT, H. R. et al. Synthesis, Characterization, and Mineralization of Polyamide-6/Calcium Lactate Composite Nanofibers for Bone Tissue Engineering. *Colloids and Surfaces B: Biointerfaces*, 2013, 102, 152-175. ISSN 0927-7765.

117. PANTHI, G. et al. Preparation and Characterization of Nylon-6/Gelatin Composite Nanofibers via Electrospinning for Biomedical Applications. *Fibers and Polymers*, 2013, 14(5), 718-723. ISSN 1229-9197.

118. PAPKOV, D. et al. Simultaneously Strong and Tough Ultrafine Continuous Nanofiber. *ACS Nano*, 2013, 7(4), 3324-3331. ISSN 1936-0851.

119. PARK, J. H. et al., Fabrication of a Multi-Walled Carbon Nanotube-Deposited Glass Fiber Air Filter for the Enhancement of Nano and Submicron Aerosol Particle Filtration and Additional Antibacterial Efficacy. *Science of Total Environmental*, 2011, 409(19), 4132-4138. ISSN 0048-9697.

120. PARK, J. Y. et al. Optimization of the Electrospinning Conditions for Preparation of Nanofibers from Polyvinylacetate (PVAc) in Ethanol Solvent. *Journal of Industrial and Engineering Chemistry*, 2008, 14(6), 707-713. ISSN 1226-086X.

121. PETRIK, S. and M. MALY. Production Nozzle-Less Electrospinning Nanofiber Technology. In *Proceedings of the Fall MRS Symposium, Boston, Mass, USA, November-December 2009*. pp. 79-90.

122. PHAM, Q. P. et al. Electrospinning of Polymeric Nanofibers for Tissue Engineering Applications: A Review. *Tissue Engineering*, 2006, 12(5), 1197-1211. ISSN 2152-4947.

123. PODGÓRSKI, A. et al. Application of Nanofibers to Improve the Filtration Efficiency of the Most Penetrating Aerosol Particles in Fibrous Filters. *Chemical Engineering Science*, 2006, 61, 6804-6815. ISSN 0009-2509.

124. QIAN, Y. F. et al. Electrospinning of Polymethyl Methacrylate Nanofibres in Different Solvents. *Iranian Polymer Journal*, 2010, 19(2), 123-129. ISSN 1026-1265.

125. QIN, X. et al. Improving Preferred Orientation and Mechanical Properties of PAN-Based Carbon Fibers by Pretreating Precursor Fibers in Nitrogen. *CARBON*, 2011, 49, 4595-4607. ISSN 0008-6223.

126. RADER, D. J. Momentum Slip Correction Factor for Small Particles in Nine Common Gases. *Journal of Aerosol Science*, 1990, 21, 161-168. ISSN 0021-8502.

127. RODOPLU, D. and M. MUTLU. Effects of Electrospinning Setup and Process Parameters on Nanofiber Morphology Intended for the Modification of Quartz Crystal Microbalance Surfaces. *Journal of Engineered Fibers and Fabrics*, 2012, 7(2), 118-123. ISSN 1558-9250.

128. ROGINA, A. Electrospinning Process: Versatile Preparation Method for Biodegradable and Natural Polymers and Biocomposite Systems Applied in Tissue Engineering and Drug Delivery. *Applied Surface Science*, 2014, 296, 221-230. ISSN 0169-4332.

129. SAMBAER, W. et al. 3D Modelling of Filtration Process via Polyurethane Nanofiber Based Nonwoven Filters Prepared by Electrospinning Process. *Chemical Engineering Science*, 2011, 66(4), 613-623. ISSN 0009-2509.

130. SASITHORN, N. and L. MARTINOVÁ. Fabrication of Silk Nanofibres with Needle and Roller Electrospinning Methods. *Journal of Nanomaterials*, 2014, Article ID 947315, 1-9. ISSN 1687-4110.

131. SCHOENMAKER, B. et al. Electrospun Polyamide 4.6 Nanofibrous Nonwovens: Parameter Study and Characterization. *Journal of Nanomaterials*, 2012, Article ID 860654, 1-9. ISSN 1687-4110.

132. SCHUEREN, L. V. et al. The Development of Polyamide 6.6 Nanofibres with a pH-Sensitive Function by Electrospinning. *European Polymer Journal*, 2010, 46, 2229-2239. ISSN 0014-3057.

133. SEN, R. et al. Preparation of Single-Walled Carbon Nanotube Reinforced Polystyrene and Polyurethane Nanofibers and Membranes by Electrospinning. *NANO LETTERS*, 2004, 4(3), 459-464. ISSN 1530-6984.

134. SHAHI, M. et al. Electrospun PVA–PANI and PVA–PANI–AgNO3 Composite Nanofibers. *Scientia Iranica*, 2011, 18 (6), 1327-1331. ISSN 1026-3098.

135. SHAHRABI, S. et al. Fabrication of Electrospun Polyamide-66 Nanofiber Layer for High-Performance Nanofiltration in Clean Room Applications. *Journal of Industrial Textile*, 2014, DOI: 10.1177/1528083714553688, 1-15. ISSN 1528-0837.

136. SOMVIPART, S. et al. Development of Electrospun Beaded Fibers from Thai Silk Fibroin and Gelatin for Controlled Release Application. *International Journal of Biological Macromolecules*, 2013, 55, 176-184. ISSN 0141-8130.

137. SUBRAMANIAN, C. et al. Electrospinning and Characterization of Highly Sulfonated Polystyrene Fibers. *Polymer*, 2010, 51, 1983-1989. ISSN 0032-3861.

138. SUN, M. et al. Mechanical and Wettable Behavior of Polyacrylonitrile Reinforced Fibrous Polystyrene Mats. *Journal of Colloid and Interface Science*, 2010, 347, 147-152. ISSN 0021-9797.

139. SUTHERLAND, K. and D. B. PURCHAS. *Handbook of Filter Media*. Elsevier, 2002. ISBN 1856173755.

140. TAYLOR, G. Electrically Driven Jets. *Proceedings of the Royal Society of London Series A*, 1969, 313, 453-475. ISSN 0080–4630.

141. TEO, W. E. and S. RAMAKRISHNA. A Review on Electrospinning Design and Nanofibre Assemblies. *Nanotechnology*, 2006, 17, R89-R106. ISSN 1361-6528.

142. THAMMAWONG, C. et al. Electrospinning of Poly(l-lactide-co-dl-lactide) Copolymers: Effect of Chemical Structures and Spinning Conditions. *Polymer Engineering and Science*, 2014, 54(2), 472-480. ISSN 1548-2634.

143. The Camfil Group. Principles of Filtration. [Viewed on 11-02-2014]. Available at: http://www.camfil.com/Filter-technology/Principles-of-Filtration/

144. TIAN, Y. et al. Electrospun Membrane of Cellulose Acetate for Heavy Metal Ion Adsorption in Water Treatment. *Carbohydrate Polymers*, 2011, 83(2), 743-748. ISSN 0144-8617.

145. TSIOPTSIAS, C. et al. Preparation and Characterization of Cellulose Acetate–Fe_2O_3 Composite Nanofibrous Materials. *Carbohydrate Polymers*, 2010, 84(4), 925-930. ISSN 0144-8617.

146. TUNGPRAPA, S. et al. Electrospun Cellulose Acetate Fibers: Effect of Solvent System on Morphology and Fiber Diameter. *Cellulose*, 2007, 14, 563-575. ISSN 0969-0239.

147. VAHTRUS, M. et al. Mechanical Characterization of TiO2 Nanofibers Produced by Different Electrospinning Techniques. *Materials Characterization*, 2015, 100, 98-103. ISSN 1044-5803.

148. VARABHAS, J. S. et al. Electrospun Nanofibers from a Porous Hollow Tube. *Polymer*, 2009, 49, 19, 4226-4229. ISSN 0032-3861.

149. VARESANO, A. et al. Experimental Investigations on the Multi-Jet Electrospinning Process. *Journal of Materials Processing Technology*, 2009, 209, 5178-5185. ISSN 0924-0136.

150. WAKEMAN, R. J. *Filtration Dictionary and Glossary*. The Filtration Society: London, 1985.

151. WANG, J. et al. Investigation of the Figure of Merit for Filters with a Single Nanofiber Layer on a Substrate. *Journal of Aerosol Science*, 2008a, 39(4), 323-33. ISSN 0021-8502.

152. WANG, J. et al. Figure of Merit of Composite Filters with Micrometer and Nanometer Fibers. *Aerosol Science and Technology*, 2008b, 42, 722-728. ISSN 0278-6826.

153. WANG, J. Effects of Particle Size and Morphology on Filtration of Airborne Nanoparticles. *KONA Powder and Particle Journal*, 2013, 30, 256-266. ISSN 0288-4534.

154. WANG, N. et al. Multilevel Structured Polyacrylonitrile/Silica Nanofibrous Membranes for High-Performance Air Filtration. *Separation and Purification Technology*, 2014, 126, 44-51. ISSN 1383-5866.

155. WANG, N. et al. Tortuously Structured Polyvinyl Chloride/Polyurethane Fibrous Membranes for High-Efficiency Fine Particulate Filtration. *Journal of Colloid Interface Science*, 2013, 398, 240-246. ISSN 0021-9797.

156. WANG, X. et al. Needleless Electrospinning of Uniform Nanofibers Using Spiral Coil Spinnerets. *Journal of Nanomaterials*, 2012, Article ID 785920, 1-9. ISSN 1687-4110.

157. WARD, G. Nanofibres: Media at the Nanoscale. *Filtration and Separation*, 2005, 42 (7), 22-24. ISSN 0015-1882.

158. World Health Organisation. Air Quality Guidelines for Particulate Matter, Ozone, Nitrogen Dioxide and Sulphur Dioxide. Global update, 2005. [Viewed on 01-04-2015]. Available at: http://www.euro.who.int/__data/assets/pdf_file/0005/78638/E90038.pdf

159. ZANDER, N. E. Hierarchically Structured Electrospun Fibers. *Polymers*, 2013, 5, 19-44. ISSN 2073-4360.

160. ZARGHAM, S. et al. The Effect of Flow Rate on Morphology and Deposition Area of Electrospun Nylon 6 Nanofiber. *Journal of Engineered Fibers and Fabrics*, 2010, 7(4), 42-49. ISSN 1558-9250.

161. ZELENYUK, A. et al. From Agglomerates of Spheres to Irregularly Shaped Particles: Determination of Dynamic Shape Factors from Measurements of Mobility and Vacuum Aerodynamic Diameters. *Aerosol Science and Technology*, 2006, 40, 197–217. ISSN 0278-6826.

162. ZHANG, H. D. et al. High-Sensitivity Gas Sensors Based on Arranged Polyaniline/PMMAcomposite Fibers. *Sensors and Actuators A: Physical*, 2014, 219, 123-127. ISSN 0924-4247.

163. ZHANG, C. et al. A Novel Two-Nozzle Electrospinning Process for Preparing Microfiber Reinforced pH-Sensitive Nano-Membrane with Enhanced Mechanical Property. *European Polymer Journal*, 2011, 47, 2228-2233. ISSN 0014-3057.

164. ZHANG, Q. et al. Improvement in Nanofiber Filtration by Multiple Thin Layers of Nanofiber Mats. *Journal of Aerosol Science*, 2010, 41(2), 230-236. ISSN 0021-8502.

165. ZHANG, S. et al. Design of Ultra-Fine Nonwovens via Electrospinning of Nylon 6: Spinning Parameters and Filtration Efficiency. *Materials and Design*, 2009, 30(9), 3659-3666. ISSN 0261-3069.

166. ZHENG, J. et al. Construction of Hierarchical Structures by Electrospinning or Electrospraying. *Polymer*, 2012, 53, 546-554. ISSN 0032-3861.

167. ZHOU, F. L. et al. Needle and Needleless Electrospinning for Nanofibers. *Journal of Applied Polymer Science*, 2010, 115, 2591-2598 . ISSN 1097-4628.

168. ZHOU, F. L. et al. Three-Jet Electrospinning Using a Flat Spinneret. *Journal of Materials Science*, 2009, 44, 5501-5508. ISSN 0022-2461.

LIST OF PUBLICATIONS ON THE TOPIC OF THE DISSERTATION

Publications corresponding to the list of the Thomson Reuters Citation Databases

1. Matulevicius, Jonas; Kliucininkas, Linas; Prasauskas, Tadas; Buivydiene, Dalia; Martuzevicius, Dainius. The Comparative Study of Aerosol Filtration by Electrospun Polyamide, Polyvinyl Acetate, Polyacrylonitrile and Cellulose Acetate Nanofiber Media // *Journal of Aerosol Science*. Oxford: Pergamon-Elsevier Science. ISSN 0021-8502. 2016, Vol. 92, pp. 27-37. [Science Citation Index Expanded (Web of Science)]. [0.200]. [IF (E): 2.236 (2014)]

2. Matulevicius, Jonas; Kliucininkas, Linas; Martuzevicius, Dainius; Krugly, Edvinas; Tichonovas, Martynas; Baltrusaitis, Jonas. Design and Characterization of Electrospun Polyamide Nanofiber Media for Air Filtration Applications // *Journal of Nanomaterials*. New York: Hindawi. ISSN 1687-4110. 2014, Vol. 2014, Article no. 859656, pp. [1-13]. DOI: 10.1155/2014/859656 [Science Citation Index Expanded (Web of Science)]. [0.167]. [IF (E): 1.644 (2014)]

3. Matulevicius, Jonas; Kliucininkas, Linas; Martuzevicius, Dainius. Electrospinning of Cellulose Acetate Fibers from a Ternary Solvent System // *CHEMIJA*. Vilnius: Lietuvos mokslų akademija. ISSN 0235-7216. 2014, Vol. 25, Iss. 2, pp. 125-129. [Science Citation Index Expanded (Web of Science)]. [0.333]. [IF (E): 0.472 (2014)]

Publications referred in the international databases

1. Matulevicius, Jonas; Krugly, Edvinas; Kliucininkas, Linas. Utilisation of Thermoplastic Polymer Waste for Nanofiber Air Filter Production // *Sustainable Development, Knowledge Society and Smart Future Manufacturing Technologies*/edited by Leal Filho, Walter; Úbelis, Arnolds; Berzina, Dina. Springer: Switzerland. ISBN 978-3-319-14882-3. 2015, pp. 283-290.

List of the presentations in the international conferences

1. Matulevicius, Jonas; Kliucininkas, Linas; Martuzevicius, Dainius; Krugly, Edvinas. Filtration Properties of Monodisperse Airborne Particles by Electrospun Nanofiber Media // Aerosol Technology 2014: International Conference, 16 - 18 June 2014, Karlsruhe, Germany/Association for Aerosol Researchers (GAeF). 2014, p. T290A14.

2. Matulevicius, Jonas; Kliucininkas, Linas; Martuzevičius, Dainius. The Comparative Study of Nanofiber Filters Fabricated by Needle and Needleless Electrospinning Techniques // Chemistry and Chemical Technology: Proceedings of

the International Conference, 25 April, 2014/Kaunas University of Technology. Kaunas: Technologija. 2014, ISSN 2351-5643, pp. 34-37.

3. Matulevicius, Jonas; Kliucininkas, Linas; Martuzevicius, Dainius. Electrospinning of Cellulose Acetate Fibers from Ternary Solvent System // EcoBalt 2013: 18th International Scientific Conference, October 25-27, 2013/Vilnius, Lithuania: Book of Abstracts. Vilnius: Vilniaus universiteto leidykla. 2013, ISBN 978-609-459-241-6, p. 116.

4. Matulevicius, Jonas; Kliucininkas, Linas; Martuzevicius, Dainius. Characterization of Polyamide Nanofiber Media for Aerosol Filtration Applications // EAC 2013: European Aerosol Conference, 1-6 September 2013, Prague/Czech Aerosol Society. 2013, p. 1.

5. Matulevicius, Jonas; Krugly, Edvinas; Grigonyte, Julija. Utilisation of Thermoplastic Polymer Waste for Nanofiber Air Filter Production // In abstracts of 3rd International Conference on Integrative Approaches towards Sustainability "Sustainable Development, Knowledge Society and Smart Future Manufacturing Technologies" (Knowledge), June 27-30, 2012, Jūrmala, Latvia/The University of Latvia. 2012, pp. 18-19.

OTHER PUBLICATIONS

1. Prasauskas, Tadas; Matulevicius, Jonas; Kliucininkas, Linas; Krugly, Edvinas; Valincius, Vitas; Martuzevicius, Dainius. Filter Media Properties of Mineral Fibers Produced by Plasma Spray // *Environmental Technology*. Oxon: Taylor & Francis. ISSN 0959-3330. 2016, p. 1-33. DOI: 10.1080/09593330.2015.1114028. [Science Citation Index Expanded (Web of Science)]. [0.167]. [IF (E): 1.560 (2014)]

2. Kliucininkas, Linas; Matulevicius, Jonas; Martuzevicius, Dainius. The life cycle assessment of alternative fuel chains for urban buses and trolleybuses // *Journal of Environmental Management*. London Elsevier. ISSN 0301-4797. 2012, Vol. 99, p. 98-103. [Science Citation Index Expanded (Web of Science)] [0.333]. [IF (E): 3.057 (2012)]

SL344. 2015-12-14, 10,5 leidyb. apsk. 1. Tiražas 10 egz. Užsakymas 463.
Išleido Kauno technologijos universitetas, K. Donelaičio g. 73, 44249 Kaunas
Spausdino leidyklos „Technologija" spaustuvė, Studentų g. 54, 51424 Kaunas